

TWO PORT RF NETWORK THEORY

LOW FREQUENCY PARAMETERS:

The purpose of this appendix is to introduce a special class of network functions that characterize linear two-port circuits. These network functions involve both the driving point and transfer functions as defined in Chapter 11. The added constraint here is that they are defined under open-circuit and short-circuit conditions.

A four-terminal network qualifies as a two port if *the net current entering each terminal pair is zero*. This means that the current exiting the lower port terminals in Figure W2-1 must be equal to the currents entering the upper terminals. One way to meet this condition is to always connect external sources and loads between the input terminal pair or between the output terminal pair.

Name	Express	In terms of	Defining equations
Impedance	V_1, V_2	I_1, I_2	$V_1 = z_{11}I_1 + z_{12}I_2$ and $V_2 = z_{21}I_1 + z_{22}I_2$
Admittance	I_1, I_2	V_1, V_2	$I_1 = y_{11}V_1 + y_{12}V_2$ and $I_2 = y_{21}V_1 + y_{22}V_2$
Hybrid	V_1, I_2	I_1, V_2	$V_1 = h_{11}I_1 + h_{12}V_2$ and $I_2 = h_{21}I_1 + h_{22}V_2$
Transmission	V_1, I_1	$V_2, -I_2$	$V_1 = AV_2 - BI_2$ and $I_1 = CV_2 - DI_2$

Before turning to specific parameters, it is important to specify the objectives of two-port network analysis. Briefly, these objectives are:

- (1) Determine two-port parameters of a given circuit.
- (2) Use two-port parameters to find port variable responses for specified input sources and output loads.

IMPEDANCE PARAMETERS:

The impedance parameters are obtained by expressing the port voltages V_1 and V_2 in terms of the port currents I_1 and I_2 .

$$\begin{aligned} V_1 &= z_{11}I_1 + z_{12}I_2 \\ V_2 &= z_{21}I_1 + z_{22}I_2 \end{aligned} \quad (\text{W2-1})$$

The network functions z_{11} , z_{12} , z_{21} , and z_{22} are called the **impedance parameters** or simply the

$$\begin{bmatrix} V_1 \\ V_2 \end{bmatrix} = \begin{bmatrix} z_{11} & z_{12} \\ z_{21} & z_{22} \end{bmatrix} \begin{bmatrix} I_1 \\ I_2 \end{bmatrix} = [\mathbf{z}] \begin{bmatrix} I_1 \\ I_2 \end{bmatrix}$$

where the matrix $[\mathbf{z}]$ is called the **impedance matrix** of a two-port network.

To measure or compute the impedance parameters we apply excitation at one port and leave the other port open circuited. When we drive at port 1 with port 2 is open ($I_2 = 0$), the expressions in Eq. (W2-1) reduce to one term each, and yield the definitions of z_{11} and z_{21} .

$$z_{11} = \left. \frac{V_1}{I_1} \right|_{I_2=0} = \text{input impedance with the output port open.}$$

$$z_{21} = \left. \frac{V_2}{I_1} \right|_{I_2=0} = \text{forward transfer impedance with the output port open.}$$

$$z_{12} = \left. \frac{V_1}{I_2} \right|_{I_1=0} = \text{reverse transfer impedance with the input port open.}$$

$$z_{22} = \left. \frac{V_2}{I_2} \right|_{I_1=0} = \text{output impedance with the input port open.}$$

All of these parameters are impedances with dimensions of ohms.

A two port is said to be **reciprocal** when the open-circuit voltage measured at one port due to a current excitation at the other port is unchanged when the measurement and excitation ports are interchanged. A two port that fails this test is said to be **nonreciprocal**. Circuits containing resistors, capacitors, and inductors (including mutual inductance) are always reciprocal. Adding dependent sources to the mix usually makes the two port nonreciprocal.

If a two port is reciprocal then $z_{12} = z_{21}$. To prove this we apply an excitation $I = I_x$ at the input port and observe that Eq. (W2-1) gives the open-circuit ($I_2 = 0$) voltage at the output port as $V_{2OC} = z_{21}I_x$. Reversing the excitation and observation ports, we find that an excitation $I_2 = I_x$ produces an open-circuit ($I_1 = 0$) voltage at the input port of $V_{1OC} = z_{12}I_x$. Reciprocity requires that $V_{1OC} = V_{2OC}$, which can only happen if $z_{12} = z_{21}$.

ADMITTANCE PARAMETERS:

The admittance parameters are obtained by expressing the port currents I_1 and I_2 in terms of the port voltages V_1 and V_2 . The resulting two-port i - v relationships are

$$\begin{aligned} I_1 &= y_{11}V_1 + y_{12}V_2 \\ I_2 &= y_{21}V_1 + y_{22}V_2 \end{aligned} \tag{W2-5}$$

The network functions y_{11} , y_{12} , y_{21} , and y_{22} are called the **admittance parameters**. In matrix form these equations are

$$\begin{bmatrix} I_1 \\ I_2 \end{bmatrix} = \begin{bmatrix} y_{11} & y_{12} \\ y_{21} & y_{22} \end{bmatrix} \begin{bmatrix} V_1 \\ V_2 \end{bmatrix} = [\mathbf{y}] \begin{bmatrix} V_1 \\ V_2 \end{bmatrix} \quad (\text{W2-6})$$

where the matrix $[\mathbf{y}]$ is called the **admittance matrix** of a two-port network.

To measure or compute the admittance parameters, we apply excitation at one port and short circuit the other port. When we drive at port 1 with port 2 is shorted ($V_2 = 0$), the

$$y_{11} = \left. \frac{I_1}{V_1} \right|_{V_2=0} = \text{input admittance with the output port shorted.}$$

$$y_{21} = \left. \frac{I_2}{V_1} \right|_{V_2=0} = \text{forward transfer admittance with the output port shorted.}$$

Conversely, when we drive at port 2 with port 1 is shorted ($V_1 = 0$), the expressions in Eq.

(W2-5) reduce to one term each that define y_{22} and y_{12} as

$$y_{12} = \left. \frac{I_1}{V_2} \right|_{V_1=0} = \text{reverse transfer admittance with the input port shorted.} \quad (\text{W2-8a})$$

$$y_{22} = \left. \frac{I_2}{V_2} \right|_{V_1=0} = \text{output admittance with the input port shorted.}$$

The admittance parameters express port currents in terms of port voltages, whereas the impedance parameters express the port voltages in terms of the port currents. In effect these parameter are inverses. To see this mathematically, we multiply Eq. (W2-2) by $[\mathbf{z}]^{-1}$ the

$$[\mathbf{z}]^{-1} \begin{bmatrix} V_1 \\ V_2 \end{bmatrix} = [\mathbf{z}]^{-1} [\mathbf{z}] \begin{bmatrix} I_1 \\ I_2 \end{bmatrix} = \begin{bmatrix} I_1 \\ I_2 \end{bmatrix}$$

Comparing this result with Eq. (W2-6) we conclude that $[\mathbf{y}] = \{\mathbf{z}\}^{-1}$. That is, the admittance matrix of a two port is the inverse of its impedance matrix. This means that the admittance parameters can be derived from the impedance parameters, provided $[\mathbf{z}]^{-1}$ exists. We will return to this idea in a later section. For the moment remember that admittance and impedance parameters are not independent descriptions of a two-port network.

HYBRID PARAMETERS:

W2-4 HYBRID PARAMETERS

The hybrid parameters are defined in terms of a mixture of port variables. Specifically, these parameters express V_1 and I_2 in terms of I_1 and V_2 . The resulting two-port *i-v* relationships are

$$\begin{aligned} V_1 &= h_{11}I_1 + h_{12}V_2 \\ I_2 &= h_{21}I_1 + h_{22}V_2 \end{aligned} \tag{W2-9}$$

Where h_{11} , h_{12} , h_{21} , and h_{22} are called the **hybrid parameters** or simply the ***h*-parameters**. In matrix form these equations are

$$\begin{bmatrix} V_1 \\ I_2 \end{bmatrix} = \begin{bmatrix} h_{11} & h_{12} \\ h_{21} & h_{22} \end{bmatrix} \begin{bmatrix} I_1 \\ V_2 \end{bmatrix} = [\mathbf{h}] \begin{bmatrix} I_1 \\ V_2 \end{bmatrix} \tag{W2-10}$$

where the matrix $[\mathbf{h}]$ is called the ***h*-matrix** of a two-port network.

The *h*-parameters can be measured or calculated as follows. When we drive at port 1

with port 2 shorted ($V_2 = 0$), the expressions in Eq. (W2-9) reduce to one term each, and yield the definitions of h_{11} and h_{21} .

$$h_{11} = \left. \frac{V_1}{I_1} \right|_{V_2=0} = \text{input impedance with the output port shorted.} \quad (\text{W2-11a})$$

$$h_{21} = \left. \frac{I_2}{I_1} \right|_{V_2=0} = \text{forward current transfer function with the output port shorted.} \quad (\text{W2-11b})$$

When we drive at port 2 with port 1 open ($I_1 = 0$), the expressions in Eq. (W2-9) reduce to one term each, and yield the definitions of h_{12} and h_{22} .

$$h_{12} = \left. \frac{V_1}{V_2} \right|_{I_1=0} = \text{reverse voltage transfer function with the input port open.} \quad (\text{W2-12a})$$

$$h_{22} = \left. \frac{I_2}{V_2} \right|_{I_1=0} = \text{output admittance with the input port open.}$$

ABCD PARAMETERS:

The ABCD-parameters are known variously as chain, cascade, or transmission line parameters. There are a number of definitions given for ABCD parameters, the most common

$$\begin{bmatrix} V_1 \\ I_1 \end{bmatrix} = \begin{bmatrix} A & B \\ C & D \end{bmatrix} \begin{bmatrix} V_2 \\ -I_2 \end{bmatrix}$$

For reciprocal networks $AD - BC = 1$ For symmetrical networks $A = D$. For networks which are reciprocal and lossless, A and D are purely real while B and C are purely imaginary.

This representation is preferred because when the parameters are used to represent a cascade of two-ports, the matrices are written in the same order that a network diagram would be drawn, that is, left to right. However, the examples given below are based on a variant definition;

$$\begin{bmatrix} V_2 \\ I_2' \end{bmatrix} = \begin{bmatrix} A' & B' \\ C' & D' \end{bmatrix} \begin{bmatrix} V_1 \\ I_1 \end{bmatrix}$$

where

$$\begin{aligned} A' &\stackrel{\text{def}}{=} \left. \frac{V_2}{V_1} \right|_{I_1=0} & B' &\stackrel{\text{def}}{=} \left. \frac{V_2}{I_1} \right|_{V_1=0} \\ C' &\stackrel{\text{def}}{=} \left. -\frac{I_2}{V_1} \right|_{I_1=0} & D' &\stackrel{\text{def}}{=} \left. -\frac{I_2}{I_1} \right|_{V_1=0} \end{aligned}$$

The negative signs in the definitions of parameters C' and D' arise because I₂' is defined with the opposite sense to I₂, that is, I₂' = -I₂. The reason for adopting this convention is so that the output current of one cascaded stage is equal to the input current of the next. Consequently, the input voltage/current matrix vector can be directly replaced with the matrix equation of the preceding cascaded stage to form a combined A'B'C'D' matrix.

The terminology of representing the parameters as a matrix of elements designated a₁₁ etc as adopted by some authors^[10] and the inverse parameters as a matrix of elements designated b₁₁ etc is used here for both brevity and to avoid confusion with circuit elements.

HIGH FREQUENCY PARAMETER

The s parameter is called as high frequency parameter

FORMULATION OF S – PARAMETER

An n-port microwave network has n arms into which power can be fed and from which power can be taken. In general, power can get from any arm (as input) to any other arm (as output). There are thus n incoming waves and n outgoing waves. We also observe that power can be reflected by a port, so the input power to a single port can partition between all the ports of the network to form outgoing waves. Associated with each port is the notion of a "reference plane" at which the wave amplitude and phase is defined. Usually the reference plane associated with a certain port is at the same place with respect to incoming and outgoing waves. The n incoming wave complex amplitudes are usually designated by the n complex quantities a_n, and the n outgoing wave complex quantities are designated by the n complex quantities b_n. The incoming wave quantities are assembled into an n-vector A and the outgoing wave quantities into an n-vector B. The outgoing waves are expressed in terms of the incoming waves by the matrix equation B = SA where S is an n by n square matrix of complex numbers called the "scattering matrix". It completely determines the behaviour of the

network. In general, the elements of this matrix, which are termed "s-parameters", are all frequency-dependent.

For example, the matrix equations for a 2-port are

$$b_1 = s_{11} a_1 + s_{12} a_2$$

$$b_2 = s_{21} a_1 + s_{22} a_2$$

And the matrix equations for a 3-port are

$$b_1 = s_{11} a_1 + s_{12} a_2 + s_{13} a_3$$

$$b_2 = s_{21} a_1 + s_{22} a_2 + s_{23} a_3$$

$$b_3 = s_{31} a_1 + s_{32} a_2 + s_{33} a_3$$

The wave amplitudes a_n and b_n are obtained from the port current and voltages by the relations $a = (V + Z_0 I) / (2 \sqrt{Z_0})$ and $b = (V - Z_0 I) / (2 \sqrt{Z_0})$. Here, a refers to an if V is V_n and I is I_n for the n th port. Note the $\sqrt{2}$ reduces the peak value to an rms value, and the $\sqrt{Z_0}$ makes the amplitude normalised with respect to power, so that the incoming power = $a a^*$ and the outgoing power is $b b^*$.

A one-port scattering parameter s is merely the reflection coefficient γ , and as we have seen we can relate γ to the load impedance $z_L = Z_L / Z_0$ by the formula $\gamma = (z_L - 1) / (z_L + 1)$.

Similarly, given an n by n "Z-matrix" for an n -port network, we obtain the S matrix from the formula $S = (Z - I)(Z + I)^{-1}$, by post-multiplying the matrix $(Z - I)$ by the inverse of the matrix $(Z + I)$. Here, I is the n by n unit matrix. The matrix of z parameters (which has n squared elements) is the inverse of the matrix of y parameters.

PROPERTIES OF S-PARAMETER

- 1) Zero diagonal elements for perfect matched network

For an ideal network with matched termination $S_{ii} = 0$, since there is no reflection from any port. Therefore under perfect matched condition the diagonal element of $[s]$ are zero

- 2) Symmetry of $[s]$ for a reciprocal network

The reciprocal device has a same transmission characteristics in either direction of a pair of ports and is characterized by a symmetric scattering matrix

$$S_{ij} = S_{ji} ; \quad i \neq j$$

Which results

$$[S]^t = [S]$$

For a reciprocal network with assumed normalized the impedance matrix equation is $[b] = ([z] + [u])^{-1} ([z] - [u]) [a]$ ----- (1)

Where u is the unit matrix

S matrix equation of network is

$$[b] = [s] [a] \text{----- (2)}$$

Compare equ (1) & (2)

$$[s] = ([z] + [u])^{-1} ([z] - [u])$$

$$[R] = [Z] - [U]$$

$$[Q] = [Z] + [U]$$

For a reciprocal network Z matrix Symmetric

$$[R] [Q] = [Q] [R]$$

$$[Q]^{-1} [R] [Q] [Q]^{-1} = [Q]^{-1} [Q] [R] [Q]^{-1}$$

$$[Q]^{-1} [R] = [R] [Q]^{-1}$$

$$[Q]^{-1} [R] [S] = [R] [Q]^{-1} \text{----- (3)}$$

TRANSPOSE OS $[s]$ IS NOW GIVEN AS

$$[S]_t = [Z-u]_t [Z+U]_t^{-1}$$

Then

$$[Z-u]_t = [Z-U]$$

$$[Z+u]_t^{-1} = [Z+U]$$

$$[S]_t = [z-u] [z+u]^{-1}$$

$$[S]_t = [R] [Q]^{-1} \text{----- (4)}$$

When compare 3 & 4

$$[S]_t = [S]$$

3) Unitary property of lossless network

For any loss less network the sum of product of each term of any one row or any one column of s matrix multiplied by its complex conjugate is unity

$$\sum_{n=1}^N S_{ni} S_{ni}^* = 1$$

For a lossless N port devices the total power leaving N ports must be equal to total input to the ports

4) Zero property

It states that the sum of the product of any each term of any one row or any one column of a s matrix is multiplied by the complex conjugate of corresponding terms of any other row is zero

$$\sum_{n=1}^N S_{ni} S_{ni}^* = 0$$

5) Phase shift propert

If any of the terminal or reference plane are mover away from the junction by anelectric distance β_k, l_k . each of the coefficient S_{ij} involving K will be multiplied by the factor $(e^{-j\beta_k l_k})$

$$S = \begin{pmatrix} 0 & e^{-j\phi_{12}} \\ e^{-j\phi_{21}} & 0 \end{pmatrix}$$

RECIPROCAL AND LOSS LESS NETWORKS:

1) Symmetry of [s] for a reciprocal network

The reciprocal device has a same transmission characteristics in either direction of a pair of ports and is characterized by a symmetric scattering matrix

$$S_{ij} = s_{ji} ; \quad i \neq j$$

Which results

$$[S]_t = [S]$$

For a reciprocal network with assumed normalized the impedance matrix equation is [b] = ([Z] + [u])⁻¹ ([Z] - [u]) [a]----- (1)

Where u is the unit matrix

S matrix equation of network is

$$[b] = [s] [a]----- (2)$$

Compare equ (1) & (2)

$$[s] = ([Z] + [u])^{-1} ([Z] - [u])$$

$$[R] = [Z] - [U]$$

$$[Q] = [Z] + [U]$$

For a reciprocal network Z matrix Symmetric

$$[R] [Q] = [Q] [R]$$

$$\begin{aligned}
 [Q]^{-1}[R][Q][Q]^{-1} &= [Q]^{-1}[Q][R][Q]^{-1} \\
 [Q]^{-1}[R] &= [R][Q]^{-1} \\
 [Q]^{-1}[R][S] &= [R][Q]^{-1}
 \end{aligned}$$

19 TRANSMISSION MATRIX

The Scattering transfer parameters or T-parameters of a 2-port network are expressed by the T-parameter matrix and are closely related to the corresponding S-parameter matrix. The Parameter matrix is related to the incident and reflected normalized waves at each of the ports as follows:

$$\begin{pmatrix} b_1 \\ a_1 \end{pmatrix} = \begin{pmatrix} T_{11} & T_{12} \\ T_{21} & T_{22} \end{pmatrix} \begin{pmatrix} a_2 \\ b_2 \end{pmatrix}$$

However, they could be defined differently, as follows :

$$\begin{pmatrix} a_1 \\ b_1 \end{pmatrix} = \begin{pmatrix} T_{11} & T_{12} \\ T_{21} & T_{22} \end{pmatrix} \begin{pmatrix} b_2 \\ a_2 \end{pmatrix}$$

The RF Toolbox add-on to MATLAB^[16] and several books (for example "Network scattering parameters"^[17]) use this last definition, so caution is necessary. The "From S to T" and "From T to S" paragraphs in this article are based on the first definition. Adaptation to the second definition is trivial (interchanging T11 for T22, and T12 for T21). The advantage of T-parameters compared to S-parameters is that they may be used to readily determine the effect of cascading 2 or more 2-port networks by simply multiplying the associated individual T-parameter matrices. If the T-parameters of say three different 2-port networks 1, 2 and 3 are (T_1) , (T_2) and (T_3) respectively then the T-parameter matrix for the cascade of all three networks (T_T) in serial order is given by:

$$(T_T) = (T_1)(T_2)(T_3)$$

As with S-parameters, T-parameters are complex values and there is a direct conversion between the two types. Although the cascaded T-parameters is a simple matrix multiplication of the individual T-parameters, the conversion for each network's S-parameters to the corresponding T-parameters and the conversion of the cascaded T-parameters back to the equivalent cascaded S-parameters, which are usually required, is not trivial. However once the operation is completed, the complex full wave interactions between all ports in both directions will be taken into account. The following equations will provide conversion between S and T parameters for 2-port networks.[18]

From S to T:

$$T_{11} = \frac{-\det(S)}{S_{21}}$$

$$T_{12} = \frac{S_{11}}{S_{21}}$$

$$T_{21} = \frac{-S_{22}}{S_{21}}$$

$$T_{22} = \frac{1}{S_{21}}$$

From T to S

$$S_{11} = \frac{T_{12}}{T_{22}}$$

$$S_{12} = \frac{\det(T)}{T_{22}}$$

$$S_{21} = \frac{1}{T_{22}}$$

$$S_{22} = \frac{-T_{21}}{T_{22}}$$

Where $\det(S)$ indicates the determinant of the matrix (S) .

INTRODUCTION TO COMPONENT BASICS:

WIRE

CAPACITOR

INDUCTOR

RESISTOR

WIRE:

RF Cable Assembly is a quality manufacturer of standard and custom cable assemblies and electromechanical wiring harnesses for medical, computer, LAN, RF, automotive, monitoring and communications equipment. We can build custom cables to meet your requirements, whether standard or special.

Complete product design, tooling design and fabrication, materials processing and selection, product manufacture, assembly, testing and packaging are available in our San Diego facility.

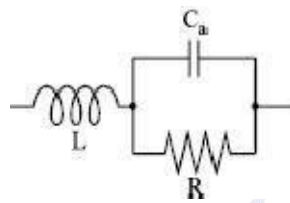
All our assembly and soldering technicians have been trained to the requirements of IPC/EIA J-STD-001 and IPC/WHMA-A-620. By creating and using hand tools and assembly jigs designed for their tasks and using them in our documented production processes, we produce quality with repeatability.

RESISTOR:

The H, Y, Z and ABCD parameters are difficult at microwave frequencies due to the following reasons.

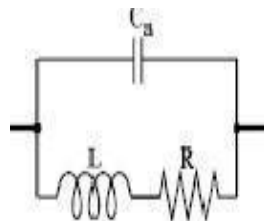
- (i) Equipment is not readily available to measure total voltage and total current at the ports of the network.
- (ii) Short circuit and open circuit are difficult to achieve over a wide range of frequencies.
- (iii) Presence of active devices makes the circuit unstable for short or open circuit.

Therefore microwave circuits are analyzed using scattering or S parameters which linearly relate the reflected wave amplitude with those of incident waves.



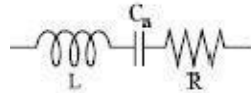
:INDUCTOR:

This inductance is exacerbated by the leads of the capacitor, which often dominate the inductance. The inductive parasitics are lumped into a single inductor L_s in series with the capacitor. The finite conductivity of the plates and the leads also results in some series loss, modeled by R_s (sometimes labeled ESR, or effective series resistance). Unless a capacitor is fabricated in a vacuum, the dielectric material that separates the plates also has loss (and resonance), which is usually modeled by a large shunt resistance, R_{di} . Furthermore, when a capacitor is soldered onto a PCB, there is parasitic capacitance from the solder pads to the ground plane, resulting in the capacitors, C_p , in the equivalent model. In a like manner, every inductor also has parasitics, as shown in the equivalent circuit model (Fig. 4), which limit operating frequency range. The series resistance, R_x , is due to the winding resistance, and the capacitance C_x models the distributed turn-to-turn capacitance of the windings. The inductor self resonates at a frequency of approximately $1/\sqrt{LC_x}$ and has a quality factor $Q = \omega L/R_x$. When the inductor is soldered onto the PCB, there is an additional capacitance to ground modeled by C_p , which lowers the self-resonant frequency to $1/\sqrt{L(C_x + C_p/2)}$.



: CAPACITOR:

now you have probably simulated your circuits with ideal passive components (inductors, capacitors, resistors), but real circuit components are far from ideal. Consider, for instance, a capacitor, which has an equivalent circuit model shown in Fig. 2. The model has many parasitic components which only become relevant at high frequencies. A plot of the impedance of the capacitor, shown in Fig. 3, shows that in addition to the ideal behavior, the most notable difference is the self-resonance that occurs for any real capacitor. The self-resonance is inevitable for any real capacitor due to the fact that as AC currents flow through a capacitor, a magnetic field is also generated by the capacitor, which leads to inductance

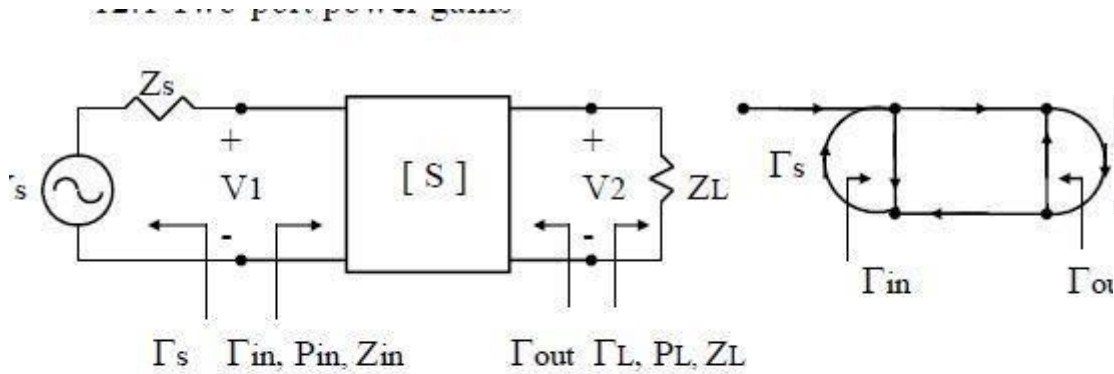


www.BrainKart.com

UNIT – 2

RF AMPLIFIERS AND MATCHING NETWORKS

AMPLIFIER POWER RELATION



$$\text{power gain } G \equiv \frac{P_L}{P_{in}}(S, \Gamma_L)$$

$$\text{available power gain } G_A \equiv \frac{P_{avn}}{P_{avs}}(S, \Gamma_s)$$

$$\text{transducer power gain } G_T \equiv \frac{P_L}{P_{avn}}(S, \Gamma_s, \Gamma_L)$$

$$P_{in}(\Gamma_{in}), P_{avs}(\Gamma_s) = P_{in}|_{\Gamma_{in}=\Gamma_s^*}, P_L(\Gamma_L), P_{avn}(\Gamma_{out}) = P_L|_{\Gamma_L=\Gamma_{out}^*}$$

$$P_{avs} = P_{in}|_{\Gamma_{in}=\Gamma_s^*} = \frac{|V_s|^2}{8Z_o} \frac{|1-\Gamma_s|^2}{1-|\Gamma_s|^2}$$

$$P_{avn} = P_L|_{\Gamma_L=\Gamma_{out}^*} = \frac{|V_s|^2}{8Z_o} \frac{|S_{21}|^2 |1-\Gamma_s|^2 (1-|\Gamma_{out}|^2)}{|1-S_{22}\Gamma_{out}^*|^2 |1-\Gamma_s\Gamma_{in}|^2}, \Gamma_{in} = S_{11} + \frac{S_{12}S_{21}\Gamma_L}{1-S_{22}\Gamma_L}$$

$$\rightarrow P_{avn} = \frac{|V_s|^2}{8Z_o} \frac{|S_{21}|^2 |1-\Gamma_s|^2}{|1-S_{11}\Gamma_s|^2 (1-|\Gamma_{out}|^2)}$$

$$4. \quad G(S, \Gamma_L) \equiv \frac{P_L}{P_{in}} = \frac{|S_{21}|^2 (1 - |\Gamma_L|^2)}{(1 - |\Gamma_{in}|^2) |1 - S_{22}\Gamma_L|^2}$$

$$G_A(S, \Gamma_s) \equiv \frac{P_{avn}}{P_{avs}} = \frac{|S_{21}|^2 (1 - |\Gamma_s|^2)}{(1 - |\Gamma_{out}|^2) |1 - S_{11}\Gamma_s|^2}$$

$$G_T(S, \Gamma_s, \Gamma_L) \equiv \frac{P_L}{P_{avs}} = \frac{|S_{21}|^2 (1 - |\Gamma_s|^2)(1 - |\Gamma_L|^2)}{|1 - \Gamma_s\Gamma_{in}|^2 |1 - S_{22}\Gamma_L|^2} (= |S_{21}|^2, \text{ if } \Gamma_s = \Gamma_L = 0)$$

STABILITY CONSIDERATION AND FREQUENCY RESPONSE:

- ✓ *Unconditional stability:* The network is unconditionally stable if $|\Gamma_{in}| < 1$ and $|\Gamma_{out}| < 1$ for all passive source and load impedances (i.e. $\Gamma_s < 1$ and $\Gamma_L < 1$)
- ✓ *Conditional stability:* The network is conditionally stable if $|\Gamma_{in}| < 1$ and $|\Gamma_{out}| < 1$ only for a certain range of passive source and load impedances. This case is also referred to as *potentially unstable*.

Stability Circles

- ✓ Applying the above requirements for unconditional stability to (12.3) gives the following conditions that must be satisfied by Γ_s and Γ_L if the amplifier is to be unconditionally

$$|\Gamma_{in}| = \left| S_{11} + \frac{S_{12}S_{21}\Gamma_L}{1 - S_{22}\Gamma_L} \right| < 1, \quad (12.19a)$$

$$|\Gamma_{out}| = \left| S_{22} + \frac{S_{12}S_{21}\Gamma_s}{1 - S_{11}\Gamma_s} \right| < 1. \quad (12.19b)$$

- ✓ We can derive the equation for the output stability circle as follows. First use (12.19a) to express the condition that $|\Gamma_{in}| = 1$ as

$$\left| S_{11} + \frac{S_{12}S_{21}\Gamma_L}{1 - S_{22}\Gamma_L} \right| = 1, \quad (12.20)$$

or

$$|S_{11}(1 - S_{22}\Gamma_L) + S_{12}S_{21}\Gamma_L| = |1 - S_{22}\Gamma_L|.$$

Now define Δ as the determinant of the scattering matrix:

$$\Delta = S_{11}S_{22} - S_{12}S_{21}. \quad (12.21)$$

Then we can write the above result as

$$|S_{11} - \Delta \Gamma_L| = |1 - S_{22} \Gamma_L|. \quad (12.22)$$

Now square both sides and simplify to obtain

$$\begin{aligned} |S_{11}|^2 + |\Delta|^2 |\Gamma_L|^2 - (\Delta \Gamma_L S_{11}^* + \Delta^* \Gamma_L^* S_{11}) &= 1 + |S_{22}|^2 |\Gamma_L|^2 - (S_{22}^* \Gamma_L^* + S_{22} \Gamma_L) \\ (|S_{22}|^2 - |\Delta|^2) \Gamma_L \Gamma_L^* - (S_{22} - \Delta S_{11}^*) \Gamma_L - (S_{22}^* - \Delta^* S_{11}) \Gamma_L^* &= |S_{11}|^2 - 1 \\ \Gamma_L \Gamma_L^* - \frac{(S_{22} - \Delta S_{11}^*) \Gamma_L + (S_{22}^* - \Delta^* S_{11}) \Gamma_L^*}{|S_{22}|^2 - |\Delta|^2} &= \frac{|S_{11}|^2 - 1}{|S_{22}|^2 - |\Delta|^2}. \end{aligned} \quad (12.23)$$

Next, complete the square by adding $|S_{22} - \Delta S_{11}^*|^2 / (|S_{22}|^2 - |\Delta|^2)^2$ to both sides:

$$\left| \Gamma_L - \frac{(S_{22} - \Delta S_{11}^*)}{|S_{22}|^2 - |\Delta|^2} \right|^2 = \frac{|S_{11}|^2 - 1}{|S_{22}|^2 - |\Delta|^2} + \frac{|S_{22} - \Delta S_{11}^*|^2}{(|S_{22}|^2 - |\Delta|^2)^2},$$

or

$$\left| \Gamma_L - \frac{(S_{22} - \Delta S_{11}^*)}{|S_{22}|^2 - |\Delta|^2} \right| = \left| \frac{S_{12} S_{21}}{|S_{22}|^2 - |\Delta|^2} \right|. \quad (12.24)$$

output stability circle with a center C_L and radius R_L , where

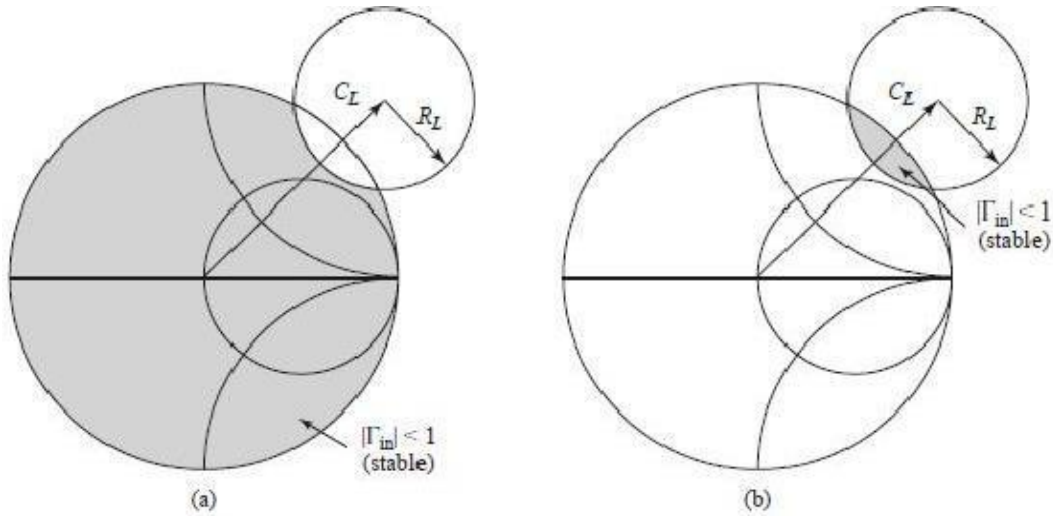
$$C_L = \frac{(S_{22} - \Delta S_{11}^*)}{|S_{22}|^2 - |\Delta|^2} \quad (\text{center}), \quad (12.25a)$$

$$R_L = \left| \frac{S_{12} S_{21}}{|S_{22}|^2 - |\Delta|^2} \right| \quad (\text{radius}). \quad (12.25b)$$

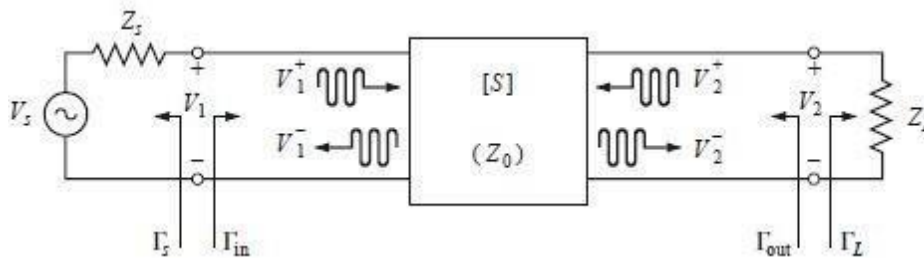
Similar results can be obtained for the input stability circle by interchanging S_{11} and S_{22} :

$$C_S = \frac{(S_{11} - \Delta S_{22}^*)}{|S_{11}|^2 - |\Delta|^2} \quad (\text{center}), \quad (12.26a)$$

$$R_S = \left| \frac{S_{12} S_{21}}{|S_{11}|^2 - |\Delta|^2} \right| \quad (\text{radius}). \quad (12.26b)$$



GAIN CONSIDERATION NOISE FIGURE



Consider an arbitrary two-port network, characterized by its scattering matrix $[S]$, connected to source and load impedances Z_S and Z_L , respectively, as shown in Figure 12.1.

We will derive expressions for three types of power gain in terms of the scattering parameters of the two-port network and the reflection coefficients, Γ_S and Γ_L , of the source and load. *Power gain* $G = P_L/P_{in}$ is the ratio of power dissipated in the load Z_L to the power delivered to the input of the two-port network.

This gain is independent of Z_S , although the characteristics of some active devices may be dependent on Z_S .

Available power gain $GA = P_{avn}/P_{avs}$ is the ratio of the power available from the two-port network to the power available from the source.

This assumes conjugate matching of both the source and the load, and depends on Z_S , but not Z_L .
Transducer power gain = $GT = PL/P_{avs}$ is the ratio of the power delivered to the load to the power available from the source. This depends on both Z_S and Z_L .

These definitions differ primarily in the way the source and load are matched to the twoport device; if the input and output are both conjugately matched to the two-port device, then the gain is maximized and $G = GA = GT$. With reference to Figure 12.1, the reflection coefficient seen looking toward the load is

$$\Gamma_L = \frac{Z_L - Z_0}{Z_L + Z_0}, \quad (12.1a)$$

while the reflection coefficient seen looking toward the source is

$$\Gamma_S = \frac{Z_S - Z_0}{Z_S + Z_0}, \quad (12.1b)$$

where Z_0 is the characteristic impedance reference for the scattering parameters of the two-port network. the following analysis. From the definition of the scattering parameters, and the fact that $V_2^- = -V_1^-$, we have

$$V_1^- = S_{11}V_1^+ + S_{12}V_2^+ = S_{11}V_1^+ + S_{12}\Gamma_L V_2^-, \quad (12.2a)$$

$$V_2^- = S_{21}V_1^+ + S_{22}V_2^+ = S_{21}V_1^+ + S_{22}\Gamma_L V_2^-. \quad (12.2b)$$

Eliminating V_2^- from (12.2a) and solving for V_1^-/V_1^+ gives

$$\Gamma_{in} = \frac{V_1^-}{V_1^+} = S_{11} + \frac{S_{12}S_{21}\Gamma_L}{1 - S_{22}\Gamma_L} = \frac{Z_{in} - Z_0}{Z_{in} + Z_0}, \quad (12.3a)$$

where Z_{in} is the impedance seen looking into port 1 of the terminated network. Similarly, the reflection coefficient seen looking into port 2 of the network when port 1 is terminated by Z_S is

$$\Gamma_{out} = \frac{V_2^-}{V_2^+} = S_{22} + \frac{S_{12}S_{21}\Gamma_S}{1 - S_{11}\Gamma_S}. \quad (12.3b)$$

By voltage division,

$$V_1 = V_S \frac{Z_{in}}{Z_S + Z_{in}} = V_1^+ + V_1^- = V_1^+ (1 + \Gamma_{in}).$$

$$Z_{in} = Z_0 \frac{1 + \Gamma_{in}}{1 - \Gamma_{in}}$$

Using

from (12.3a) and solving for V_1^+

1 in terms of V_S gives

$$V_1^+ = \frac{V_S (1 - \Gamma_S)}{2 (1 - \Gamma_S \Gamma_{in})}. \quad (12.4)$$

If peak values are assumed for all voltages, the average power delivered to the network is

$$P_{in} = \frac{1}{2Z_0} |V_1^+|^2 (1 - |\Gamma_{in}|^2) = \frac{|V_S|^2 |1 - \Gamma_S|^2}{8Z_0 |1 - \Gamma_S \Gamma_{in}|^2} (1 - |\Gamma_{in}|^2), \quad (12.5)$$

where (12.4) was used. The power delivered to the load is

$$P_L = \frac{|V_2^-|^2}{2Z_0} (1 - |\Gamma_L|^2). \quad (12.6)$$

Solving for V_2^-

2 from (12.2b), substituting into (12.6), and using (12.4) gives

$$P_L = \frac{|V_1^+|^2 |S_{21}|^2 (1 - |\Gamma_L|^2)}{2Z_0 |1 - S_{22} \Gamma_L|^2} = \frac{|V_S|^2 |S_{21}|^2 (1 - |\Gamma_L|^2) |1 - \Gamma_S|^2}{8Z_0 |1 - S_{22} \Gamma_L|^2 |1 - \Gamma_S \Gamma_{in}|^2}. \quad (12.7)$$

The power gain can then be expressed as

$$G = \frac{P_L}{P_{in}} = \frac{|S_{21}|^2 (1 - |\Gamma_L|^2)}{(1 - |\Gamma_{in}|^2) |1 - S_{22} \Gamma_L|^2}. \quad (12.8)$$

The power available from the source, P_{avs} , is the maximum power that can be delivered to the network.

This occurs when the input impedance of the terminated network is conjugately matched to the source

impedance, as discussed in Section 2.6. Thus, from (12.5),

$$P_{avs} = P_{in} \Big|_{\Gamma_{in}=\Gamma_S^*} = \frac{|V_S|^2}{8Z_0} \frac{|1 - \Gamma_S|^2}{(1 - |\Gamma_S|^2)}. \quad (12.9)$$

Similarly, the power available from the network, P_{avn} , is the maximum power that can be delivered to the load. Thus, from (12.7),

$$P_{avn} = P_L \Big|_{\Gamma_L=\Gamma_{out}^*} = \frac{|V_S|^2 |S_{21}|^2 (1 - |\Gamma_{out}|^2) |1 - \Gamma_S|^2}{8Z_0 |1 - S_{22}\Gamma_{out}^*|^2 |1 - \Gamma_S\Gamma_{in}|^2} \Big|_{\Gamma_L=\Gamma_{out}^*} \quad (12.10)$$

In (12.10), Γ_{in} must be evaluated for $\Gamma_L = \Gamma_{out}^*$. From (12.3a), it can be shown that

$$|1 - \Gamma_S\Gamma_{in}|^2 \Big|_{\Gamma_L=\Gamma_{out}^*} = \frac{|1 - S_{11}\Gamma_S|^2 (1 - |\Gamma_{out}|^2)^2}{|1 - S_{22}\Gamma_{out}^*|^2},$$

(12.10) to

which reduces (12.10) to

$$P_{avn} = \frac{|V_S|^2}{8Z_0} \frac{|S_{21}|^2 |1 - \Gamma_S|^2}{|1 - S_{11}\Gamma_S|^2 (1 - |\Gamma_{out}|^2)}. \quad (12.11)$$

Observe that P_{avs} and P_{avn} have been expressed in terms of the source voltage, V_S , which is independent of the input or load impedances. There would be confusion if these quantities were expressed in terms of V_{+1} since V_{+1} is different for each of the calculations of P_L , P_{avs} , and P_{avn} . Using (12.11) and (12.9), we obtain the available power gain as

$$G_A = \frac{P_{avn}}{P_{avs}} = \frac{|S_{21}|^2 (1 - |\Gamma_S|^2)}{|1 - S_{11}\Gamma_S|^2 (1 - |\Gamma_{out}|^2)}. \quad (12.12)$$

From (12.7) and (12.9), the transducer power gain is

$$G_T = \frac{P_L}{P_{avs}} = \frac{|S_{21}|^2 (1 - |\Gamma_S|^2) (1 - |\Gamma_L|^2)}{|1 - \Gamma_S\Gamma_{in}|^2 |1 - S_{22}\Gamma_L|^2}. \quad (12.13)$$

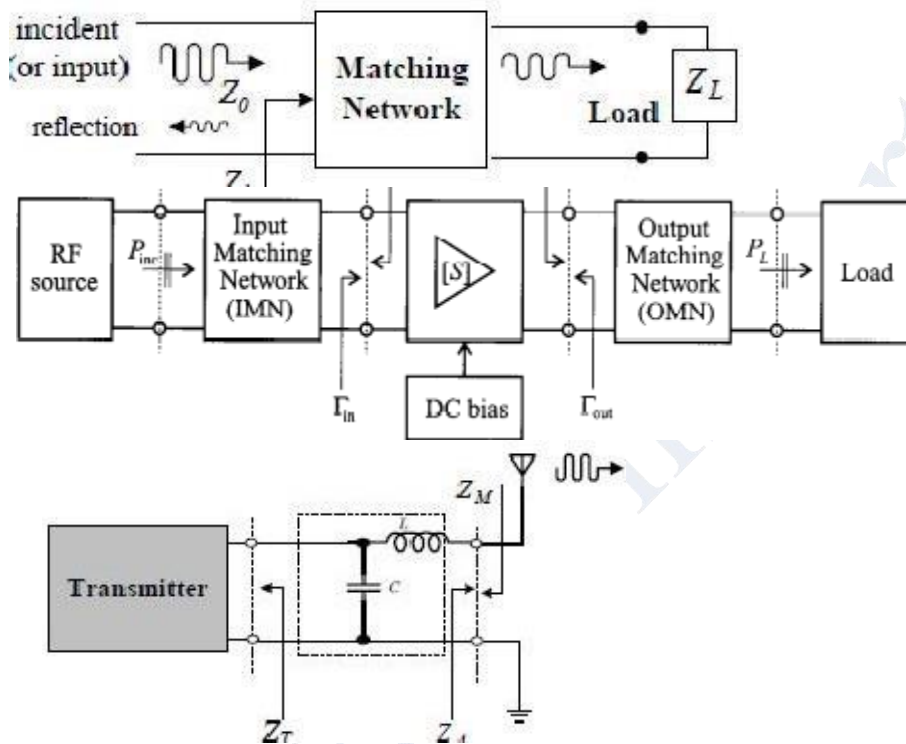
A special case of the transducer power gain occurs when both the input and output are matched for zero reflection (in contrast to conjugate matching). Then $\Gamma_L = \Gamma_S = 0$, and (12.13) reduces to

$$G_T = |S_{21}|^2. \quad (12.14)$$

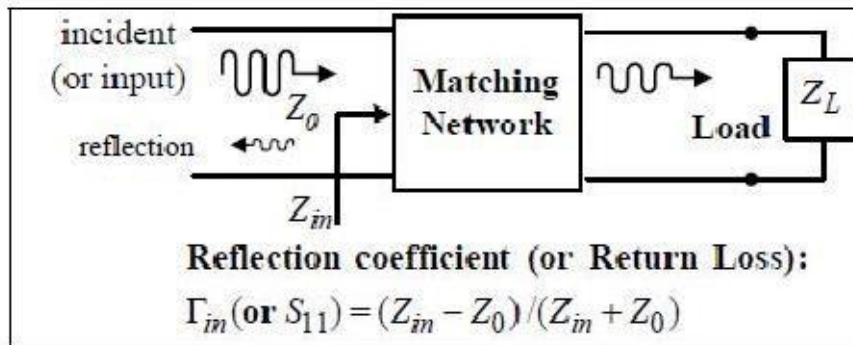
Another special case is the *unilateral transducer power gain, G_{TU}* , where $S_{12} = 0$ (or is negligibly small). This nonreciprocal characteristic is approximately true for many transistors devices. From (12.3a), $\Gamma_{in} = S_{11}$ when $S_{12} = 0$, so (12.13) gives the unilateral transducer power gain as

$$G_{TU} = \frac{|S_{21}|^2 (1 - |\Gamma_S|^2)(1 - |\Gamma_L|^2)}{|1 - S_{11}\Gamma_S|^2 |1 - S_{22}\Gamma_L|^2} \quad (12.15)$$

IMPEDANCE MATCHING NETWORKS



Impedance matching (or tuning) is important for the following reasons



- ✓ minimum power loss in the feed line & maximum power delivery
- ✓ linearizing the frequency response of the circuit
- ✓ improving the S/N ratio of the system for sensitive receiver components (*lownoise amplifier, etc.*)
- ✓ reducing amplitude & phase errors in a power distribution network (such as *antenna array-feed network*)

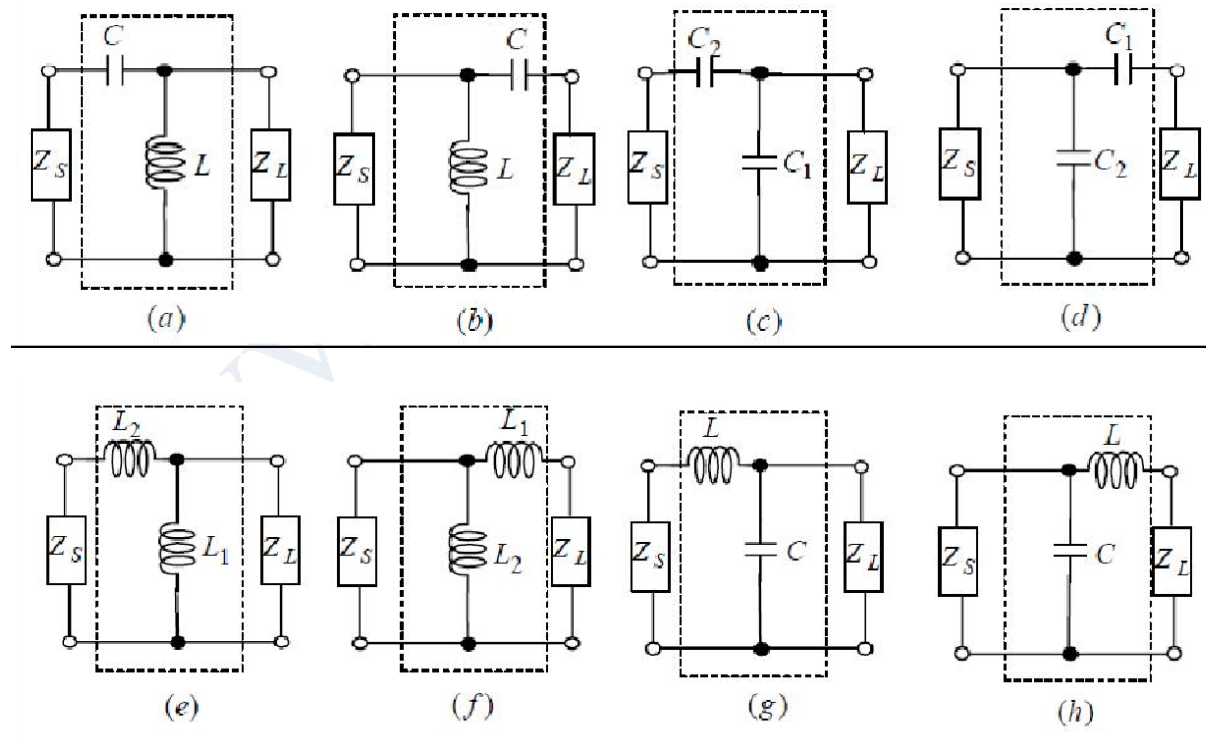
Factors in the selection of matching networks

- ✓ complexity -bandwidth requirement (such as broadband design) - *adjustability*
- ✓ implementation (by using transmission line, chip R/L/C elements ..)

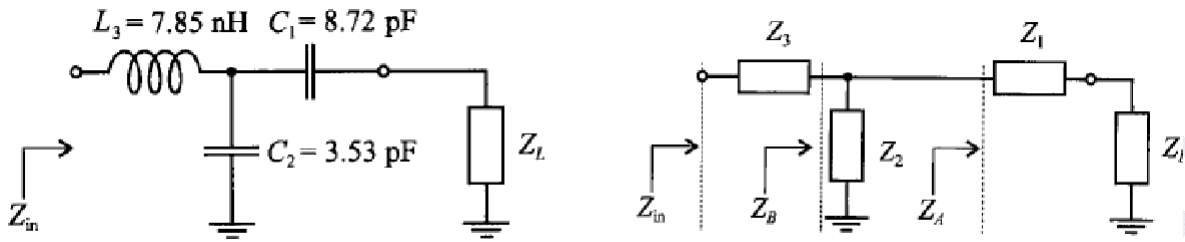
T AND PI MATCHING NETWORKS L-

section Networks (Two-component) Lumped

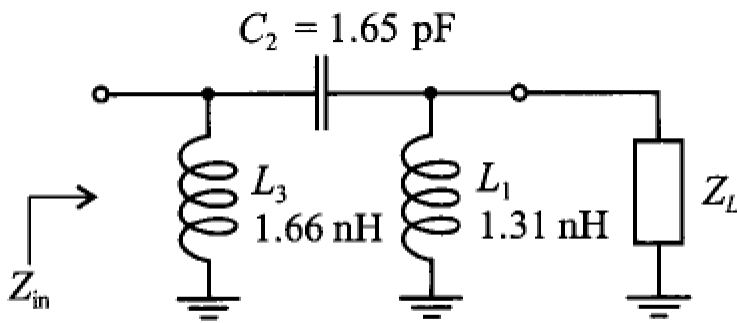
elements: R/L/C



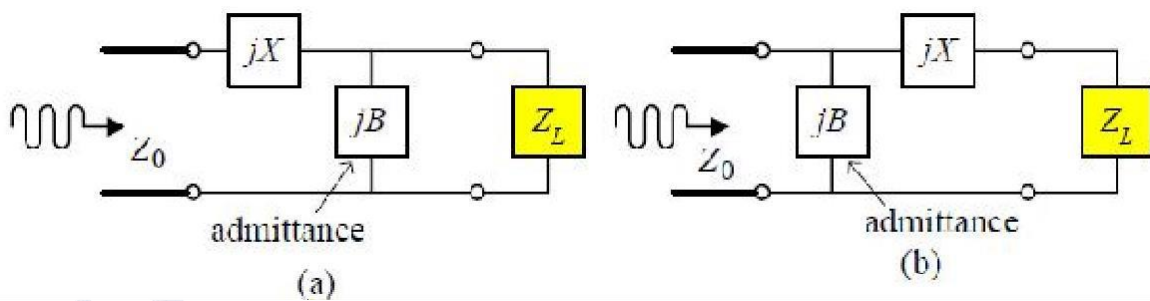
T-section Networks



π -section Networks



Matching with Lumped Elements: L-section Network



How to determine jX and jB ? Let $z_L = Z_L / Z_0 = (R_L + jX_L) / Z_0 = r + jx$

1. Analytic Solutions

2. Smith Chart Solution (p254)

(1) if $R_L > Z_0$ ($r > 1$) [z_L is **inside** the $(1 + jx)$ circle] => choose **(a)** why?

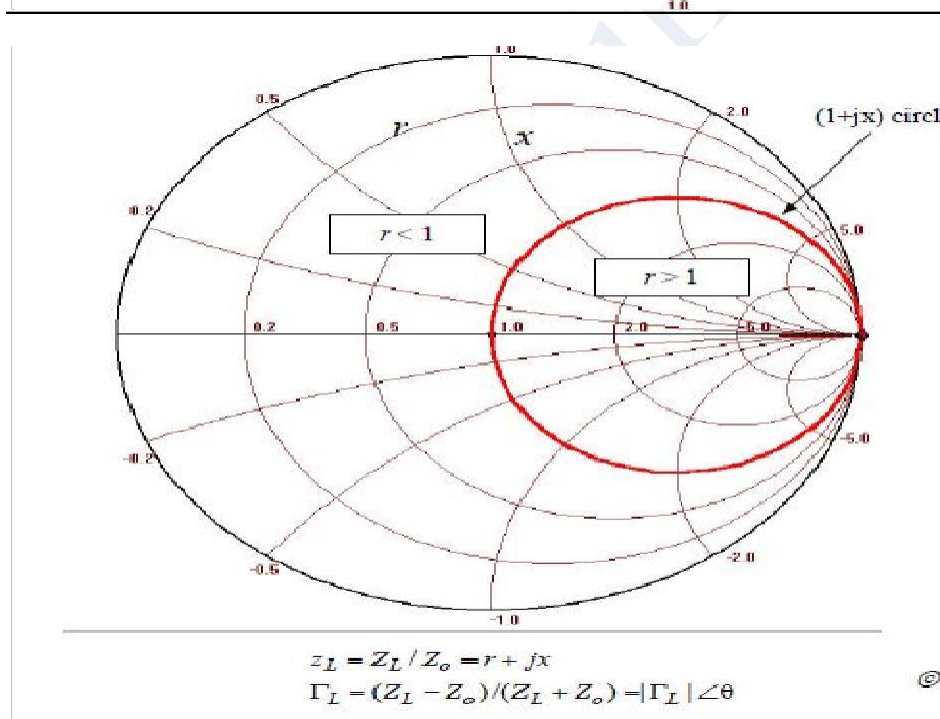
for impedance matching (to Z_0) $\rightarrow jX + \frac{1}{jB + 1/(R_L + jX_L)} = Z_0$

$$\therefore \begin{cases} B(XR_L - X_L Z_0) = R_L - Z_0 \\ X(1 - BX_L) = BZ_0 R_L - X_L \end{cases} \Rightarrow \begin{cases} B = \frac{X_L \pm \sqrt{R_L/Z_0} \sqrt{R_L^2 + X_L^2} - Z_0 R_L}{R_L^2 + X_L^2} \\ X - (1/B) + (X_L Z_0 / R_L) - (Z_0 / B R_L) \end{cases}$$

(2) if $R_L < Z_0$ ($r < 1$) [z_L is **outside** the $(1 + jx)$ circle] => choose **(b)** why?

for impedance matching (to Z_0) $\Rightarrow jB + \frac{1}{R_L + j(X + X_L)} = \frac{1}{Z_0}$

$$\therefore \begin{cases} BZ_0(X + X_L) = Z_0 - R_L \\ (X + X_L) - BZ_0 R_L \end{cases} \Rightarrow \begin{cases} X - \pm \sqrt{R_L(Z_0 - R_L)} - X_L \\ B = \pm \sqrt{(Z_0 - R_L) / R_L} / Z_0 \end{cases}$$



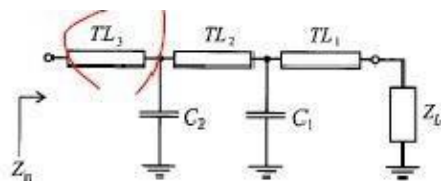
MICROSTRIP MATCHING NETWORKS

Microstrip Line Matching Networks

- ✓ In the **mid-GHz** and higher frequency range, the discrete R/L/C lumped elements will have more noticeable **parasitic effects** (see chapter 2) and let to complicating the circuit design process
- ✓ Distributed components such as **transmission line segments** can be used to mix with lumped elements

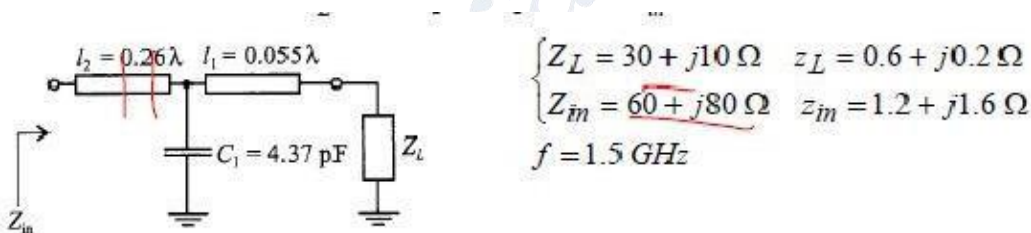
From Discrete Components to Microstrip Lines

- ✓ Avoid using **inductors** (if possible) due to higher resistive loss (& higher price)



- ✓ In general, one shunt capacitor & two series transmission lines is sufficiently to transform any load to any input impedance.

EX: transform load Z_L to an input impedance Z_{in}



○ Single-Stub Matching Networks

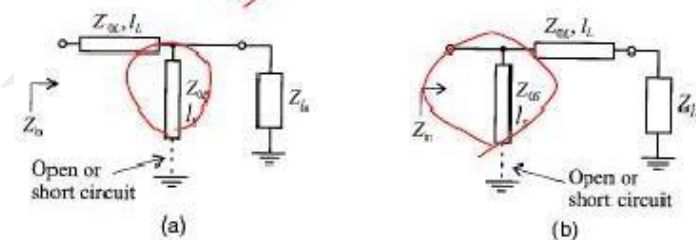


Figure 8-23 Two topologies of single-stub matching networks.

- **4 adjustable parameters:**
 $(l_s, Z_{0s}, l_L, Z_{0L})$

UNIT – 3

MICROWAVE PASSIVE COMPONENTS

:MICROWAVE FREQUENCY RANGE:

Microwaves are electromagnetic waves with wavelengths ranging from 1 mm to 1 m, or frequencies between 300 MHz and 300 GHz.

L band 1 to 2 GHz

S band 2 to 4 GHz

C band 4 to 8 GHz

X band 8 to 12 GHz

K_u band 12 to 18GHz
GHz

K band 18 to 26.5
GHz

K_a band 26.5 to 40
GHz

Q band 30 to 50
GHz

U band 40 to 60
GHz

V band 50 to 75
GHz

:SIGNIFICANCE MICROWAVE FREQUENCY RANGE:

Wireless LAN protocols, such as Bluetooth and the IEEE 802.11 specifications, also use microwaves in the 2.4 GHz ISM band, although 802.11a uses ISM band and U-NII frequencies in the 5 GHz range. Licensed long-range (up to about 25 km) Wireless Internet Access services can be found in many countries (but not the USA) in the 3.5–4.0 GHz range. Metropolitan Area Networks: MAN protocols, such as WiMAX (Worldwide Interoperability for Microwave Access) based in the IEEE 802.16 specification. The IEEE 802.16 specification was designed to operate between 2 to 11 GHz. The commercial implementations are in the 2.3GHz, 2.5 GHz, 3.5 GHz and 5.8 GHz ranges.

Wide Area Mobile Broadband Wireless Access: MBWA protocols based on standards specifications such as IEEE 802.20 or ATIS/ANSI HC-SDMA (e.g. iBurst) are designed to operate between 1.6 and 2.3 GHz to give mobility and in-building penetration characteristics similar to mobile phones but with vastly greater spectral efficiency.

Cable TV and Internet access on coaxial cable as well as broadcast television use some of the lower microwave frequencies. Some mobile phone networks, like GSM, also use the lower microwave frequencies.

:APPLICATION OF MICROWAVE:

- 1.FM Broadcasting
- 2.CDMA mobile phone
- 3.GSM Mobile phone
4. Cable television relay
- 5.Geostationary fixed satellite service
- 6.Marine airborne radar
- 7.Remote sensing radar

: SCATTERING MATRIX:

"Scattering" is an idea taken from billiards, or pool. One takes a cue ball and fires it up the table at a collection of other balls. After the impact, the energy and momentum in the cue ball is divided between all the balls involved in the impact. The cue ball "scatters" the stationary target balls and in turn is deflected or "scattered" by them.

In a microwave circuit, the equivalent to the energy and momentum of the cue ball is the amplitude and phase of the incoming wave on a transmission line. (A rather loose analogy, this). This incoming wave is "scattered" by the circuit and its energy is partitioned between all the possible outgoing waves on all the other transmission lines connected to the circuit. The scattering parameters are fixed properties of the (linear) circuit which describe how the energy couples between each pair of ports or transmission lines connected to the circuit.

Formally, s-parameters can be defined for any collection of linear electronic components, whether or not the wave view of the power flow in the circuit is necessary. They are algebraically related to the impedance parameters (z-parameters), also to the admittance parameters (y-parameters) and to a notional characteristic impedance of the transmission lines.

COCEPT OF N PORT SCATTERING MATRIX REPRESENTATION:

An n-port microwave network has n arms into which power can be fed and from which power can be taken. In general, power can get from any arm (as input) to any other arm (as output). There are thus n incoming waves and n outgoing waves.

We also observe that power can be reflected by a port, so the input power to a single port can partition between all the ports of the network to form outgoing waves. Associated with each port is the notion of a "reference plane" at which the wave amplitude and phase is defined.

Usually the reference plane associated with a certain port is at the same place with respect to incoming and outgoing waves. The n incoming wave complex amplitudes are usually designated by the n complex quantities a_n , and the n outgoing wave complex quantities are designated by the n complex quantities b_n . The incoming wave quantities are assembled into an n-vector

A and the outgoing wave quantities into an n-vector B. The outgoing waves are expressed in terms of the incoming waves by the matrix equation $B = SA$ where S is an n by n square matrix of complex numbers called the "scattering matrix". It completely determines the behaviour of the network. In general, the elements of this matrix, which are termed "s-parameters", are all frequency-dependent.

For example, the matrix equations for a 2-port are

$$b_1 = s_{11} a_1 + s_{12} a_2$$

$$b_2 = s_{21} a_1 + s_{22} a_2$$

And the matrix equations for a 3-port are

$$b_1 = s_{11} a_1 + s_{12} a_2 + s_{13} a_3$$

$$b_2 = s_{21} a_1 + s_{22} a_2 + s_{23} a_3$$

$$b_3 = s_{31} a_1 + s_{32} a_2 + s_{33} a_3$$

The wave amplitudes a_n and b_n are obtained from the port current and voltages by the relations $a = (V + Z_0 I) / (2 \sqrt{2 Z_0})$ and $b = (V - Z_0 I) / (2 \sqrt{2 Z_0})$. Here, a refers to an if V is V_n and I is I_n for the nth port. Note the $\sqrt{2}$ reduces the peak value to an rms value, and the $\sqrt{Z_0}$ makes the amplitude normalised with respect to power, so that the incoming power = $a a^*$ and the outgoing power is $b b^*$.

A one-port scattering parameter s is merely the reflection coefficient γ , and as we have seen we can relate γ to the load impedance $Z_L = Z_L / Z_0$ by the formula $\gamma = (Z_L - 1) / (Z_L + 1)$.

Similarly, given an n by n "Z-matrix" for an n-port network, we obtain the S matrix from the formula $S = (Z - I)(Z + I)^{-1}$, by post-multiplying the matrix (Z-I) by the inverse of the matrix (Z+I). Here, I is the n by n unit matrix. The matrix of z parameters (which has n squared elements) is the inverse of the matrix of y parameters.

PROPERTIES OF S MATRIX

- 1) Zero diagonal elements for perfect matched network

For an ideal network with matched termination $S_{ii}=0$, since there is no reflection from any port. Therefore under perfect matched condition the diagonal element of [s] are zero

- 2) Symmetry of [s] for a reciprocal network

The reciprocal device has a same transmission characteristics in either direction of a pair of ports and is characterized by a symmetric scattering matrix

$$S_{ij} = S_{ji} ; \quad i \neq j$$

Which results

$$[S]_t = [S]$$

For a reciprocal network with assumed normalized the impedance matrix equation is [b] = ([Z] + [u])⁻¹ ([Z] - [u]) [a]----- (1)

Where u is the unit matrix

S matrix equation of network is

$$[b] = [s] [a]----- (2)$$

Compare equ (1) & (2)

$$[s] = ([Z] + [u])^{-1} ([Z] - [u])$$

$$[R] = [Z] - [U]$$

$$[Q] = [Z] + [U]$$

For a reciprocal network Z matrix Symmetric

$$[R] [Q] = [Q] [R]$$

$$[Q]^{-1} [R] [Q] [Q]^{-1} = [Q]^{-1} [Q] [R] [Q]^{-1}$$

$$[Q]^{-1} [R] = [R] [Q]^{-1}$$

$$[Q]^{-1} [R] [S] = [R] [Q]^{-1}----- (3)$$

TRANSPOSE OS [s] IS NOW GIVEN AS

$$[S]_t = [Z-u]_t [Z+U]_t^{-1}$$

Then

$$[Z-u]_t = [Z-U]$$

$$[Z+u]_t^{-1} = [Z+U]$$

$$[S]_t = [z-u] [z+u]^{-1}$$

$$[S]_t = [R] [Q]^{-1}----- (4)$$

When compare 3 & 4

$$[S]_t = [S]$$

3) Unitary property of lossless network

For any loss less network the sum of product of each term of any one row or any one column of s matrix multiplied by its complex conjugate is unity

$$\sum_{n=1}^N S_{ni} S_{ni}^* = 1$$

For a lossless N port devices the total power leaving N ports must be equal to total input to the ports

4) Zero property

It states that the sum of the product of any each term of any one row or any one column of a s matrix is multiplied by the complex conjugate of corresponding terms of any other row is zero

$$\sum_{n=1}^N S_{ni} S_{nj}^* = 0$$

5) Phase shift propert

If any of the terminal or reference plane are mover away from the junction by anelectric distance $\beta_k l_k$. each of the coefficient S_{ij} involving K will be multiplied by the factor $(e^{-j\beta_k l_k})$

$$S = \begin{pmatrix} 0 & e^{-j\phi_{12}} \\ e^{-j\phi_{21}} & 0 \end{pmatrix}$$

S MATRIX FORMULATION OF TWO PORT JUNCTION

In the case of a microwave network having two ports only, an input and an output, the s-matrix has four s-parameters, designated s_{11} s_{12} s_{21} s_{22}

These four complex quantities actually contain eight separate numbers; the real and imaginary parts, or the modulus and the phase angle, of each of the four complex scattering parameters. Let us consider the physical meaning of these s-parameters. If the output port 2 is terminated, that is, the transmission line is connected to a matched load impedance giving rise to no reflections, then there is no input wave on port 2.

The input wave on port 1 (a_1) gives rise to a reflected wave at port 1 ($s_{11}a_1$) and a transmitted wave at port 2 which is absorbed in the termination on 2.

The transmitted wave size is ($s_{21}a_1$). If the network has no loss and no gain, the output power must equal the input power and so in this case $|s_{11}|^2 + |s_{21}|^2$ must equal unity. We see therefore that the sizes of S_{11} and S_{21} determine how the input power splits between the possible output paths.

MICROWAVE JUNCTIONS:

E PLANE TEE

H PLANE TEE

MAGIC TEE OR HYBRID TEE

: TEE JUNCTIONS:

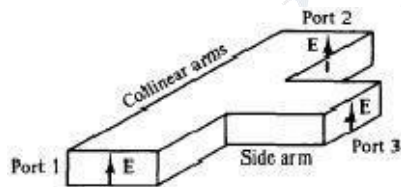
Tee junctions. In microwave circuits a waveguide or coaxial-line junction with three independent ports is commonly referred to as a *tee junction*.

From the S parameter theory of a microwave junction it is evident that a tee junction should be characterized by a matrix of third order containing nine elements, six of which should be independent.

The characteristics of a three-port junction can be explained by three theorems of the tee junction. These theorems are derived from the equivalent- circuit representation of the tee junction. Their statements follow

1. A short circuit may always be placed in one of the arms of a three-port junction in such a way that no power can be transferred through the other two arms.
2. If the junction is symmetric about one of its arms, a short circuit can always be placed in that arm so that no reflections occur in power transmission between the other two arms. (That is, the arms present matched impedances.)
3. It is impossible for a general three-port junction of arbitrary symmetry to present matched impedances at all three arms.

H-plane tee (shunt tee). An H -plane tee is a waveguide tee in which the axis of its side arm is "shunting" the E field or parallel to the H field of the main guide as shown in Fig.



It can be seen that if two input waves are fed into port 1 and port 2 of the collinear arm, the output wave at port 3 will be in phase and additive. On the other hand, if the input is fed into port 3, the wave will split equally into port 1 and port 2 in phase and in the same magnitude.

Therefore the S matrix of the H -plane tee is similar to Eqs.

$$S_{13} = S_{23}$$

$$[S] = \begin{bmatrix} S_{11} & S_{12} & S_{13} \\ S_{21} & S_{22} & S_{23} \\ S_{31} & S_{32} & S_{33} \end{bmatrix}$$

$$S_{13} = S_{23}$$

$$S_{33} = 0$$

$$S_{11} = S_{22}$$

$$S_{13} = 1/\sqrt{2}$$

$$S_{11} = 1/2$$

$$[S] = \begin{bmatrix} 1/2 & -1/2 & 1/\sqrt{2} \\ -1/2 & 1/2 & 1/\sqrt{2} \\ 1/\sqrt{2} & 1/\sqrt{2} & 0 \end{bmatrix}$$

E -plane tee (series tee). An E -plane tee is a waveguide tee in which the axis of its side arm is parallel to the E field of the main guide

If the collinear arms are symmetric about the side arm, there are two different transmission characteristics

It can be seen from Fig. 4-4-4 that if the Eplane tee is perfectly matched with the aid of screw tuners or inductive or capacitive windows at the junction, the diagonal components of the scattering matrix, S_{11} , S_{22} , and S_{33} , are zero because there will be no reflection.

When the waves are fed into the side arm (port 3), the waves appearing at port 1 and port 2 of the collinear arm will be in opposite phase and in the same magnitude. Therefore It should be noted that Eq. does not mean that S_{13} is always positive and S_{23}

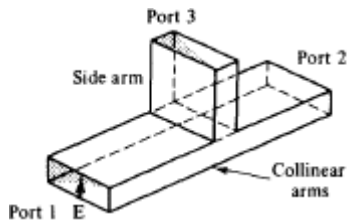


Figure 4-4-4 E-plane tee

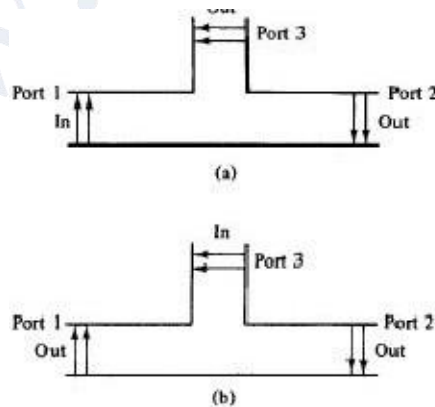


Figure 4-4-5 Two-way transmission of E-plane tee. (a) Input through main arm. (b) Input from side arm.

is always negative. The negative sign merely means that S_{13} and S_{23} have opposite signs. For a matched junction, the S matrix is given by

$$\mathbf{S} = \begin{bmatrix} 0 & S_{12} & S_{13} \\ S_{21} & 0 & S_{23} \\ S_{31} & S_{32} & 0 \end{bmatrix} \quad (4-4-13)$$

From the symmetry property of S matrix, the symmetric terms in Eq. (4-4-13) are equal and they are

$$S_{12} = S_{21} \quad S_{13} = S_{31} \quad S_{23} = S_{32} \quad (4-4-14)$$

From the zero property of S matrix, the sum of the products of each term of any column (or row) multiplied by the complex conjugate of the corresponding terms of any other column (or row) is zero and it is

$$S_{11}S_{12}^* + S_{21}S_{22}^* + S_{31}S_{32}^* = 0 \quad (4-4-15)$$

Hence

$$S_{12}S_{23}^* = 0 \quad (4-4-16)$$

This means that either S_{13} or S_{23} , or both, should be zero. However, from the unity property of S matrix, the sum of the products of each term of any one row (or column) multiplied by its complex conjugate is unity; that is,

$$S_{21}S_{21}^* + S_{31}S_{31}^* = 1 \quad (4-4-17)$$

$$S_{12}S_{12}^* + S_{32}S_{32}^* = 1 \quad (4-4-18)$$

$$S_{13}S_{13}^* + S_{23}S_{23}^* = 1 \quad (4-4-19)$$

Substitution of Eq. (4-4-14) in (4-4-17) results in

$$|S_{12}|^2 = 1 - |S_{13}|^2 = 1 - |S_{23}|^2 \quad (4-4-20)$$

zero and thus Eq. (4-4-19) is false. In a similar fashion, if $S_{23} = 0$, then S_{13} becomes zero and therefore Eq. (4-4-20) is not true.

This inconsistency proves the statement that the tee junction cannot be matched to the three arms. In other words, the diagonal elements of the S matrix of a tee junction are not all zeros.

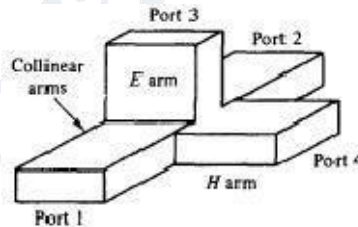
In general, when an E-plane tee is constructed of an empty waveguide, it is poorly matched at the tee junction. Hence $S_{ii} \neq 0$ if $i = j$.

However, since the collinear arm is usually symmetric about the side arm, $S_{13} = S_{23}$ and $S_{11} = S_{22}$. Then the S matrix can be simplified to

$$S = \begin{bmatrix} S_{11} & S_{12} & S_{13} \\ S_{12} & S_{11} & -S_{13} \\ S_{13} & -S_{13} & S_{13} \end{bmatrix} \quad (4-4-21)$$

MAGIC TEE:

A magic tee is a combination of the E-plane tee and H-plane tee (refer to Fig. 4-4-7). The magic tee has several characteristics:



1. If two waves of equal magnitude and the same phase are fed into port 1 and port 2, the output will be zero at port 3 and additive at port 4.
2. If a wave is fed into port 4 (the H arm), it will be divided equally between port 1 and port 2 of the collinear arms and will not appear at port 3 (the E arm).
3. If a wave is fed into port 3 (the E arm), it will produce an output of equal magnitude

and opposite phase at port 1 and port 2. The output at port 4 is zero. That is, $S_{43} = S_{34} = 0$.

4. If a wave is fed into one of the collinear arms at port 1 or port 2, it will not appear in the other collinear arm at port 2 or port 1 because the E arm causes a phase delay while the H arm causes a phase advance. That is, $S_{z1} = S_{1z} = 0$.

Therefore the S matrix of a magic tee can be expressed as

The magic tee is commonly used for mixing, duplexing, and impedance measurements. Suppose, for example, there are two identical radar transmitters in equipment stock.

A particular application requires twice more input power to an antenna than either transmitter can deliver. A magic tee may be used to couple the two transmitters to the antenna in such a way that the transmitters do not load each other.

The two transmitters should be connected to ports 3 and 4, respectively, as shown in Fig. 4-4-8. Transmitter 1, connected to port 3, causes a wave to emanate from port 1 and another to emanate from port 2; these waves are equal in magnitude but opposite in phase.

Similarly, transmitter 2, connected to port 4, gives rise to a wave at port 1 and another at port 2, both equal in magnitude and in phase.

At port 1 the two opposite waves cancel each other. At port 2 the two in-phase waves add together; so double output power at port 2 is obtained for the antenna as shown in Fig.

4-4-8.

$$[S] = \begin{bmatrix} S_{11} & S_{12} & S_{13} & S_{14} \\ S_{21} & S_{22} & S_{23} & S_{24} \\ S_{31} & S_{32} & S_{33} & S_{34} \\ S_{41} & S_{42} & S_{43} & S_{44} \end{bmatrix}$$

But $S_{21} = 0, S_{12} = 0, S_{43} = 0, S_{34} = 0$

$S_{11} = 0, S_{22} = 0, S_{33} = 0, S_{44} = 0$

and $S_{14} = S_{24}, S_{13} = -S_{23}$

For port-3 and port-4 matched

∴ S-matrix becomes

$$[S] = \begin{bmatrix} 0 & 0 & S_{13} & S_{14} \\ 0 & 0 & -S_{13} & S_{14} \\ S_{31} & S_{32} & 0 & 0 \\ S_{41} & S_{42} & 0 & 0 \end{bmatrix}$$

$$= \begin{bmatrix} 0 & 0 & S_{13} & S_{13} \\ 0 & 0 & -S_{13} & S_{13} \\ S_{13} & -S_{13} & 0 & 0 \\ S_{13} & S_{13} & 0 & 0 \end{bmatrix} = \frac{1}{\sqrt{2}} \begin{bmatrix} 0 & 0 & 1 & 1 \\ 0 & 0 & -1 & 1 \\ 1 & -1 & 0 & 0 \\ 1 & 1 & 0 & 0 \end{bmatrix}$$

:RATE RACE –CORNERS

Applications of rat-race couplers are numerous, and include mixers and phase shifters. The rat-race gets its name from its circular shape, shown below. The circumference is 1.5 wavelengths. For an equal-split rat-race coupler, the impedance of the entire ring is fixed at $1.41 \times Z_0$, or 70.7 ohms for a 50 ohm system. For an input signal V_{in} , the outputs at ports 2 and 4 (thanks, Tom!) are equal in magnitude, but 180 degrees out of phase.

The coupling of the two arms is shown in the figure below, for an ideal rat-race coupler centered at 10 GHz (10,000 MHz). An equal power split of 3 dB occurs at only the center frequency. The 1-dB bandwidth of the coupled port (S_{41}) is shown by the markers to be 3760 MHz, or 37.6 percent.

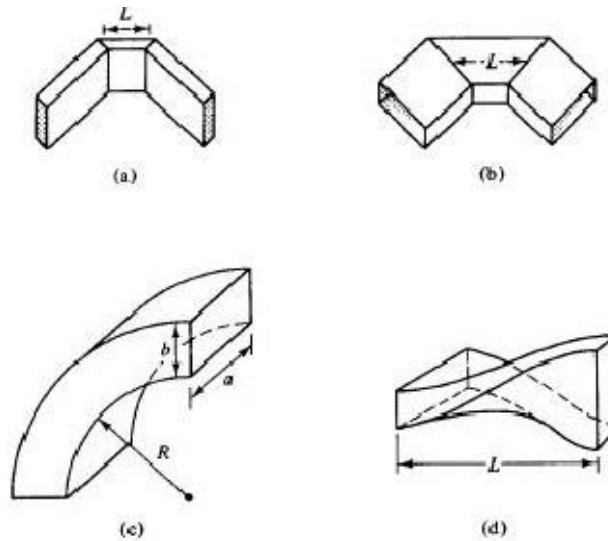
:BENTS &TWISTS:

The waveguide corner, bend, and twist are shown in Fig. 4-4-10. These waveguide components are normally used to change the direction of the guide through an arbitrary angle. In order to minimize reflections from the discontinuities, it is desirable to have the mean length L between continuities equal to an odd number of quarter-wavelengths. That is,

where $n = 0, 1, 2, 3, \dots$, and λ_g is the wavelength in the waveguide. If the mean length L is an odd number of quarter wavelengths, the reflected waves from both ends of the waveguide section are completely canceled. For the waveguide bend, the minimum radius of curvature for a small reflection is given by Southworth [2] as

$$R = 1.5b \text{ for an } E \text{ bend}$$

$$R = 1.5a \text{ for an } H \text{ bend}$$



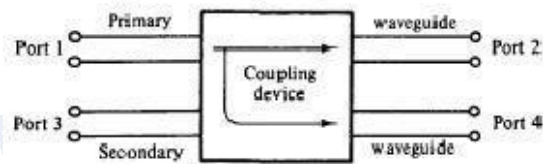
: DIRECTIONAL COUPLERS:

A *directional coupler* is a four-port waveguide junction as shown in Fig. 4-5-1. It consists of a primary waveguide 1-2 and a secondary waveguide 3-4.

When all ports are terminated in their characteristic impedances, there is free transmission of power, without reflection, between port 1 and port 2, and there is no transmission of power between port 1 and port 3 or between port 2 and port 4 because no coupling exists between these two pairs of ports.

The degree of coupling between port 1 and port 4 and between port 2 and port 3 depends on the structure of the coupler. The characteristics of a directional coupler can be expressed in terms of its coupling factor and its directivity.

Assuming that the wave is propagating from port 1 to port 2 in the primary line, the coupling factor and the directivity are defined,



respectively, by

$$\text{Coupling factor (dB)} = 10 \log_{10} \frac{P_1}{P_4}$$

$$\text{Directivity (dB)} = 10 \log_{10} \frac{P_4}{P_3}$$

where P_1 = power input to port 1
 P_3 = power output from port 3
 P_4 = power output from port 4

It should be noted that port 2, port 3, and port 4 are terminated in their characteristic impedances. *The coupling factor is a measure of the ratio of power levels in the primary and secondary lines.* Hence if the coupling factor is known, a fraction of power measured at port 4 may be used to determine the power input at port

1. This significance is desirable for microwave power measurements because no disturbance, which may be caused by the power measurements, occurs in the primary line.
2. The directivity is a measure of how well the forward traveling wave in the primary waveguide couples only to a specific port of the secondary waveguide. An ideal directional coupler should have infinite directivity. In other words, the power at port 3 must be zero because port 2 and port 4 are perfectly matched.
3. Actually, well-designed directional couplers have a directivity of only 30 to 35 dB. Several types of directional couplers exist, such as a two-hole directional coupler, four-hole directional coupler, reverse-coupling directional coupler (Schwinger coupler), and Bethe-hole directional coupler (refer to Fig. 4-5-2). Only the very commonly used two-hole directional coupler is described here.

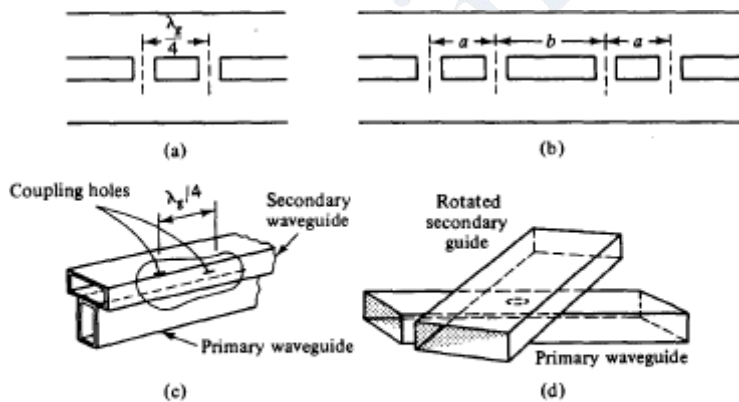


Figure 4-5-2 Different directional couplers. (a) Two-hole directional coupler. (b) Four-hole directional coupler. (c) Schwinger coupler. (d) Bethe-hole directional coupler.

$$S_{11} = S_{22} = S_{33} = S_{44} = 0$$

As noted, there is no coupling between port 1 and port 3 and between port 2 and port 4. Thus

$$S_{13} = S_{31} = S_{24} = S_{42} = 0$$

Consequently, the S matrix of a directional coupler becomes

$$\mathbf{S} = \begin{bmatrix} 0 & S_{12} & 0 & S_{14} \\ S_{21} & 0 & S_{23} & 0 \\ 0 & S_{32} & 0 & S_{34} \\ S_{41} & 0 & S_{43} & 0 \end{bmatrix}$$

Equation (4-5-6) can be further reduced by means of the zero property of the S matrix, so we have

$$S_{12}S_{14}^* + S_{32}S_{34}^* = 0$$

$$S_{21}S_{23}^* + S_{41}S_{43}^* = 0$$

Also from the unity property of the S matrix, we can write

$$S_{12}S_{12}^* + S_{14}S_{14}^* = 1$$

Equations (4-5-7) and (4-5-8) can also be written

$$|S_{12}| |S_{14}| = |S_{32}| |S_{34}|$$

$$|S_{21}| |S_{23}| = |S_{41}| |S_{43}|$$

Since $S_{12} = S_{21}$, $S_{14} = S_{41}$, $S_{23} = S_{32}$, and $S_{34} = S_{43}$, then

$$|S_{12}| = |S_{34}|$$

$$|S_{14}| = |S_{23}|$$

Let

$$S_{12} = S_{34} = p$$

where p is positive and real. Then from Eq. (4-5-8)

$$p(S_{23}^* + S_{43}) = 0$$

Let

$$S_{23} = S_{41} = jq$$

where q is positive and real. Then from Eq. (4-5-9)

$$p^2 + q^2 = 1$$

The S matrix of a directional coupler is reduced to

$$S = \begin{bmatrix} 0 & p & 0 & jq \\ p & 0 & jq & 0 \\ 0 & jq & 0 & p \\ jq & 0 & p & 0 \end{bmatrix}$$

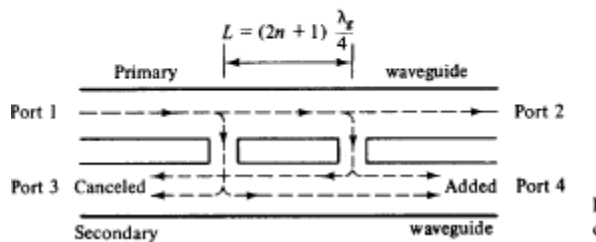
: TWO HOLE DIRECTIONAL COUPLERS:

Two-Hole Directional Couplers

A two-hole directional coupler with traveling waves propagating in it is illustrated in Fig. 4-5-3. The spacing between the centers of two holes must be

$$L = (2n + 1) \frac{\lambda_g}{4}$$

where n is any positive integer.



A fraction of the wave energy entered into port 1 passes through the holes and is radiated into the secondary guide as the holes act as slot antennas.

The forward waves in the secondary guide are in the same phase, regardless of the hole space, and are added at port 4.

The backward waves in the secondary guide (waves are progressing from right to left) are out of phase by $(2L/\lambda_g)2\pi$ rad and are canceled at port 3.

In a directional coupler all four ports are completely matched. Thus the diagonal elements of the S matrix are zeros

:FERRITES:

An *isolator* is a nonreciprocal transmission device that is used to isolate one component from reflections of other components in the transmission line. An ideal isolator completely absorbs the power for propagation in one direction and provides lossless transmission in the opposite direction.

Thus the isolator is usually called *uniline*. Isolators are generally used to improve the frequency stability of microwave generators, such as klystrons and magnetrons, in which the reflection from the load affects the generating frequency.

In such cases, the isolator placed between the generator and load prevents the reflected power from the unmatched load from returning to the generator. As a result, the isolator maintains the frequency stability of the generator. Isolators can be constructed in many ways.

They can be made by terminating ports 3 and 4 of a four-port circulator with matched loads. On the other hand, isolators can be made by inserting a ferrite rod along the axis of a rectangular waveguide as shown in Fig. 4-6-5. The isolator here is a Faraday-rotation isolator. Its operating principle can be explained as follows [5]. The input resistive card is in the y - z plane, and the output resistive card is displaced 45° with respect to the input card.

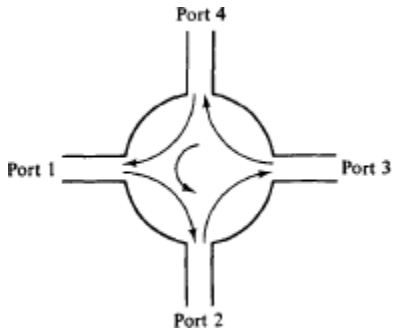
The de magnetic field, which is applied longitudinally to the ferrite rod, rotates the wave plane of polarization by 45° . The degrees of rotation depend on the length and diameter of the rod and on the applied de magnetic field. An input TE₁₀ dominant mode is incident to the left end of the isolator. Since the TE₁₀ mode wave is perpendicular to the input resistive card, the wave passes through the ferrite rod without attenuation.

The wave in the ferrite rod section is rotated clockwise by 45° and is normal to the output resistive card. As a result of rotation, the wave arrives at the output

:TERMINATION:

A *microwave circulator* is a multiport waveguide junction in which the wave can flow only from the n th port to the $(n + 1)$ th port in one direction

Although there is no restriction on the number of ports, the four-port microwave circulator is the most common. One type of four-port microwave circulator is a combination of two 3-dB side-hole directional couplers and a rectangular waveguide with two nonreciprocal phase shifters as shown in Fig



The operating principle of a typical microwave circulator can be analyzed with the aid of Fig. Each of the two 3-dB couplers in the circulator introduces a phase shift of 90° , and each of the two phase shifters produces a certain amount of phase change in a certain direction as indicated.

When a wave is incident to port 1, the wave is split into two components by coupler 1. The wave in the primary guide arrives at port 2 with a relative phase change of 180° . The second wave propagates through the two couplers and the secondary guide and arrives at port 2 with a relative phase shift of 180° . Since the two waves reaching port 2 are in phase, the power transmission is obtained from port 1 to port 2.

However, the wave propagates through the primary guide, phase shifter, and coupler 2 and arrives at port 4 with a phase change of 270° . The wave travels through coupler 1 and the secondary guide, and it arrives at port 4 with a phase shift of 90° . Since the two waves reaching port 4 are out of phase by 180° , the power transmission from port 1 to port 4 is zero. In general, the differential propagation constants in the two directions of propagation in a waveguide containing ferrite phase shifters should be

$$\omega_1 - \omega_3 = (2m + 1)\pi \quad \text{rad/s}$$

$$\omega_2 - \omega_4 = 2n\pi \quad \text{rad/s}$$

:GYRATOR:

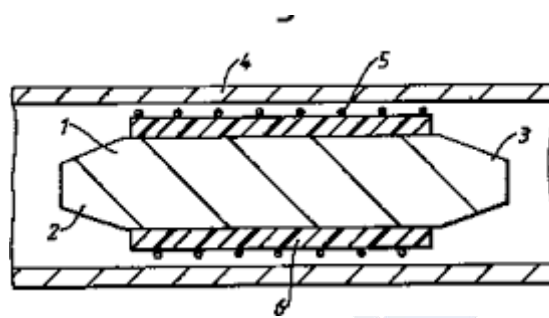
A **gyrator** is a passive, linear, lossless, two-port electrical network element proposed in 1948 by Bernard D. H. Tellegen as a hypothetical fifth linear element after the resistor, capacitor, inductor and ideal transformer. Unlike the four conventional elements, the gyrator is non-reciprocal. Gyrators permit network realizations of two-(or-more)-port devices which cannot be realized with just the conventional four elements.

In particular, gyrators make possible network realizations of isolators and circulators. Gyrators do not however change the range of one-port devices that can be realized. Although the gyrator was conceived as a fifth linear element, its adoption makes both the ideal transformer and either the capacitor or inductor

redundant. Thus the number of necessary linear elements is in fact reduced to three. Circuits that function as gyrators can be built with transistors and op amps using feedback.

Wyller invented a circuit symbol for the gyrator and suggested a number of ways in which a practical gyrator might be built.

An important property of a gyrator is that it inverts the current-voltage characteristic of an electrical component or network. In the case of linear elements, the impedance is also inverted. In other words, a gyrator can make a capacitive circuit behave inductively, a series LC circuit behave like a parallel LC circuit, and so on. It is primarily used in active filter design and miniaturization.



: ISOLATOR CIRCULATOR:

An *isolator* is a nonreciprocal transmission device that is used to isolate one component from reflections of other components in the transmission line. An ideal isolator completely absorbs the power for propagation in one direction and provides lossless transmission in the opposite direction. Thus the isolator is usually called *uniline*.

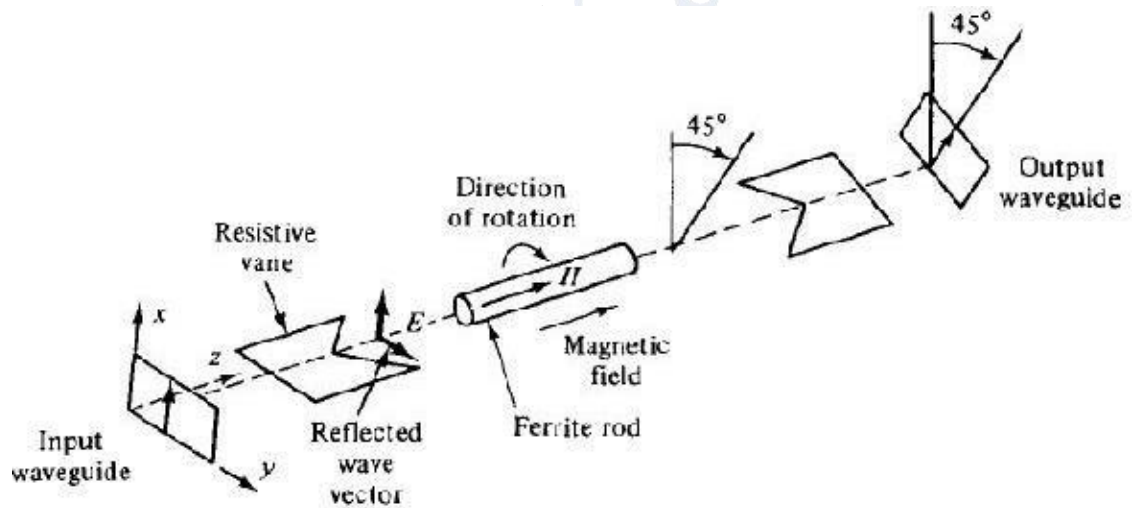
Isolators are generally used to improve the frequency stability of microwave generators, such as klystrons and magnetrons, in which the reflection from the load affects the generating frequency. In such cases, the isolator placed between the generator and load prevents the reflected power from the unmatched load from returning to the generator.

As a result, the isolator maintains the frequency stability of the generator. Isolators can be constructed in many ways. They can be made by terminating ports 3 and 4 of a four-port circulator with matched loads. On the other hand, isolators can be made by inserting a ferrite rod along the axis of a rectangular waveguide as shown in Fig. 4-6-5.

The isolator here is a Faraday-rotation isolator. Its operating principle can be explained as follows [5]. The input resistive card is in the y - z plane, and the output resistive card is displaced 45° with respect to the input card. The de magnetic field, which is applied longitudinally to the ferrite rod, rotates the wave plane of polarization by 45° . The degrees of rotation depend on the length and diameter of the rod and on the applied de magnetic field. An input TE₁₀ dominant mode is incident to the left end of the isolator. Since the TE₁₀ mode wave is perpendicular to the input resistive card, the wave passes through the ferrite rod without attenuation.

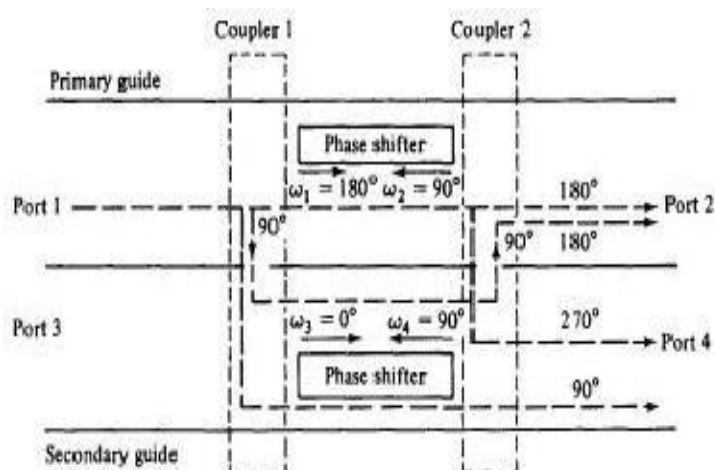
The wave in the ferrite rod section is rotated clockwise by 45° and is normal to the output resistive card. As a result of rotation, the wave arrives at the output end without attenuation at all. On the contrary, a reflected wave from the output end is similarly rotated clockwise 45° by the ferrite rod.

However, since the reflected wave is parallel to the input resistive card, the wave is thereby absorbed by the input card. The typical performance of these isolators is about 1-dB insertion loss in forward transmission and about 20- to 30-dB isolation in reverse attenuation



:ATTENUATOR:

A *microwave circulator* is a multiport waveguide junction in which the wave can flow only from the n th port to the $(n + 1)$ th port in one direction (see Fig. 4-6-2). Although there is no restriction on the number of ports, the four-port microwave circulator is the most common. One type of four-port microwave circulator is a combination of two 3-dB side-hole directional couplers and a rectangular waveguide with two nonreciprocal phase shifters as shown in Fig. 4-6-3.



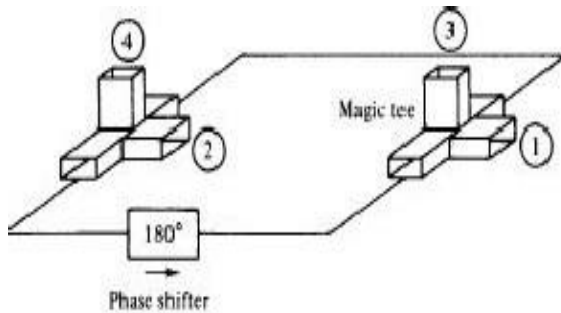
The operating principle of a typical microwave circulator can be analyzed with the aid of Fig. 4-6-3. Each of the two 3-dB couplers in the circulator introduces a phase shift of 90° , and each of the two phase shifters produces a certain amount of phase change in a certain direction as indicated.

When a wave is incident to port 1, the wave is split into two components by coupler 1. The wave in the primary guide arrives at port 2 with a relative phase change of 180° . The second wave propagates through the two couplers and the secondary guide and arrives at port 2 with a relative phase shift of 180° .

Since the two waves reaching port 2 are in phase, the power transmission is obtained from port 1 to port 2. However, the wave propagates through the primary guide, phase shifter, and coupler 2 and arrives at port 4 with a phase change of 270° . The wave travels through coupler 1 and the secondary guide, and it arrives at port 4 with a phase shift of 90° . Since the two waves reaching port 4 are out of phase by 180° , the power transmission from port 1 to port 4 is zero.

In general, the differential propagation constants in the two directions of propagation in a waveguide containing ferrite phase shifters should be where m and n are any integers, including zeros. A similar analysis shows that a wave incident to port 2 emerges at port 3 and so on. As a result, the sequence of power flow is designated as $1 \sim 2 \sim 3 \sim 4 \sim 1$. Many types of microwave circulators are in use today.

However, their principles of operation remain the same. Figure 4-6-4 shows a four-port circulator constructed of two magic tees and a phase shifter. The phase shifter produces a phase shift of 180°. The explanation of how this circulator works is left as an exercise for the reader.



$$S = \begin{bmatrix} 0 & S_{12} & S_{13} & S_{14} \\ S_{21} & 0 & S_{23} & S_{24} \\ S_{31} & S_{32} & 0 & S_{34} \\ S_{41} & S_{42} & S_{43} & 0 \end{bmatrix}$$

$$S = \begin{bmatrix} 0 & 0 & 0 & 1 \\ 1 & 0 & 0 & 0 \\ 0 & 1 & 0 & 0 \\ 0 & 0 & 1 & 0 \end{bmatrix}$$

PHASE CHANGER:

:S MARIX FOR MICROWAVE COMPONENTS:

H palne tee:

$$[S] = \begin{bmatrix} 1/2 & -1/2 & 1/\sqrt{2} \\ -1/2 & 1/2 & 1/\sqrt{2} \\ 1/\sqrt{2} & 1/\sqrt{2} & 0 \end{bmatrix}$$

Circulator:

$$S = \begin{bmatrix} 0 & 0 & 0 & 1 \\ 1 & 0 & 0 & 0 \\ 0 & 1 & 0 & 0 \\ 0 & 0 & 1 & 0 \end{bmatrix}$$

Directional coupler:

$$\mathbf{S} = \begin{bmatrix} 0 & p & 0 & jq \\ p & 0 & jq & 0 \\ 0 & jq & 0 & p \\ jq & 0 & p & 0 \end{bmatrix}$$

E palne Tee

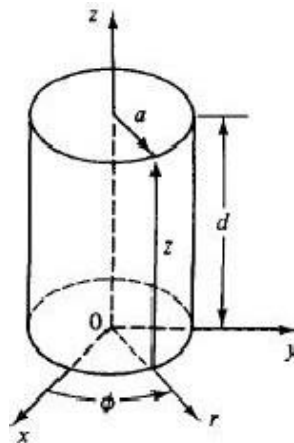
$$\mathbf{S} = \begin{bmatrix} S_{11} & S_{12} & S_{13} \\ S_{12} & S_{11} & -S_{13} \\ S_{13} & -S_{13} & S_{33} \end{bmatrix} \quad (4-4-21)$$

:CYLINDRICAL CAVITY RESONATORS:

In general, a cavity resonator is a metallic enclosure that confines the electromagnetic energy. The stored electric and magnetic energies inside the cavity determine its equivalent inductance and capacitance. The energy dissipated by the finite conductivity of the cavity walls determines its equivalent resistance.

In practice, the rectangular-cavity resonator, circular-cavity resonator, and reentrant-cavity resonator are commonly used in many microwave applications. Theoretically a given resonator has an infinite number of resonant modes, and each mode corresponds to a definite resonant frequency.

When the frequency of an impressed signal is equal to a resonant frequency, a maximum amplitude of the standing wave occurs, and the peak energies stored in the electric and magnetic fields are equal. The mode having the lowest resonant frequency is known as the *dominant mode*.



Circular-cavity resonator. A circular-cavity resonator is a circular waveguide with two ends closed by a metal wall (see Fig. 4-3-3). The wave function in the circular resonator should satisfy Maxwell's equations, subject to the same boundary conditions described for a rectangular-cavity resonator. It is merely necessary to choose the harmonic functions in z to satisfy the boundary conditions at the remaining two end walls. These can be achieved if

$$H_z = H_{0z} J_n \left(\frac{X'_{np} r}{a} \right) \cos (n\phi) \sin \left(\frac{q\pi z}{d} \right) \quad (\text{TE}_{npq})$$

where $n = 0, 1, 2, 3, \dots$ is the number of the periodicity in the ϕ direction

$p = 1, 2, 3, 4, \dots$ is the number of zeros of the field in the radial direction

$q = 1, 2, 3, 4, \dots$ is the number of half-waves in the axial direction

J_n = Bessell's function of the first kind

H_{0z} = amplitude of the magnetic field

$$E_z = E_{0z} J_n \left(\frac{X_{np} r}{a} \right) \cos (n\phi) \cos \left(\frac{q\pi z}{d} \right) \quad (\text{TM}_{npq})$$

UNIT -4

MICROWAVE SEMICONDUCTOR DEVICES

MICROWAVE SEMICONDUCTOR

DEVICES OPERATION

Microwave solid-state devices are becoming increasingly important at microwave frequencies. These devices can be broken down into four groups. In the first group are the microwave bipolar junction transistor (BJT), the heterojunction bipolar transistor (HBT), and the tunnel diodes.

This group is discussed in this chapter. The second group includes microwave field-effect transistors (FETs) such as the junction field-effect transistors (JFETs), metal-semiconductor field-effect transistors (MESFETs), high electron mobility transistors (HEMTs), metal-oxide-semiconductor field-effect transistors (MOSFETs), the metal-oxide-semiconductor transistors and memory devices, and the charge-coupled devices (CCDs).

This group is described in The third group, which is characterized by the bulk effect of the semiconductor, is called the transferred electron device (TED). These devices include the Gunn diode, limited space-charge-accumulation diode (LSA diode), indium phosphide diode (InP diode), and cadmium telluride diode (CdTe diode).

This group is analyzed in Chapter 7. The devices of the fourth group, which are operated by the avalanche effect of the semiconductor, are referred to as avalanche diodes: the impact ionization avalanche transit-time diodes (IMPATT diodes), the trapped plasma avalanche triggered transit-time diodes (TRAPATT diodes), and the barrier injected transit-time diodes (BARITT diodes).

The avalanche diodes are studied in . All those microwave solid-state devices are tabulated in Table 5-0-1. In studying microwave solid-state devices, the electrical behavior of solids is the first item to be investigated. In this section it will be seen that the transport of charge through a semiconductor depends not only on the properties of the electron but also on the arrangement of atoms in the solids.

Semiconductors are a group of substances having electrical conductivities that are intermediate between metals and insulators. Since the conductivity of the semiconductors can be varied over wide ranges by changes in their temperature, optical excitation, and impurity content, they are the natural choices for

electronic devices. The properties of important semiconductors are tabulated in Table 5-0-2. The energy bands of a semiconductor play a major role in their electrical behavior. For any semiconductor, there is a forbidden energy region in which no allowable states can exist.

The energy band above the forbidden region is called the *conduction band*, and the bottom of the conduction band is designated by E_c . The energy band below the forbidden region is called the *valence band*, and the top of the valence band is designated by E_v . The separation between the energy of the lowest conduction band and that of the highest valence band is called the *bandgap energy E_g* , which is the most important parameter in semiconductors.

APPLICATION OF BJTS & FETS

TABLE 5-0-3 APPLICATIONS OF MICROWAVE SOLID-STATE DEVICES

Devices	Applications	Advantages
Transistor	L-band transmitters for telemetry systems and phased array radar systems L- and S-band transmitters for communications systems	Low cost, low power supply, reliable, high CW power output, light weight
TED	C-, X-, and Ku-band ECM amplifiers for wideband systems X- and Ku-band transmitters for radar systems, such as traffic control	Low power supply (12 V), low cost, light weight, reliable, low noise, high gain
IMPATT	Transmitters for millimeter-wave communications systems	Low power supply, low cost, reliable, high CW power output, light weight
TRAPATT	S-band pulsed transmitters for phased array radar systems	High peak and average power, reliable, low power supply, low cost
BARITT	Local oscillators in communications and radar receivers	Low cost, low power supply, reliable, low noise

PRICIPLE OF TUNNEL DIODE

MICROWAVE TUNNEL DIODES

Tunnel diodes are heavily doped PN junction diode that have a negative resistance over a portion of its V-I characteristics

Principles of Operation

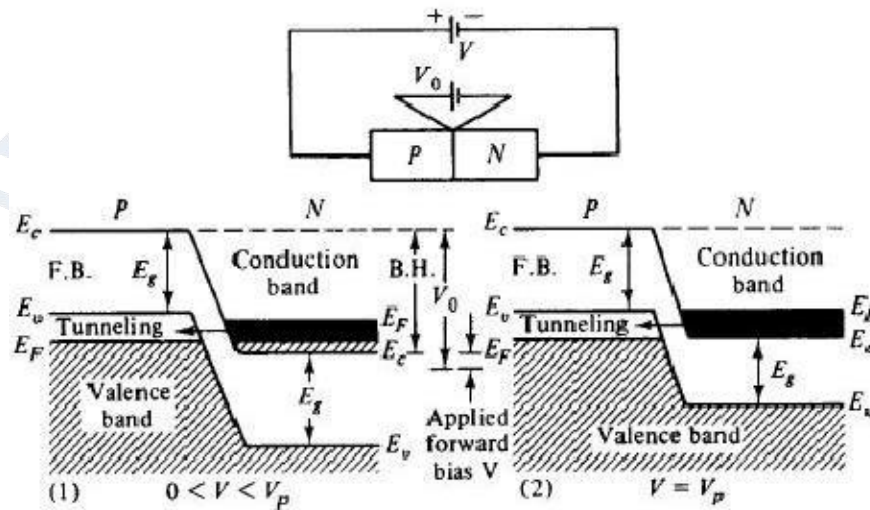
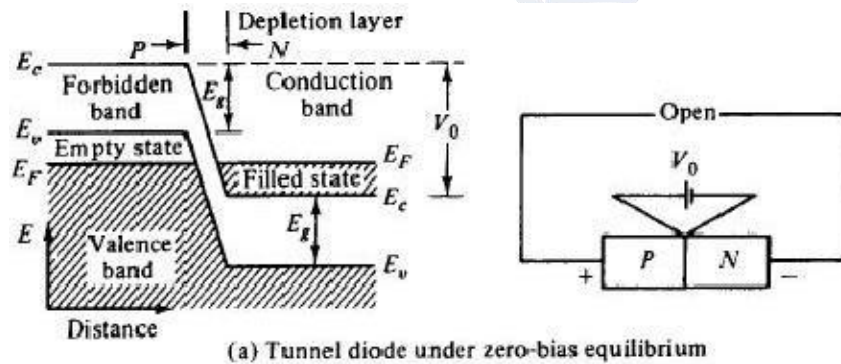
The tunnel diode is a negative-resistance semiconductor *p-n* junction diode. The negative resistance is created by the tunnel effect of electrons in the *p-n* junction.

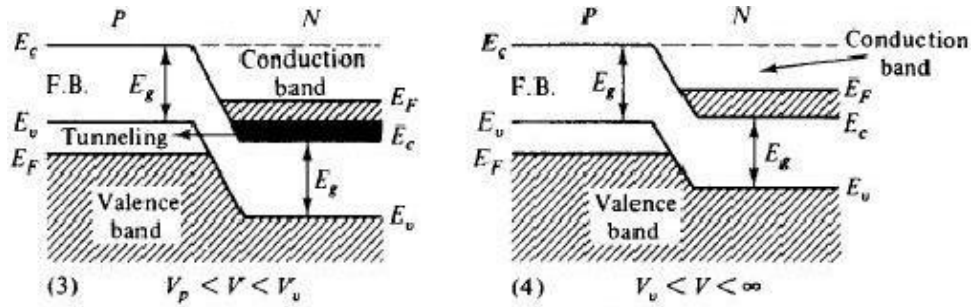
The doping of both the p and n regions of the tunnel diode is very high-impurity concentrations of 10^{19} to 10^{20} atoms/cm³ are used-and the depletion-layer barrier at the junction is very thin, on the order of 100 \AA or 10^{-6} cm. Classically, it is possible for those particles to pass over the barrier if and only if they have an energy equal to or greater than the height of the potential barrier.

Quantum mechanically, however, if the barrier is less than 3 \AA there is an appreciable probability that particles will tunnel through the potential barrier even though they do not have enough kinetic energy to pass over the same barrier.

In addition to the barrier thinness, there must also be filled energy states on the side from which particles will tunnel and allowed empty states on the other side into which particles penetrate through at the same energy level.

In order to understand the tunnel effects fully, let us analyze the energy-band pictures of a heavily doped p - n diode.





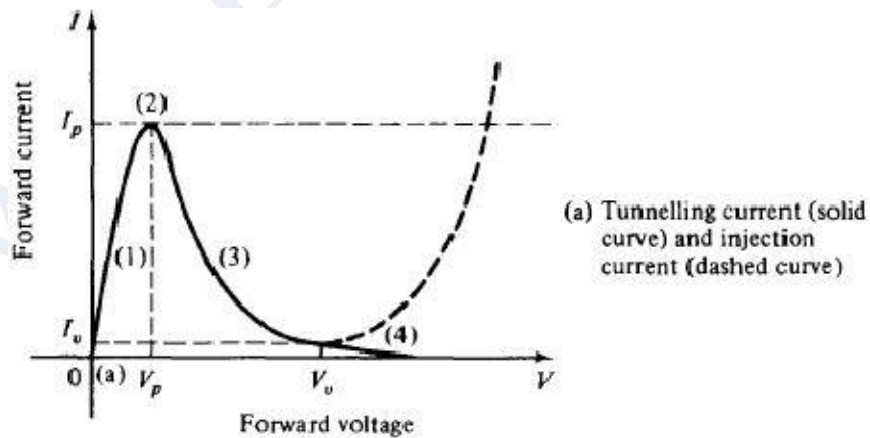
(b) Tunnel diode with applied forward bias

E_F is the Fermi level representing the energy state with 50% probability of being filled if no forbidden band exists
 V_0 is the potential barrier of the junction
 E_g is the energy required to break a covalent bond, which is 0.72 eV for germanium and 1.10 eV for silicon
 E_c is the lowest energy in the conduction band
 E_v is the maximum energy in the valence band
 V is the applied forward bias
 F.B. stands for the forbidden band
 B.H. represents the barrier height

Figure 5-3-1 Energy-band diagrams of tunnel diode.

Under open-circuit conditions or at zero-bias equilibrium, the upper levels of electron energy of both the p type and n type are lined up at the same Fermi level as shown in Fig. 5-3-1(a).

Since there are no filled states on one side of the junction that are at the same energy level as empty allowed states on the other side, there is no flow of charge in either direction across the junction and the current is zero, as shown at point (a) of the volt-ampere characteristic curve of a tunnel diode in Fig.



(a) Tunnelling current (solid curve) and injection current (dashed curve)

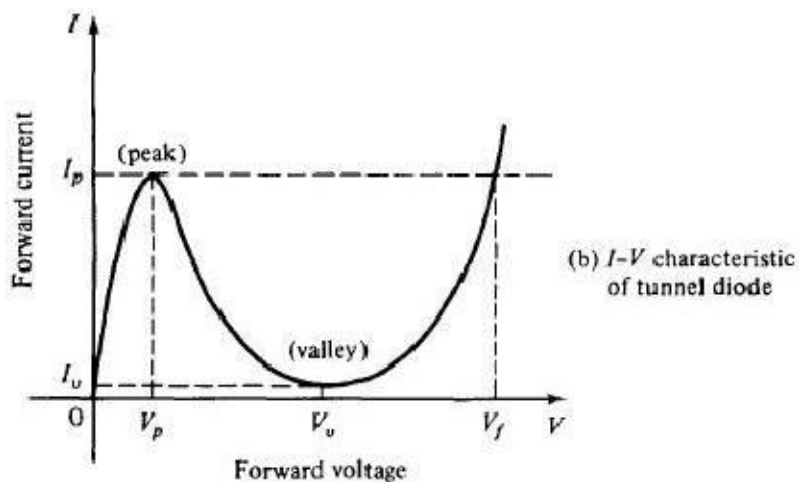


Figure 5-3-2 Ampere-voltage characteristics of tunnel diode.

In ordinary diodes the Fermi level exists in the forbidden band. Since the tunnel diode is heavily doped, the Fermi level exists in the valence band in p -type and in the conduction band in n -type semiconductors. When the tunnel diode is forward biased by a voltage between zero and the value that would produce peak tunneling current I_p ($0 < V < V_p$), the energy diagram is shown in part (1) of Fig. 5-3-1(b).

Accordingly, the potential barrier is decreased by the magnitude of the applied forward-bias voltage. A difference in Fermi levels in both sides is created.

Since there are filled states in the conduction band of the n type at the same energy level as allowed empty states in the valence band of the p type, the electrons tunnel through the barrier from the n type to the p type, giving rise to a forward tunneling current from the p type to n type as shown in sector (1) of Fig. 5-3-2(a). As the forward bias is increased to V_p , the picture of the energy band is as shown in part (2) of Fig. 5-3-1(b).

A maximum number of electrons can tunnel through the barrier from the filled states in the n type to the empty states in the p type, giving rise to the peak current I_p in Fig. 5-3-2(a). If the bias voltage is further increased, the condition shown in part (3) of Fig. 5-3-1(b) is reached.

The tunneling current decreases as shown in sector (3) of Fig. 5-3-2(a). Finally, at a very large bias voltage, the band structure of part (4) of Fig. 5-3-1(b) is obtained.

Since there are now no allowed empty states in the p type at the same energy level as filled states in the n type, no electrons can tunnel through the barrier and the tunneling current drops to zero as shown at point (4) of Fig. 5-3-2(a).

When the forward-bias voltage V is increased above the valley voltage V_v , the ordinary injection current I at the p - n junction starts to flow.

This injection current is increased exponentially with the forward voltage as indicated by the dashed curve of Fig. 5-3-2(a). The total current, given by the sum of the tunneling current and the injection current, results in the volt-ampere characteristic of the tunnel diode as shown in Fig. 5-3-2(b).

It can be seen from the figure that the total current reaches a minimum value I_v (or valley current) somewhere in the region where the tunnel diode characteristic meets the ordinary p - n diode characteristic. The ratio of peak current to valley current (I_p/I_v) can theoretically reach 50 to 100. In practice, however, this ratio is about 15.

VARACTOR AND STEP RECOVERY DIODE

It is a high-efficiency microwave generator capable of operating from several hundred megahertz to several gigahertz. The basic operation of the oscillator is a semiconductor p - n junction diode reverse biased to current densities well in excess of those encountered in normal avalanche operation.

High-peak-power diodes are typically silicon $n^+ - p - p^+$ (or $p^+ - n - n^+$) structures with thin-type depletion region width varying from 2.5 to 12.5 μm . The doping of the depletion region is generally such that the diodes are well "punched through" at breakdown; that is, the electric field in the depletion region just prior to breakdown is well above the saturated drift-velocity level. The device's p^+ region is kept as thin as possible at 2.5 to 7.5 μm . The TRAPATT diode's diameter ranges from as small as 50 μm for CW operation to 750 μm at lower frequency for high peak- power devices.

Principles of Operation

high-field avalanche zone propagates through the diode and fills the depletion layer with a dense plasma of electrons and holes that become trapped in the low-field region behind the zone.

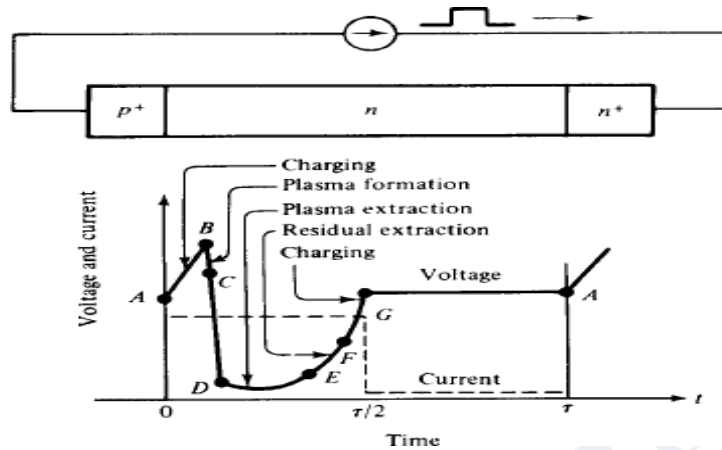
At point A the electric field is uniform throughout the sample and its magnitude is large but less than the value required for avalanche breakdown. The current density is expressed by

The current density is expressed by

$$J = \epsilon_s \frac{dE}{dt} \quad (8-3-1)$$

where ϵ_s is the semiconductor dielectric permittivity of the diode.

At the instant of time at point A, the diode current is turned on. Since the only charge carriers present are those caused by the thermal generation, the diode initially charges up like a linear capacitor, driving the magnitude of the electric field above the breakdown voltage.



When a sufficient number of carriers is generated, the particle current exceeds the external current and the electric field is depressed throughout the depletion region, causing the voltage to decrease. This portion of the cycle is shown by the curve from point B to point C.

During this time interval the electric field is sufficiently large for the avalanche to continue, and a dense plasma of electrons and holes is created. As some of the electrons and holes drift out of the ends of the depletion layer, the field is further depressed and "traps" the remaining plasma.

The voltage decreases to point D. A long time is required to remove the plasma because the total plasma charge is large compared to the charge per unit time in the external current.

At point E the plasma is removed, but a residual charge of electrons remains in one end of the depletion layer and a residual charge of holes in the other end. As the residual charge is removed, the voltage increases from point E to point F.

At point F all the charge that was generated internally has been removed. This charge must be greater than or equal to that supplied by the external current; otherwise the voltage will exceed that at point A.

From point F to point G the diode charges up again like a fixed capacitor. At point G the diode current goes to zero for half a period and the voltage and the cycle repeats. The electric field can be expressed as

$$E(x, t) = E_m - \frac{qN_A}{\epsilon_s} x + \frac{Jt}{\epsilon_s} \quad (8-3-2)$$

where N_A is the doping concentration of *then* region and x is the distance. Thus the value of t at which the electric field reaches E_m at a given distance x into the depletion region is obtained by setting $E(x, t) = E_m$, yielding

$$t = \frac{qN_A}{J} x \quad (8-3-3)$$

Differentiation of Eq. (8-3-3) with respect to time t results in

$$v_z \equiv \frac{dx}{dt} = \frac{J}{qN_A} \quad (8-3-4)$$

where V_z is the avalanche-zone velocity.

the low-field mobilities, and the transit time of the carriers can become much longer than

$$\tau_s = \frac{L}{v_s} \quad (8-3-5)$$

Power Output and Efficiency

RF power is delivered by the diode to an external load when the diode is placed in a proper circuit with a load. The main function of this circuit is to match the diode effective negative resistance to the load at the output frequency while reactively terminating (trapping) frequencies above the oscillation frequency in order to ensure TRAPATT operation. To date, the highest pulse power of 1.2 kW has been obtained at 1.1 GHz (five diodes in series) [10], and the highest efficiency of 75% has been achieved at 0.6 GHz (11). Table 8-3-1 shows the current state of TRAPATT diodes

TRANSFERRED ELECTRON DEVICES

The application of two-terminal semiconductor devices at microwave frequencies has been increased usage during the past decades. The CW, average, and peak power outputs of these devices at higher microwave frequencies are much larger than those obtainable with the best power transistor. The common characteristic of all active

two-terminal solid-state devices is their negative resistance. The real part of their impedance is negative over a range of frequencies. In a positive resistance the current through the resistance and the voltage across it are in phase. The voltage drop across a positive resistance is positive and a power of $(I^2 R)$ is dissipated in the resistance. In a negative resistance, however, the current and voltage are out of phase by 180° . The voltage drop across a negative resistance is negative, and a power of $(-I^2 R)$ is generated by the power supply associated with the negative resistance. In other words, positive resistances absorb power (passive devices), whereas negative resistances generate power (active devices). In this chapter the transferred electron devices (TEDs) are analyzed. The differences between microwave transistors and transferred electron devices (TEDs) are fundamental. Transistors operate with either junctions or gates, but TEDs are bulk devices having no junctions or gates. The majority of transistors are fabricated from elemental semiconductors, such as silicon or germanium, whereas TEDs are fabricated from compound semiconductors, such as gallium arsenide (GaAs), indium phosphide (InP), or cadmium telluride (CdTe). Transistors operate with "warm" electrons whose energy is not much greater than the thermal energy (0.026 eV at room temperature) of electrons in the semiconductor, whereas TEDs operate with "hot" electrons whose energy is very much greater than the thermal energy. Because of these fundamental differences, the theory and technology of transistors cannot be applied to TEDs.

GUNN DIODE

Gunn Effect:

Gun effect was first observed by GUNN in n_type GaAs bulk diode. According to GUNN, above some critical voltage corresponding to an electric field of 2000-4000v/cm, the current in every specimen became a fluctuating function of time. The frequency of oscillation was determined mainly by the specimen and not by the external circuit.

RIDLEY-WATKINS-HILSUM (RWH) THEORY

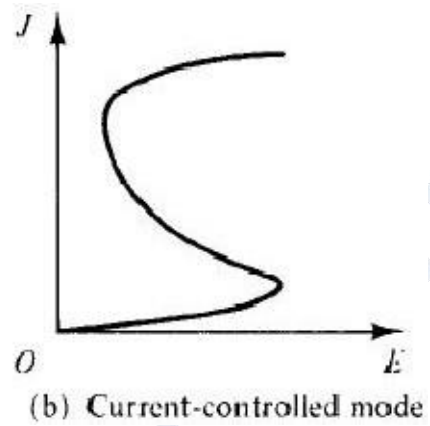
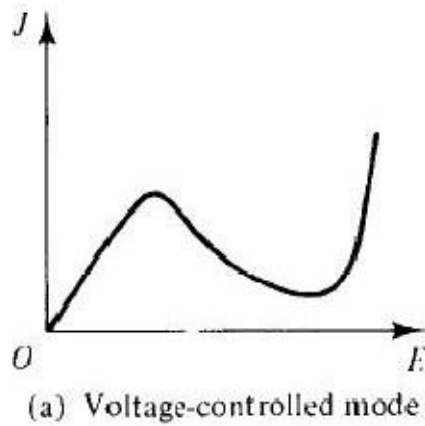
Differential Negative Resistance

The fundamental concept of the Ridley-Watkins-Hilsum (RWH) theory is the differential negative resistance developed in a bulk solid-state III-V compound when either a voltage (or electric field) or a current is applied to the terminals of the sample.

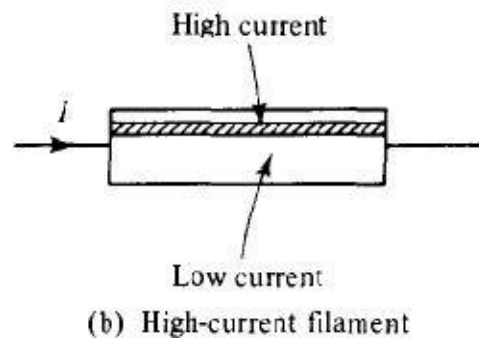
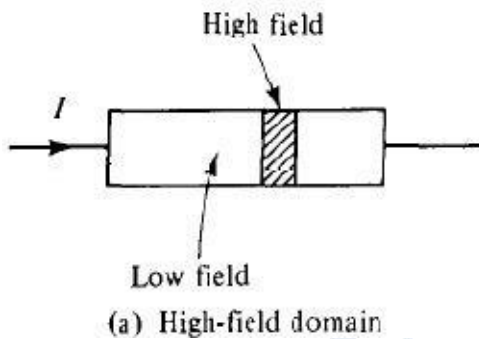
There are two modes of negative-resistance devices:

i) Voltage-controlled and

ii) current controlled modes as shown in Fig.



In the voltage-controlled mode the current density can be multivalued, whereas in the current-controlled mode the voltage can be multivalued.



The major effect of the appearance of a differential negative-resistance region in the current-density-field curve is to render the sample electrically unstable. As a result, the initially homogeneous sample becomes electrically heterogeneous in an attempt to reach stability.

In the voltage-controlled negative-resistance mode high-field domains are formed, separating two low-field regions. The interfaces separating low and high-field domains lie along equipotentials;

thus they are in planes perpendicular to the current direction as shown in Fig. 7-2-2(a). In the current-controlled negative-resistance mode splitting the sample results in high-current filaments running along the field direction as shown in Fig. 7-2-2(b).

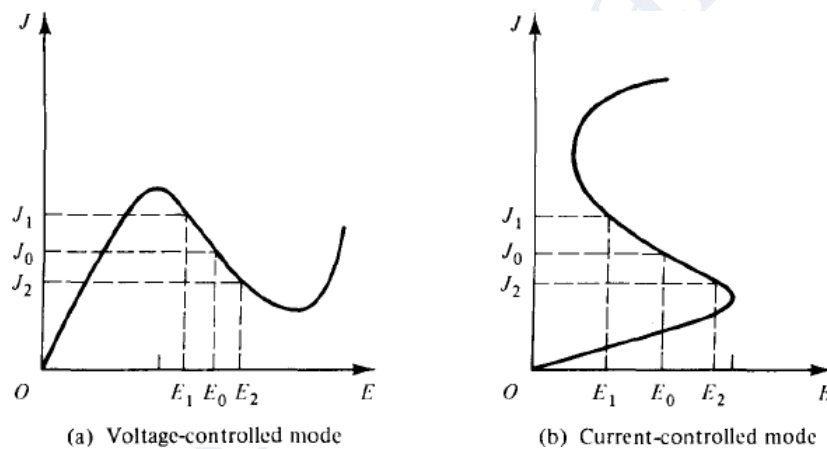
Expressed mathematically, the negative resistance of the sample at a particular region is

$$\frac{dI}{dV} = \frac{dJ}{dE} = \text{negative resistance} \quad (7-2-1)$$

If an electric field E_0 (or voltage V_0) is applied to the sample, for example, the current density is generated. As the applied field (or voltage) is increased to E_2 (or V_2), the current density is decreased to J_2 .

When the field (or voltage) is decreased to E_1 (or V_1), the current density is increased to J_1 . These phenomena of the voltage controlled negative resistance are shown in Fig. 7-2-3(a).

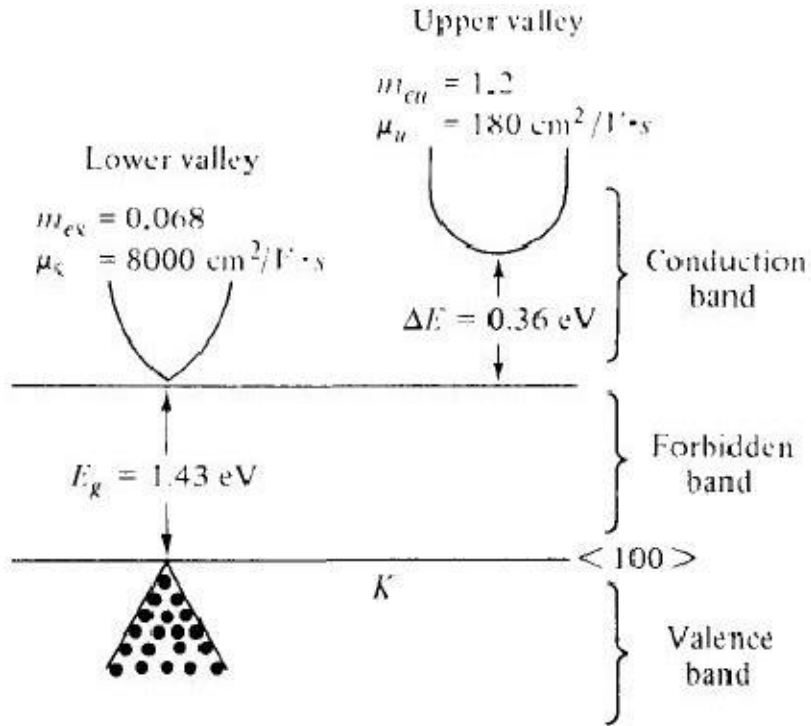
Similarly, for the current controlled mode, the negative-resistance profile is as shown in Fig. 7-2-3(b).



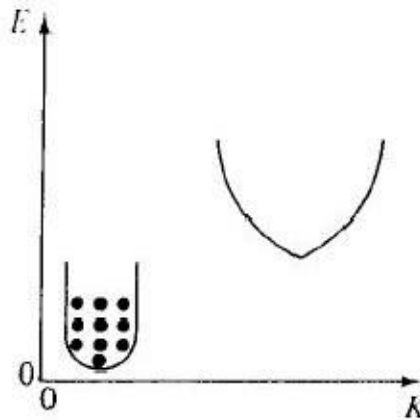
Two-Valley Model Theory

According to the energy band theory of then-type GaAs, a high-mobility lower valley is separated by an energy of 0.36 eV from a low-mobility upper valley

Valley	Effective Mass M_e	Mobility μ	Separation ΔE
Lower	$M_{e\ell} = 0.068$	$\mu_{\ell} = 8000 \text{ cm}^2/\text{V-sec}$	$\Delta E = 0.36 \text{ eV}$
Upper	$M_{eu} = 1.2$	$\mu_u = 180 \text{ cm}^2/\text{V-sec}$	$\Delta E = 0.36 \text{ eV}$

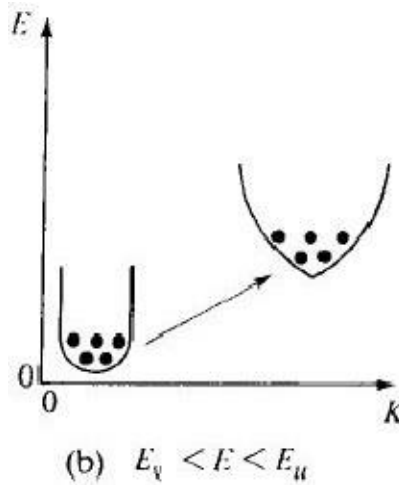


When the applied electric field is lower than the electric field of the lower valley ($\mathcal{E} < E_c$), no electrons will transfer to the upper valley as show in Fig. 7-2-S(a).

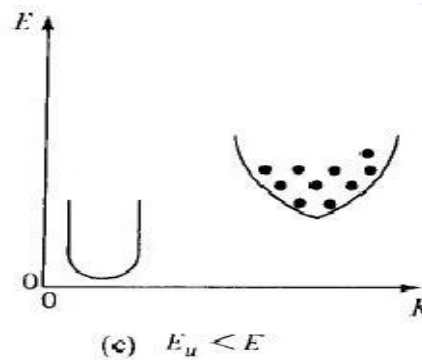


(a) $E < E_c$

When the applied electric field is higher than that of the lower valley and lower than that of the upper valley ($E_c < E < E_u$), electrons will begin to transfer to the upper valley as shown in Fig. 7-2-S(b).



And when the applied electric field is higher than that of the upper valley ($E_u < E$), all electrons will transfer to the upper valley as shown in Fig. 7-2-S(c).



If electron densities in the lower and upper valleys are n_l and n_u , the conductivity of the n -type GaAs is

$$\sigma = e(\mu_l n_l + \mu_u n_u) \quad (7-2-2)$$

where e = the electron charge
 μ = the electron mobility
 $n = n_l + n_u$ is the electron density

When a sufficiently high field E is applied to the specimen, electrons are accelerated and their effective temperature rises above the lattice temperature. Furthermore, the lattice temperature also increases. Thus electron density n and mobility $f-L$ are both functions of electric field E . Differentiation of Eq. (7-2-2) with respect to E yields

$$\frac{d\sigma}{dE} = e\left(\mu_l \frac{dn_l}{dE} + \mu_u \frac{dn_u}{dE}\right) + e\left(n_l \frac{d\mu_l}{dE} + n_u \frac{d\mu_u}{dE}\right) \quad (7-2-3)$$

If the total electron density is given by $n = n_t + n_u$ and it is assumed that $f.L_e$ and $/L_u$ are proportional to EP , where p is a constant, then

$$\frac{d}{dE} (n_t + n_u) = \frac{dn}{dE} = 0 \quad (7-2-4)$$

$$\frac{dn_t}{dE} = - \frac{dn_u}{dE} \quad (7-2-5)$$

$$\frac{d\mu}{dE} \propto \frac{dE^p}{dE} = pE^{p-1} = p \frac{E^p}{E} \propto p \frac{\mu}{E} = \mu \frac{p}{E} \quad (7-2-6)$$

Substitution of Eqs. (7-2-4) to (7-2-6) into Eq. (7-2-3) results in

$$\frac{d\sigma}{dE} = e(\mu_t - \mu_u) \frac{dn_t}{dE} + e(n_t\mu_t + n_u\mu_u) \frac{p}{E} \quad (7-2-7)$$

Then differentiation of Ohm's law $J = \sigma E$ with respect to E yields

$$\frac{dJ}{dE} = \sigma + \frac{d\sigma}{dE} E \quad (7-2-8)$$

Equation (7-2-8) can be rewritten

$$\frac{1}{\sigma} \frac{dJ}{dE} = 1 + \frac{d\sigma/dE}{\sigma/E} \quad (7-2-9)$$

Clearly, for negative resistance, the current density J must decrease with increasing field E or the ratio of dJ/dE must be negative. Such would be the case only if the right-hand term of Eq. (7-2-9) is less than zero. In other words, the condition for negative resistance is

$$- \frac{d\sigma/dE}{\sigma/E} > 1 \quad (7-2-10)$$

Substitution of Eqs. (7-2-2) and (7-2-7) with μ_e/μ_n results in [2]

$$\left[\left(\frac{\mu_e - \mu_n}{\mu_e + \mu_n} \right) \left(-\frac{E}{n_e} \frac{dn_e}{dE} \right) - p \right] > 1 \quad (7-2-11)$$

AVALANCE TRANSIT TIME DEVICES:

Avalanche transit-time diode oscillators rely on the effect of voltage breakdown across a reverse-biased $p-n$ junction to produce a supply of holes and electrons. Ever since the development of modern semiconductor device theory scientists have speculated on whether it is possible to make a two-terminal negative-resistance device.

The tunnel diode was the first such device to be realized in practice. Its operation depends on the properties of a forward-biased $p-n$ junction in which both the p and n regions are heavily doped. The other two devices are the transferred electron devices and the avalanche transit-time devices. In this chapter the latter type is discussed.

The transferred electron devices or the Gunn oscillators operate simply by the application of a dc voltage to a bulk semiconductor. There are no $p-n$ junctions in this device. Its frequency is a function of the load and of the natural frequency of the circuit. The avalanche diode oscillator uses carrier impact ionization and drift in the high-field region of a semiconductor junction to produce a negative resistance at microwave frequencies.

The device was originally proposed in a theoretical paper by Read in which he analyzed the negative-resistance properties of an idealized $n+p-i-p+$ diode. Two distinct modes of avalanche oscillator have been observed. One is the IMPATT mode, which stands for *impact ionization avalanche transit-time* operation. In this mode the typical dc-to-RF conversion efficiency is 5 to 10%, and frequencies are as high as 100 GHz with silicon diodes.

The other mode is the TRAPATT mode, which represents *trapped plasma avalanche triggered transit* operation. Its typical conversion efficiency is from 20 to 60%. Another type of active microwave device is the BARITT (*barrier injected transit-time*) diode [2]. It has long drift

regions similar to those of IMPATT diodes. The carriers traversing the drift regions of BARITT diodes, however, are generated by minority carrier injection from forward-biased junctions rather than being extracted from the plasma of an avalanche region. Several different structures have been operated as BARITT diodes, such as $p-n-p$, $p-n-v-p$, $p-n$ -metal, and metal-nmetal. BARITT diodes have low noise figures of 15 dB, but their bandwidth is relatively narrow with low output power.

IMPATT AND TRAPATT DIODE:

Physical Structures

A theoretical Read diode made of $n-p-i-p$ or $p-n-i-n$ structure has been analyzed. Its basic physical mechanism is the interaction of the impact ionization avalanche and the transit time of charge carriers. Hence the Read-type diodes are called IMPATT diodes. These diodes exhibit a differential negative resistance by two effects:

- 1) The impact ionization avalanche effect, which causes the carrier current $i_o(t)$ and the ac voltage to be out of phase by 90°
- 2) The transit-time effect, which further delays the external current $i_e(t)$ relative to the ac voltage by 90°

The first IMPATT operation as reported by Johnston et al. [4] in 1965, however, was obtained from a simple $p-n$ junction. The first real Read-type IMPATT diode was reported by Lee et al. [3], as described previously.

From the small-signal theory developed by Gilden [5] it has been confirmed that a negative resistance of the IMPATT diode can be obtained from a junction diode with any doping profile.

Many IMPATT diodes consist of a high doping avalanching region followed by a drift region where the field is low enough that the carriers can traverse through it without avalanching.

The Read diode is the basic type in the IMPATT diode family. The others are the one-sided abrupt $p-n$ junction, the linearly graded $p-n$ junction (or double-drift region), and the $p-i-n$ diode, all of which are shown in Fig. 8-2-1.

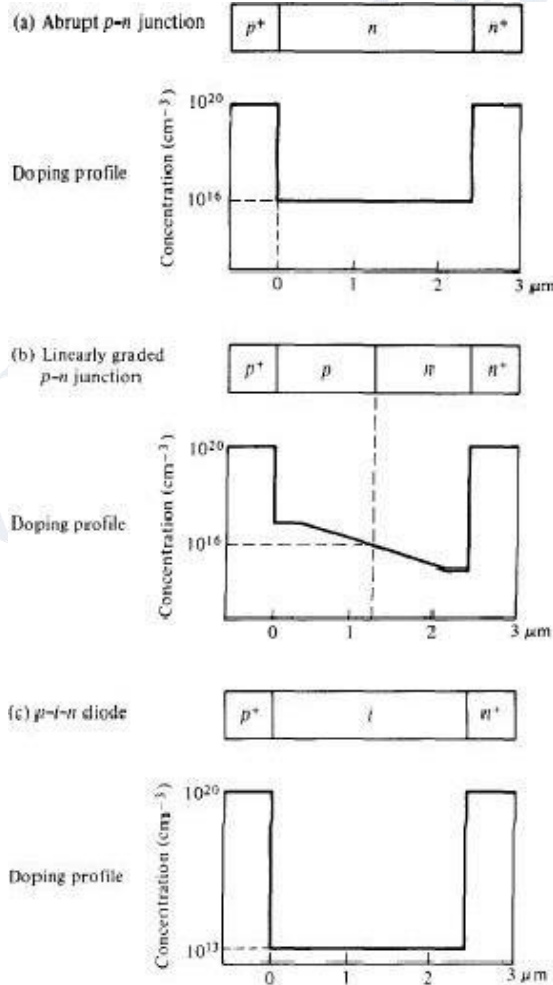
The principle of operation of these devices, however, is essentially similar to the mechanism described for the Read diode.

Negative Resistance

Small-signal analysis of a Read diode results in the following expression for the real part of the diode terminal impedance [5]:

$$R = R_s + \frac{2L^2}{v_d \epsilon_s A} \frac{1}{1 - \omega^2/\omega_c^2} \frac{1 - \cos \theta}{\theta} \tag{8-2-1}$$

- where R_s = passive resistance of the inactive region
- v_d = carrier drift velocity
- L = length of the drift space-charge region
- A = diode cross section
- ϵ_s = semiconductor dielectric permittivity



Moreover, θ is the transit angle, given by

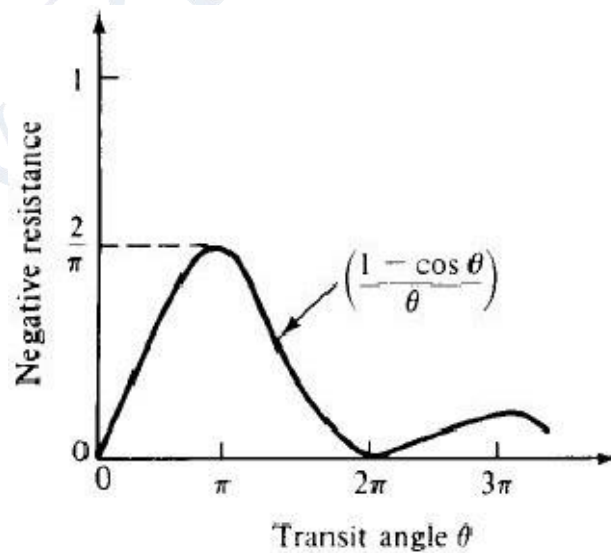
$$\theta = \omega\tau = \omega \frac{L}{v_d} \quad (8-2-2)$$

and ω_r is the avalanche resonant frequency, defined by

$$\omega_r \equiv \left(\frac{2\alpha' v_d I_0}{\epsilon_s A} \right)^{1/2} \quad (8-2-3)$$

The variation of the negative resistance with the transit angle when $\omega > \omega_r$ is plotted in Fig. 8-2-2. The peak value of the negative resistance occurs near $\theta = \pi$. For transit angles larger than π and approaching $3\pi/2$, the negative resistance of the diode decreases rapidly. For practical purposes, the Read-type IMPATT diodes work well only in a frequency range around the π transit angle. That is,

$$f = \frac{1}{2\tau} = \frac{v_d}{2L} \quad (8-2-4)$$



Power Output and Efficiency

For a uniform avalanche, the maximum voltage that can be applied across the diode is given by

$$V_m = E_m L \quad (8-2-5)$$

where

L is the depletion length

E_m is the maximum electric field.

This maximum applied voltage is limited by the breakdown voltage. Furthermore, the maximum current that can be carried by the diode is also limited by the avalanche breakdown process, for the current in the space-charge region causes an increase in the electric field. The maximum current is given by

$$I_m = J_m A = \sigma E_m A = \frac{\epsilon_s}{\tau} E_m A = \frac{v_d \epsilon_s E_m A}{L} \quad (8-2-6)$$

Therefore the upper limit of the power input is given by

$$P_m = I_m V_m = E_m^2 \epsilon_s v_d A \quad (8-2-7)$$

The capacitance across the space-charge region is defined as

$$C = \frac{\epsilon_s A}{L} \quad (8-2-8)$$

Substitution of Eq. (8-2-8) in Eq. (8-2-7) and application of $2\pi fL = 1$ yield

$$P_m f^2 = \frac{E_m^2 v_d^2}{4\pi^2 X_c} \quad (8-2-9)$$

It is interesting to note that this equation is identical to Eq. (5-1-60) of the power-frequency limitation for the microwave power transistor. The maximum power that can be given to the mobile carriers decreases as $1/f$. For silicon, this electronic limit is dominant at frequencies as high as 100 GHz. The efficiency of the IMPATT diodes is given by

$$\eta = \frac{P_{ac}}{P_{dc}} = \left(\frac{V_a}{V_d}\right)\left(\frac{I_a}{I_d}\right) \quad (8-2-10)$$

PARAMETRIC DEVICES:

Parametric Amplifiers

In a super heterodyne receiver a radio frequency signal may be mixed with a signal from the local oscillator in a nonlinear circuit (the mixer) to generate the sum and difference frequencies.

In a parametric amplifier the local oscillator is replaced by a pumping generator such as a reflex klystron and the nonlinear element by a time varying capacitor such as a varactor diode (or inductor) as shown in Fig.

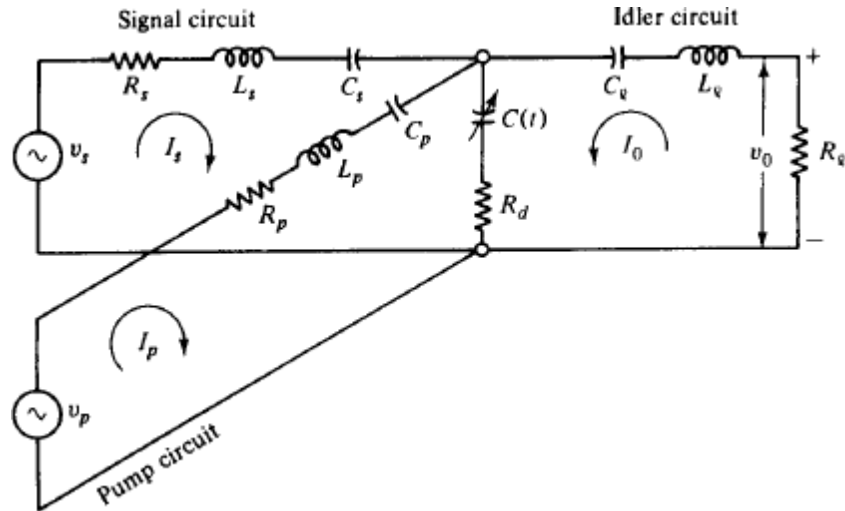
In Fig. 8-5-2, the signal frequency f_s and the pump frequency f_p are mixed in the nonlinear capacitor C . Accordingly, a voltage of the fundamental frequencies f_s and f_p , as well as the sum and the difference frequencies $mfp \pm nfs$ appears across C .

If a resistive load is connected across the terminals of the idler circuit, an output voltage can be generated across the load at the output frequency f_a . The output circuit, which does not require external excitation, is called the *idler circuit*.

The output (or idler) frequency f_a in the idler circuit is expressed as the sum and the difference frequencies of the signal frequency f_s and the pump frequency f_p . That is,

where m and n are positive integers from zero to infinity.

If $f_o > f_s$, the device is called a parametric *up-converter*. Conversely, if $f_o < f_s$, the device is known as a parametric *down-converter*.



Parametric up-converter.

A parametric up-converter has the following properties:

- 1) The output frequency is equal to the sum of the signal frequency and the pump frequency.
- 2) There is no power flow in the parametric device at frequencies other than the signal, pump, and output frequencies.

Power Gain.

When these two conditions are satisfied, the maximum power gain of a parametric up-converter [21] is expressed as

$$\text{Gain} = \frac{f_0}{f_s} \frac{x}{(1 + \sqrt{1 + x})^2} \tag{8-5-30}$$

where $f_0 = f_p + f_s$

$$x = \frac{f_s}{f_0} (\gamma Q)^2$$

$$Q = \frac{1}{2\pi f_s C R_d}$$

Moreover, R_d is the series resistance of a $p-n$ junction diode and γQ is the figure of merit for the nonlinear capacitor. The quantity of $x/(1 + \sqrt{1 + x})^2$ may be regarded as a gain-degradation factor. As R_d approaches zero, the figure of merit γQ goes to infinity and the gain-degradation factor becomes equal to unity. As a result, the power gain of a parametric up-converter for a lossless diode is equal to f_0/f_s ,

which is predicted by the Manley-Rowe relations as shown in Eq. (8-5-27). In a typical microwave diode yQ could be equal to 10. If $f_o/f_s = 15$, the maximum gain given by Eq. (8-5-30) is 7.3 dB.

Noise Figure.

One advantage of the parametric amplifier over the transistor amplifier is its low-noise figure because a pure reactance does not contribute thermal noise to the circuit. The noise figure F for a parametric up-converter [21] is given by

$$F = 1 + \frac{2T_d}{T_0} \left[\frac{1}{\gamma Q} + \frac{1}{(\gamma Q)^2} \right] \tag{8-5-31}$$

where T_d = diode temperature in degrees Kelvin
 $T_0 = 300^\circ\text{K}$ is the ambient temperature in degrees Kelvin
 γQ = figure of merit for the nonlinear capacitor

Bandwidth.

The bandwidth of a parametric up-converter is related to the gain-degradation factor of the merit figure and the ratio of the signal frequency to the output frequency. The bandwidth equation [21] is given by

$$BW = 2\gamma \sqrt{\frac{f_o}{f_s}} \tag{8-5-32}$$

If $f_o/f_s = 10$ and $\gamma = 0.2$, the bandwidth (BW) is equal to 1.264.

Parametric down-converter.

The down-conversion gain (actually a loss) is given by

$$\text{Gain} = \frac{f_s}{f_o} \frac{x}{(1 + \sqrt{1 + x})^2} \tag{8-5-33}$$

Negative-resistance parametric amplifier.

If a significant portion of power flows only at the signal frequency f_s , the pump frequency f_p , and the idler frequency f_i , a regenerative condition with the possibility of oscillation at both the signal frequency and the idler frequency will occur.

The idler frequency is $f_i = f_p - f_s$.

When the mode operates below the oscillation threshold, the device behaves as a bilateral negative-resistance parametric amplifier.

Power Gain.

The output power is taken from the resistance R ; at a frequency f_s , and the conversion gain from f_s to f_i [21] is given by

$$\text{Gain} = \frac{4f_i}{f_s} \cdot \frac{R_g R_i}{R_{T_s} R_{T_i}} \cdot \frac{a}{(1 - a)^2} \quad (8-5-34)$$

- where f_s = signal frequency
- f_p = pump frequency
- $f_i = f_p - f_s$ is the idler frequency
- R_g = output resistance of the signal generator
- R_i = output resistance of the idler generator
- R_{T_s} = total series resistance at f_s
- R_{T_i} = total series resistance at f_i
- $a = R/R_{T_s}$
- $R = \gamma^2/(\omega_s \omega_i C^2 R_{T_i})$ is the equivalent negative resistance

Noise Figure.

The optimum noise figure of a negative-resistance parametric amplifier [21] is expressed as

$$F = 1 + 2 \frac{T_d}{T_0} \left[\frac{1}{\gamma Q} + \frac{1}{(\gamma Q)^2} \right] \quad (8-5-35)$$

- where γQ = figure of merit for the nonlinear capacitor
- $T_0 = 300^\circ\text{K}$ is the ambient temperature in degrees Kelvin
- T_d = diode temperature in degrees Kelvin

The optimum noise figure of a negative-resistance parametric amplifier [21] is expressed as

Bandwidth.

The maximum gain bandwidth of a negative-resistance parametric amplifier [21] is given by

$$\text{BW} = \frac{\gamma}{2} \sqrt{\frac{f_i}{f_s \text{ gain}}}$$

Degenerate parametric amplifier.

The degenerate parametric amplifier or oscillator is defined as a negative-resistance amplifier with the signal frequency equal to the idler frequency.

Power Gain and Bandwidth.

The power gain and bandwidth characteristics of a degenerate parametric amplifier are exactly the same as for the parametric up converter.

With $f_s = f_i$ and $f_p = 2f_s$, the power transferred from pump to signal frequency is equal to the power transferred from pump to idler frequency.

Noise Figure.

The noise figures for a single-sideband and a double-sideband degenerate parametric amplifier [21] are given by, respectively,

$$F_{\text{ssb}} = 2 + \frac{2\bar{T}_d R_d}{T_0 R_g} \quad (8-5-37)$$

$$F_{\text{dsb}} = 1 + \frac{\bar{T}_d R_d}{T_0 R_g} \quad (8-5-38)$$

where \bar{T}_d = average diode temperature in degrees Kelvin
 $T_0 = 300^\circ\text{K}$ is the ambient noise temperature in degrees Kelvin
 R_d = diode series resistance in ohms
 R_g = external output resistance of the signal generator in ohms

It can be seen that the noise figure for double-sideband operation is 3 dB less than that for single-sideband operation.

APPLICATION OF PARAMETRIC DEVICES

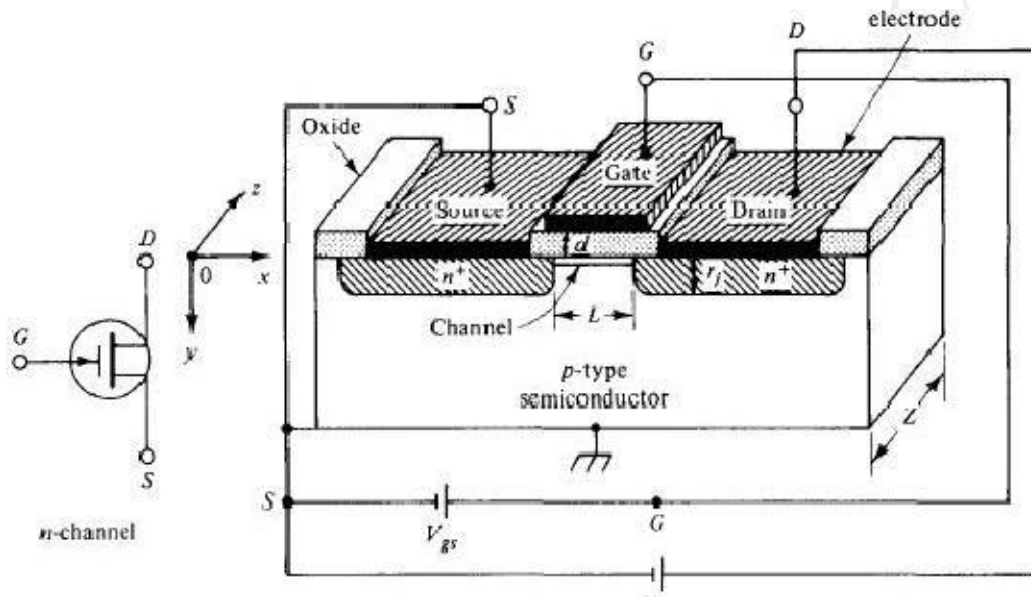
Applications

1. A positive input impedance
2. Unconditionally stable and unilateral
3. Power gain independent of changes in its source impedance
4. No circulator required
5. A typical bandwidth on the order of 5%

: MICROWAVE MONOLITHIC INTEGRATED CIRCUITES

The metal-oxide-semiconductor field-effect transistor (MOSFET) is a four-terminal device. There are both n-channel and p-channel MOSFETs. The n-channel MOSFET consists of a slightly doped p -type semiconductor substrate into which two highly doped $n+$ sections are diffused, as shown in Fig. 6-4-1.

These n^+ sections, which act as the source and the drain, are separated by about $0.5 \lambda_m$. A thin layer of insulating silicon dioxide (SiO_2) is grown over the surface of the structure. The metal contact on the insulator is called the *gate*. Similarly, the p -channel MOSFET is made of a slightly doped n -type semiconductor with two highly doped p^+ -type regions for the source and drain. The heavily doped polysilicon or a combination of silicide and polysilicon can also be used as the gate electrode. In practice, a MOSFET is commonly surrounded by a thick oxide to isolate it from the adjacent devices in a microwave integrated circuit. The basic device parameters of a MOSFET are as follows: L is the channel length, which is the distance between the two $n^+ - p$ junctions just beneath the insulator (say, $0.5 \lambda_m$), Z is the channel depth (say, $5 \lambda_m$), d_{ox} is the insulator thickness (say, $0.1 \lambda_m$), and r_1 is the junction thickness of the n^+ section (say, $0.2 \lambda_m$).



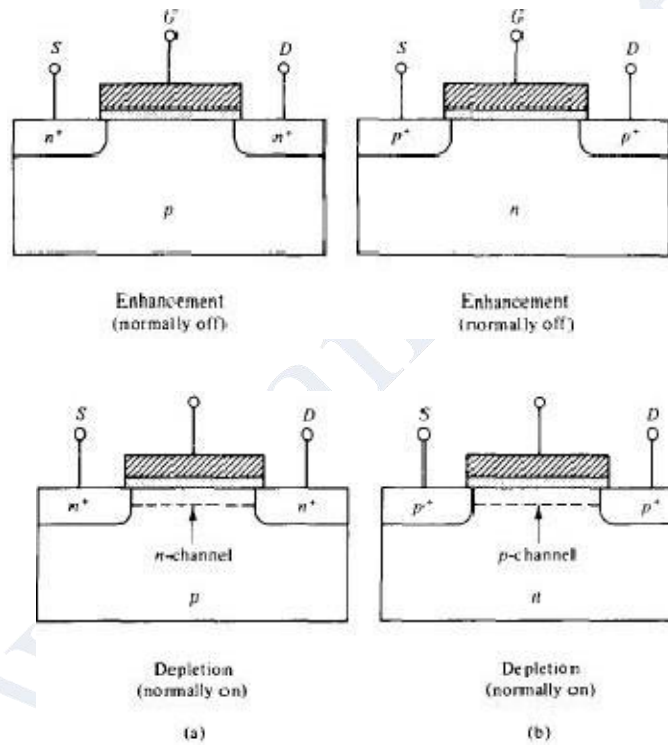
MATERIALS AND FABRICATION TECHNIQUES

1. **n-Channel Enhancement Mode (normally OFF).** When the gate voltage is zero, the channel conductance is very low and it is not conducting. A positive voltage must be applied to the gate to form an n channel for conduction. The drain current is enhanced by the positive voltage. This type is called the enhancement-mode (normally OFF) n-channel MOSFET.

n-Channel Depletion Mode (normally ON). If an n channel exists at equilibrium (that is, at zero bias), a negative gate voltage must be applied to deplete the carriers in the channel. In effect, the channel conductance is reduced, and the device is turned OFF. This type is called the depletion-mode (normally ON) n-channel MOSFET.

p -Channel Enhancement Mode (normally OFF). A negative voltage must be applied to the gate to induce a p channel for conduction. This type is called the enhancement-mode (normally OFF) p -channel MOSFET.

p -Channel Depletion Mode (normally ON). A positive voltage must be applied to the gate to deplete the carriers in the channel for nonconduction. This type is called the depletion-mode (normally ON) p -channel MOSFET.

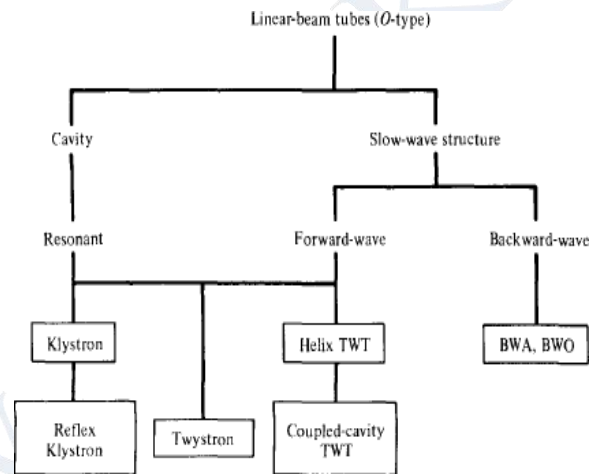


UNIT – 5

MICROWAVE TUBES AND MEASUREMENTS

MICROWAVE TUBES

We turn now to a quantitative and qualitative analysis of several conventional vacuum tubes and microwave tubes in common use. The conventional vacuum tubes, such as triodes, tetrodes, and pentodes, are still used as signal sources of low output power at low microwave frequencies. The most important microwave tubes at present are the linear-beam tubes (O type) tabulated in Table 9-0-1. The paramount O-type tube is the two-cavity klystron, and it is followed by the reflex klystron. The helix traveling-wave tube (TWT), the coupled-cavity TWT, the forward-wave amplifier (FWA), and the backward-wave amplifier and oscillator (BWA and BWO) are also O-type tubes, but they have nonresonant periodic structures for electron interactions. The Twystron is a hybrid amplifier that uses combinations of klystron and TWT components. The switching tubes such as krytron, thyatron, and planar triode are very useful in laser modulation. Although it is impossible to discuss all such tubes in detail, the common operating principles of many will be described.



OPERATION OF MULTICAVIDITY KLYSTRON

Two cavity klystron:

The two-cavity klystron is a widely used microwave amplifier operated by the principles of velocity and current modulation. All electrons injected from the cathode arrive at the first cavity with uniform velocity. Those electrons passing the first cavity gap at zeros of the gap voltage (or signal voltage) pass through with unchanged velocity; those passing through the positive half cycles of the gap voltage undergo an increase in velocity; those passing through the negative swings of the gap voltage undergo a decrease in velocity.

As a result of these actions, the electrons gradually bunch together as they travel down the drift space. The variation in electron velocity in the drift space is known as *velocity modulation*. The density of the electrons in the second cavity gap varies cyclically with time.

The electron beam contains an ac component and is said to be current-modulated. The maximum bunching should occur approximately midway between the second cavity grids during its retarding phase; thus the kinetic energy is transferred from the electrons to the field of the second cavity.

The electrons then emerge from the second cavity with reduced velocity and finally terminate at the collector. The characteristics of a two-cavity klystron amplifier are as follows:

1. Efficiency: about 40%.
2. Power output: average power (CW power) is up to 500 kW and pulsed power is up to 30 MW at 10 GHz.
3. Power gain: about 30 dB.

Reentrant Cavities

The coaxial cavity is similar to a coaxial line shorted at two ends and joined at the center by a capacitor.

The input impedance to each shorted coaxial line is given by

$$Z_0 = \frac{1}{2\pi} \sqrt{\frac{\mu}{\epsilon}} \ln \frac{b}{a} \quad \text{ohms} \quad (9-2-1)$$

where e is the length of the coaxial line.

Substitution of Eq. (9-2-1) in (9-2-2) results in

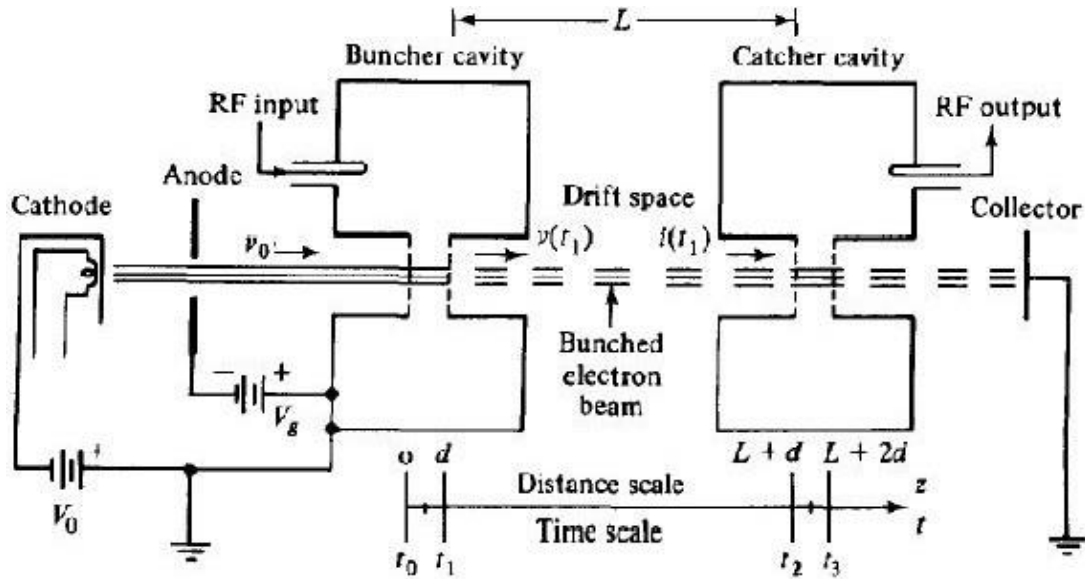


Figure 9-2-2 Two-cavity klystron amplifier.

The inductance of the cavity is given by

$$L = \frac{2X_{in}}{\omega} = \frac{1}{\pi\omega} \sqrt{\frac{\mu}{\epsilon}} \ln \frac{b}{a} \tan(\beta \ell) \quad (9-2-4)$$

and the capacitance of the gap by

$$C_g = \frac{\epsilon\pi a^2}{d} \quad (9-2-5)$$

At resonance the inductive reactance of the two shorted coaxial lines in series is equal in magnitude to the capacitive reactance of the gap. That is, $\omega L = 1/(\omega C_g)$.

Thus where $v = 1/\gamma\epsilon\epsilon_0$ is the phase velocity in any medium

Velocity-Modulation Process

When electrons are first accelerated by the high de voltage V_0 before entering the buncher grids, their velocity is uniform:

$$v_0 = \sqrt{\frac{2eV_0}{m}} = 0.593 \times 10^6 \sqrt{V_0} \quad \text{m/s} \quad (9-2-10)$$

In Eq. (9-2-10) it is assumed that electrons leave the cathode with zero velocity. When a microwave signal is applied to the input terminal, the gap voltage between the buncher grids appears as

$$V_s = V_1 \sin(\omega t) \quad (9-2-11)$$

where V_1 is the amplitude of the signal and $V_1 \ll V_0$ is assumed.

In order to find the modulated velocity in the buncher cavity in terms of either the entering time t_0 or the exiting time t_1 and the gap transit angle θ as shown in Fig. 9-2-2 it is necessary to determine the average microwave voltage in the buncher gap as indicated in Fig. 9-2-6. Since $V_1 \ll V_0$, the average transit time through the buncher gap distance d is

$$\tau \approx \frac{d}{v_0} = t_1 - t_0 \quad (9-2-12)$$

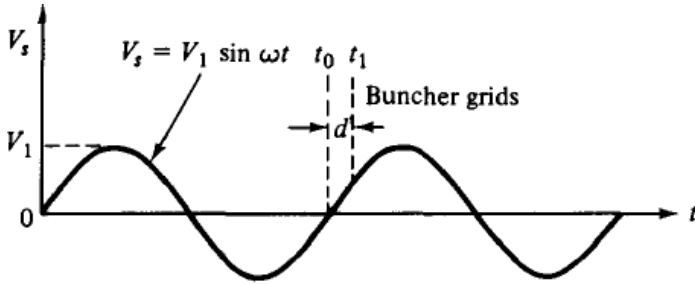


Figure 9-2-6 Signal voltage in the buncher gap.

The average gap transit angle can be expressed as

$$\theta_g = \omega\tau = \omega(t_1 - t_0) = \frac{\omega d}{v_0} \quad (9-2-13)$$

The average microwave voltage in the buncher gap can be found in the following way:

$$\begin{aligned} \langle V_s \rangle &= \frac{1}{\tau} \int_{t_0}^{t_1} V_1 \sin(\omega t) dt = -\frac{V_1}{\omega\tau} [\cos(\omega t_1) - \cos(\omega t_0)] \\ &= \frac{V_1}{\omega\tau} \left[\cos(\omega t_0) - \cos\left(\omega_0 + \frac{\omega d}{v_0}\right) \right] \end{aligned} \quad (9-2-14)$$

Let

$$\omega t_0 + \frac{\omega d}{2v_0} = \omega t_0 + \frac{\theta_g}{2} = A$$

and

$$\frac{\omega d}{2v_0} = \frac{\theta_g}{2} = B$$

Then using the trigonometric identity that $\cos(A - B) - \cos(A + B) = 2 \sin A \sin B$, Eq. (9-2-14) becomes

$$\langle V_s \rangle = V_1 \frac{\sin[\omega d/(2v_0)]}{\omega d/(2v_0)} \sin\left(\omega t_0 + \frac{\omega d}{2v_0}\right) = V_1 \frac{\sin(\theta_g/2)}{\theta_g/2} \sin\left(\omega t_0 + \frac{\theta_g}{2}\right) \quad (9-2-15)$$

It is defined as

$$\beta_i \equiv \frac{\sin[\omega d/(2v_0)]}{\omega d/(2v_0)} = \frac{\sin(\theta_g/2)}{\theta_g/2} \quad (9-2-16)$$

Note that β_i is known as the *beam-coupling coefficient* of the input cavity gap (see Fig. 9-2-7).

It can be seen that increasing the gap transit angle θ_g decreases the coupling between the electron beam and the buncher cavity; that is, the velocity modulation

It can be seen that increasing the gap transit angle θ_g decreases the coupling between the electron beam and the buncher cavity; that is, the velocity modulation of the beam for a given microwave signal is decreased. Immediately after velocity modulation, the exit velocity from the buncher gap is given by

$$\begin{aligned} v(t_1) &= \sqrt{\frac{2e}{m} \left[V_0 + \beta_i V_1 \sin \left(\omega t_0 + \frac{\theta_g}{2} \right) \right]} \\ &= \sqrt{\frac{2e}{m} V_0 \left[1 + \frac{\beta_i V_1}{V_0} \sin \left(\omega t_0 + \frac{\theta_g}{2} \right) \right]} \end{aligned} \quad (9-2-17)$$

where the factor $\beta_i V_1/V_0$ is called the *depth of velocity modulation*.

Using binomial expansion under the assumption of

$$\beta_i V_1 \ll V_0 \quad (9-2-18)$$

Eq. (9-2-17) becomes

$$v(t_1) = v_0 \left[1 + \frac{\beta_i V_1}{2V_0} \sin \left(\omega t_0 + \frac{\theta_g}{2} \right) \right] \quad (9-2-19)$$

Equation (9-2-19) is the equation of velocity modulation. Alternatively, the equation of velocity modulation can be given by

$$v(t_1) = v_0 \left[1 + \frac{\beta_i V_1}{2V_0} \sin \left(\omega t_1 - \frac{\theta_g}{2} \right) \right] \quad (9-2-20)$$

Bunching Process

Once the electrons leave the buncher cavity, they drift with a velocity given by Eq. (9-2-19) or (9-2-20) along in the field-free space between the two cavities. The effect of velocity modulation produces bunching of the electron beam-or current modulation.

The electrons that pass the buncher at $V_s = 0$ travel through with unchanged velocity v_0 and become the bunching center. Those electrons that pass the buncher cavity during the positive half cycles of the microwave input voltage V_s travel faster than the electrons that passed the gap when $V_s = 0$. Those electrons that pass the buncher cavity during the negative half cycles of the voltage V_s travel slower than the electrons that passed the gap when $V_s = 0$. At a distance of L along the beam from the buncher

cavity, the beam electrons have drifted into dense clusters. Figure 9-2-8 shows the trajectories of minimum, zero, and maximum electron acceleration.

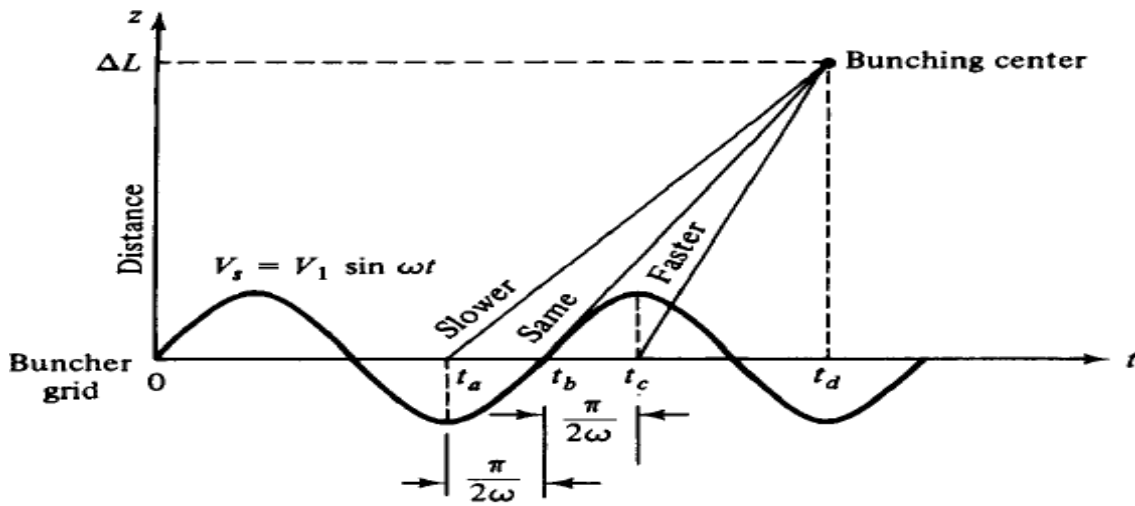


Figure 9-2-8 Bunching distance.

The distance from the buncher grid to the location of dense electron bunching for the electron at t_b is

$$\Delta L = v_0(t_d - t_b) \quad (9-2-21)$$

Similarly, the distances for the electrons at t_a and t_c are

$$\Delta L = v_{\min}(t_d - t_a) = v_{\min}\left(t_d - t_b + \frac{\pi}{2\omega}\right) \quad (9-2-22)$$

$$\Delta L = v_{\max}(t_d - t_c) = v_{\max}\left(t_d - t_b - \frac{\pi}{2\omega}\right) \quad (9-2-23)$$

From Eq. (9-2-19) or (9-2-20) the minimum and maximum velocities are

$$v_{\min} = v_0\left(1 - \frac{\beta_i V_1}{2V_0}\right) \quad (9-2-24)$$

$$v_{\max} = v_0 \left(1 + \frac{\beta_i V_1}{2V_0} \right) \quad (9-2-25)$$

Substitution of Eqs. (9-2-24) and (9-2-25) in Eqs. (9-2-22) and (9-2-23), respectively, yields the distance

$$\Delta L = v_0(t_d - t_b) + \left[v_0 \frac{\pi}{2\omega} - v_0 \frac{\beta_i V_1}{2V_0} (t_d - t_b) - v_0 \frac{\beta_i V_1}{2V_0} \frac{\pi}{2\omega} \right] \quad (9-2-26)$$

and

$$\Delta L = v_0(t_d - t_b) + \left[-v_0 \frac{\pi}{2\omega} + v_0 \frac{\beta_i V_1}{2V_0} (t_d - t_b) + v_0 \frac{\beta_i V_1}{2V_0} \frac{\pi}{2\omega} \right] \quad (9-2-27)$$

The necessary condition for those electrons at t_a , t_b , and t_c to meet at the same distance ΔL is

$$v_0 \frac{\pi}{2\omega} - v_0 \frac{\beta_i V_1}{2V_0} (t_d - t_b) - v_0 \frac{\beta_i V_1}{2V_0} \frac{\pi}{2\omega} = 0 \quad (9-2-28)$$

and

$$-v_0 \frac{\pi}{2\omega} + v_0 \frac{\beta_i V_1}{2V_0} (t_d - t_b) + v_0 \frac{\beta_i V_1}{2V_0} \frac{\pi}{2\omega} = 0 \quad (9-2-29)$$

Consequently,

$$t_d - t_b \approx \frac{\pi V_0}{\omega \beta_i V_1} \quad (9-2-30)$$

and

$$\Delta L = v_0 \frac{\pi V_0}{\omega \beta_i V_1} \quad (9-2-31)$$

$$T = t_2 - t_1 = \frac{L}{v(t_1)} = T_0 \left[1 - \frac{\beta_i V_1}{2V_0} \sin \left(\omega t_1 - \frac{\theta_g}{2} \right) \right] \quad (9-2-32)$$

where the binomial expansion of $(1 + x)^{-1}$ for $|x| \ll 1$ has been replaced and $T_0 = L/v_0$ is the dc transit time. In terms of radians the preceding expression can be written

$$\omega T = \omega t_2 - \omega t_1 = \theta_0 - X \sin \left(\omega t_1 - \frac{\theta_g}{2} \right) \quad (9-2-33)$$

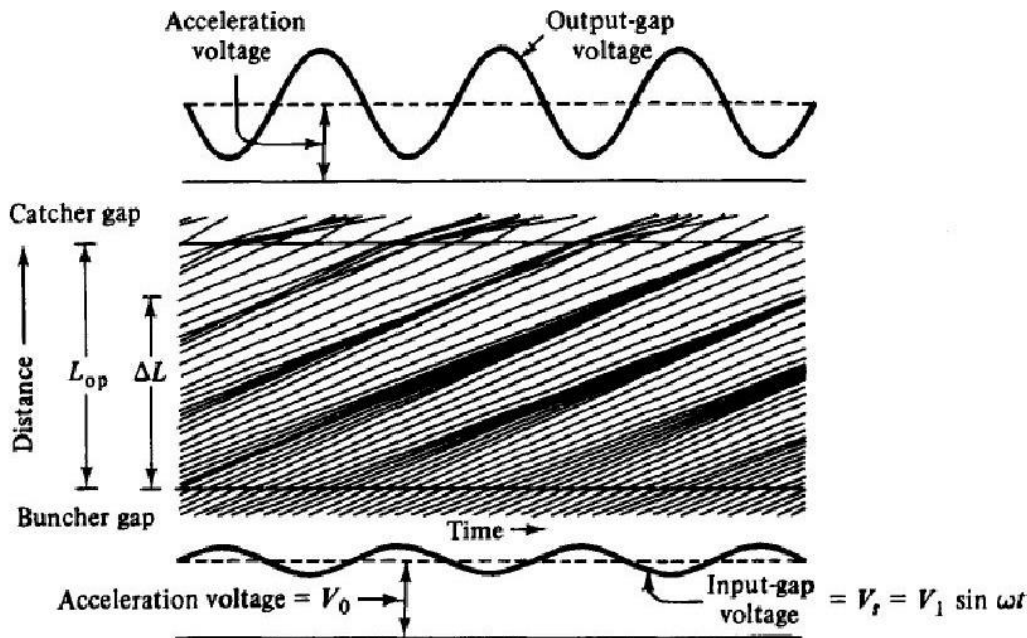


Figure 9-2-9 Applegate diagram.

where

$$\theta_0 = \frac{\omega L}{v_0} = 2\pi N \quad (9-2-34)$$

is the dc transit angle between cavities, N is the number of electron transit cycles in the drift space, and

$$X \equiv \frac{\beta_i V_1}{2V_0} \theta_0 \quad (9-2-35)$$

is defined as the *bunching parameter* of a klystron.

At the buncher gap a charge dQ_0 passing through at a time interval dt_0 is given by

$$dQ_0 = I_0 dt_0 \quad (9-2-36)$$

where I_0 is the dc current. From the principle of conservation of charges this same amount of charge dQ_0 also passes the catcher at a later time interval dt_2 . Hence

$$I_0 |dt_0| = i_2 |dt_2| \quad (9-2-37)$$

where the absolute value signs are necessary because a negative value of the time ratio would indicate a negative current. Current i_2 is the current at the catcher gap. Rewriting Eq. (9-2-32) in terms of Eq. (9-2-19) yields

$$t_2 = t_0 + \tau + T_0 \left[1 - \frac{\beta_i V_1}{2V_0} \sin \left(\omega t_0 + \frac{\theta_g}{2} \right) \right] \quad (9-2-38)$$

Alternatively,

$$\omega t_2 - \left(\theta_0 + \frac{\theta_g}{2} \right) = \left(\omega t_0 + \frac{\theta_g}{2} \right) - X \sin \left(\omega t_0 + \frac{\theta_g}{2} \right) \quad (9-2-39)$$

SC where $(\omega t_0 + \theta_g/2)$ is the buncher cavity departure angle and $\omega t_2 - (\theta_0 + \theta_g/2)$ is the catcher cavity arrival angle. Figure 9-2-10 shows the curves for the catcher cav-

Differentiation of Eq. (9-2-38) with respect to t_0 results in

$$dt_2 = dt_0 \left[1 - X \cos \left(\omega t_0 + \frac{\theta_s}{2} \right) \right] \quad (9-2-40)$$

The current arriving at the catcher cavity is then given as

$$i_2(t_0) = \frac{I_0}{1 - X \cos (\omega t_0 + \theta_s/2)} \quad (9-2-41)$$

In terms of t_2 the current is

$$i_2(t_2) = \frac{I_0}{1 - X \cos (\omega t_2 - \theta_0 - \theta_s/2)} \quad (9-2-42)$$

The optimum distance L at which the maximum fundamental component of current occurs is computed from Eqs. (9-2-34), (9-2-35), and (9-2-54) as

$$L_{\text{optimum}} = \frac{3.682 v_0 V_0}{\omega \beta_i V_1} \quad (9-2-55)$$

REFLUX KLYSTRON

If a fraction of the output power is fed back to the input cavity and if the loop gain has a magnitude of unity with a phase shift of multiple 2π , the klystron will oscillate. However, a two-cavity klystron oscillator is usually not constructed because, when the oscillation frequency is varied, the resonant frequency of each cavity and the feedback path phase shift must be readjusted for a positive feedback.

The reflex klystron is a single-cavity klystron that overcomes the disadvantages of the two-cavity klystron oscillator. It is a low-power generator of 10 to 500-mW output at a frequency range of 1 to 25 GHz. The efficiency is about 20 to 30%. This type is widely used in the laboratory for microwave measurements and in microwave receivers as local oscillators in commercial, military, and airborne Doppler radars as well as missiles.

The theory of the two-cavity klystron can be applied to the analysis of the reflex klystron with slight modification. A schematic diagram of the reflex klystron is shown in Fig. 9-4-1.

The electron beam injected from the cathode is first velocity-modulated by the cavity-gap voltage. Some electrons accelerated by the accelerating field enter the repeller space with greater velocity than those with unchanged velocity. Some electrons decelerated by the retarding field enter the repeller region with less velocity.

All electrons turned around by the repeller voltage then pass through the cavity gap in bunches that occur once per cycle. On their return journey the bunched electrons pass through the gap during the retarding phase of the alternating field and give up their kinetic energy to the electromagnetic energy of the field in the cavity. Oscillator output energy is then taken from the cavity. The electrons are finally collected by the walls of the cavity or other grounded metal parts of the tube. Figure 9-4-2 shows an Applegate diagram for the 1~ mode of a reflex klystron.

Velocity Modulation

The analysis of a reflex klystron is similar to that of a two-cavity klystron. For simplicity, the effect of space-charge forces on the electron motion will again be neglected. The electron entering the cavity gap from the cathode at $z = 0$ and time t_0 is assumed to have uniform velocity

$$v_0 = 0.593 \times 10^6 \sqrt{V_0} \quad (9-4-1)$$

The same electron leaves the cavity gap at $z = d$ at time t_1 with velocity

$$v(t_1) = v_0 \left[1 + \frac{\beta_1 V_1}{2V_0} \sin \left(\omega t_1 - \frac{\theta_g}{2} \right) \right] \quad (9-4-2)$$

This expression is identical to Eq. (9-2-17), for the problems up to this point are identical to those of a two-cavity klystron amplifier. The same electron is forced back to the cavity $z = d$ and time t_2 by the retarding electric field E , which is given by

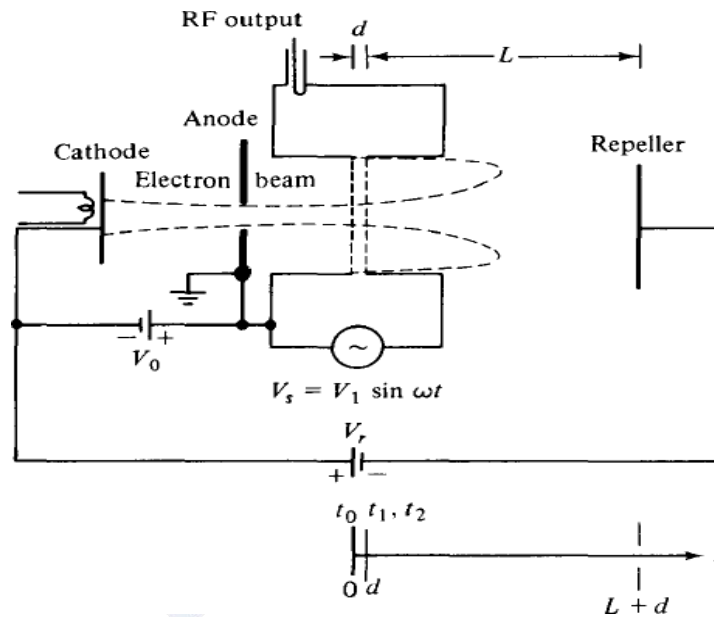
$$E = \frac{V_r + V_0 + V_1 \sin(\omega t)}{L} \quad (9-4-3)$$

This retarding field E is assumed to be constant in the z direction. The force equation for one electron in the repeller region is

$$m \frac{d^2 z}{dt^2} = -eE = -e \frac{V_r + V_0}{L} \quad (9-4-4)$$

where $E = -VY$ is used in the z direction only, Y_r is the magnitude of the repeller voltage, and $I Yt \sin wt$
 $I \sim (Y_r + Y_0)$ is assumed. Integration of Eq. (9-4-4) twice yields

$$\frac{dz}{dt} = \frac{-e(V_r + V_0)}{mL} \int_{t_1}^t dt = \frac{-e(V_r + V_0)}{mL} (t - t_1) + K_1 \quad (9-4-5)$$

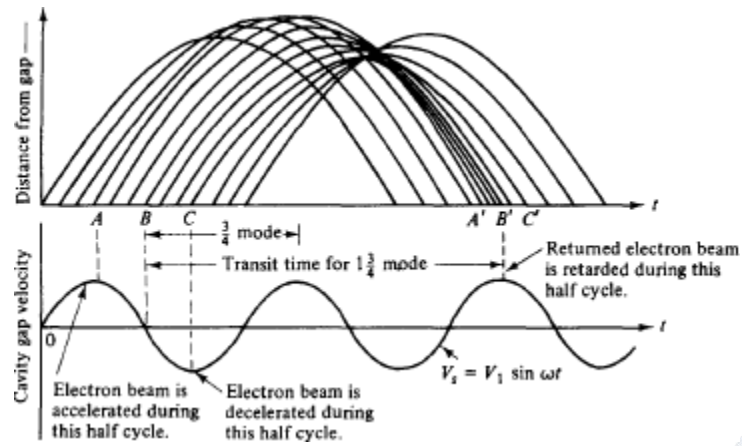


t_0 time for electron entering cavity gap at $z = 0$

t_1 time for same electron leaving cavity gap at $z = d$

time for same electron returned by retarding field

$z = d$ and collected on walls of cavity



at $t = t_1$, $dz/dt = v(t_1) = K_1$; then

$$z = \frac{-e(V_r + V_0)}{mL} \int_{t_1}^t (t - t_1) dt + v(t_1) \int_{t_1}^t dt$$

$$z = \frac{-e(V_r + V_0)}{2mL} (t - t_1)^2 + v(t_1)(t - t_1) + K_2$$

at $t = t_2$, $z = d = K_3$; then

$$z = \frac{-e(V_r + V_0)}{2mL} (t - t_1)^2 + v(t_1)(t - t_1) + d \tag{9-4-6}$$

On the assumption that the electron leaves the cavity gap at $z = d$ and time t_1 with a velocity of $v(t_1)$ and returns to the gap at $z = d$ and time t_2 , then, at $t = t_2, z = d$,

$$0 = \frac{-e(V_r + V_0)}{2mL}(t_2 - t_1)^2 + v(t_1)(t_2 - t_1)$$

The round-trip transit time in the repeller region is given by

$$T' = t_2 - t_1 = \frac{2mL}{e(V_r + V_0)}v(t_1) = T'_0 \left[1 + \frac{\beta_1 V_1}{2V_0} \sin \left(\omega t_1 - \frac{\theta_\xi}{2} \right) \right] \quad (9-4-7)$$

where

$$T'_0 = \frac{2mLv_0}{e(V_r + V_0)} \quad (9-4-8)$$

is the round-trip dc transit time of the center-of-the-bunch electron.

Multiplication of Eq. (9-4-7) through by a radian frequency results in

$$\omega(t_2 - t_1) = \theta'_0 + X' \sin \left(\omega t_1 - \frac{\theta_\xi}{2} \right) \quad (9-4-9)$$

where

$$\theta'_0 = \omega T'_0 \quad (9-4-10)$$

is the round-trip dc transit angle of the center-of-the-bunch electron and

$$X' = \frac{\beta_1 V_1}{2V_0} \theta'_0 \quad (9-4-11)$$

is the bunching parameter of the reflex klystron oscillator.

TRAVELING WAVE TUBE

Since Kompfner invented the helix traveling-wave tube (TWT) in 1944 [11], its basic circuit has changed little. For broadband applications, the helix TWTs are almost exclusively used, whereas for high-average-power purposes, such as radar transmitters, the coupled-cavity TWTs are commonly used.

In previous sections klystrons and reflex klystrons were analyzed in some detail. Before starting to describe the TWT, it seems appropriate to compare the basic operating principles of both the TWT and the klystron. In the case of the TWT, the microwave circuit is nonresonant and the wave propagates with the same speed as the electrons in the beam. The initial effect on the beam is a small amount of velocity modulation caused by the weak electric fields associated with the traveling wave.

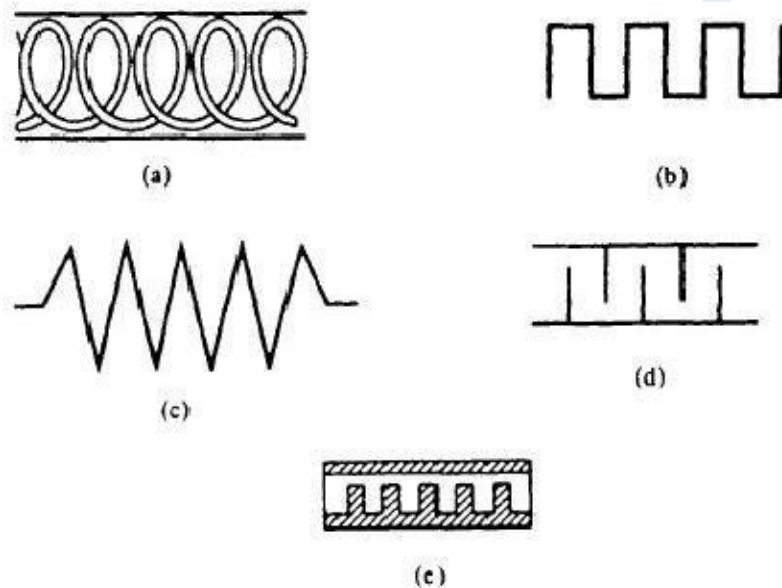
Just as in the klystron, this velocity modulation later translates to current modulation, which then induces an RF current in the circuit, causing amplification. However, there are some major differences between the TWT and the klystron:

The interaction of electron beam and RF field in the TWT is continuous over the entire length of the circuit, but the interaction in the klystron occurs only at the gaps of a few resonant cavities.

The wave in the TWT is a propagating wave; the wave in the klystron is not.

In the coupled-cavity TWT there is a coupling effect between the cavities, whereas each cavity in the klystron operates independently.

As the operating frequency is increased, both the inductance and capacitance of the resonant circuit must be decreased in order to maintain resonance at the operating frequency. Because the gain-bandwidth product is limited by the resonant circuit, the ordinary resonator cannot generate a large output. Several nonresonant periodic circuits or slow-wave structures (see Fig. 9-5-2) are designed for producing large gain over a wide bandwidth.



Slow-wave structures are special circuits that are used in microwave tubes to reduce the wave velocity in a certain direction so that the electron beam and the signal wave can interact. The phase velocity of a wave in ordinary waveguides is greater than the velocity of light in a vacuum.

In the operation of traveling-wave and magnetron-type devices, the electron beam must keep in step with the microwave signal. Since the electron beam can be accelerated only to velocities that are about a fraction of the velocity of light, a slow-wave structure must be incorporated in the microwave devices so that the phase velocity of the microwave signal can keep pace with that of the electron beam for effective interactions. Several types of slow-wave structures are shown in figure.

$$\frac{v_p}{c} = \frac{P}{\sqrt{P^2 + (\pi d)^2}} = \sin \psi$$

MAGNETRON

MAGNETRON OSCILLATORS

Hull invented the magnetron in 1921 [1], but it was only an interesting laboratory device until about 1940. During World War II, an urgent need for high-power microwave generators for radar transmitters led to the rapid development of the magnetron to its present state.

All magnetrons consist of some form of anode and cathode operated in a de magnetic field normal to of the crossed field between the cathode and anode, the electrons emitted from the cathode are influenced by the crossed field to move in curved paths. If the de magnetic field is strong enough, the electrons will not arrive in the anode but return instead to the cathode. Consequently, the anode current is cut off.

Magnetrons can be classified into three types:

1. *Split-anode magnetron*: This type of magnetron uses a static negative resistance between two anode segments.
2. *Cyclotron-frequency magnetrons*: This type operates under the influence of synchronism between an alternating component of electric field and a periodic oscillation of electrons in a direction parallel to the field.
3. *Traveling-wave magnetrons*: This type depends on the interaction of electrons with a traveling electromagnetic field of linear velocity. They are customarily referred to simply as *magnetrons*.

Cylindrical Magnetron

A schematic diagram of a cylindrical magnetron oscillator is shown in Fig. 10-1-1. This type of magnetron is also called a *conventional magnetron*.

In a cylindrical magnetron, several reentrant cavities are connected to the gaps. The de voltage V_0 is applied between the cathode and the anode. The magnetic flux density B_0 is in the positive z direction. When the de voltage and the magnetic flux are adjusted properly, the electrons will follow cycloidal paths

in the cathode-anode space under the combined force of both electric and magnetic fields as shown in Fig. 10-1-2.

Equations of electron motion. The equations of motion for electrons in a cylindrical magnetron can be written with the aid of Eqs.(1-2-Sa) and (1-2-Sb) as

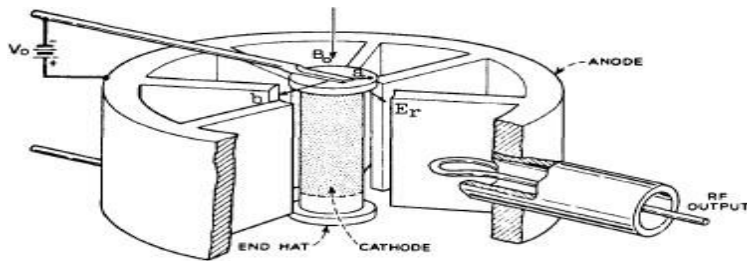


Figure 10-1-1 Schematic diagram of a cylindrical magnetron.

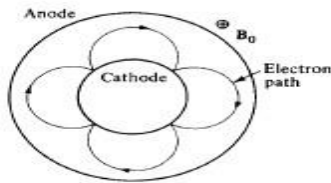


Figure 10-1-2 Electron path in a cylindrical magnetron.

$$\frac{d^2r}{dt^2} - r \left(\frac{d\phi}{dt} \right)^2 = \frac{e}{m} E_r - \frac{e}{m} r B_z \frac{d\phi}{dt} \quad (10-1-1)$$

$$\frac{1}{r} \frac{d}{dt} \left(r^2 \frac{d\phi}{dt} \right) = \frac{e}{m} B_z \frac{dr}{dt} \quad (10-1-2)$$

where $\frac{e}{m} = 1.759 \times 10^{11}$ C/kg is the charge-to-mass ratio of the electron and

$B_0 = B_z$ is assumed in the positive z direction.

Rearrangement of Eq. (10-1-2) results in the following form

$$\frac{d}{dt} \left(r^2 \frac{d\phi}{dt} \right) = \frac{e}{m} B_z r \frac{dr}{dt} = \frac{1}{2} \omega_c \frac{d}{dt} (r^2) \quad (10-1-3)$$

where $\omega_c = \frac{e}{m} B_z$ is the cyclotron angular frequency. Integration of Eq. (10-1-3)

yields

$$r^2 \frac{d\phi}{dt} = \frac{1}{2} \omega_c r^2 + \text{constant} \quad (10-1-4)$$

at $r = a$, where a is the radius of the cathode cylinder, and $\frac{d\phi}{dt} = 0$, constant = $-\frac{1}{2}\omega_c a^2$. The angular velocity is expressed by

$$\frac{d\phi}{dt} = \frac{1}{2}\omega_c \left(1 - \frac{a^2}{r^2}\right) \quad (10-1-5)$$

Since the magnetic field does no work on the electrons, the kinetic energy of the electron is given by

$$\frac{1}{2}mV^2 = eV \quad (10-1-6)$$

However, the electron velocity has r and ϕ components such as

$$V^2 = \frac{2e}{m}V = V_r^2 + V_\phi^2 = \left(\frac{dr}{dt}\right)^2 + \left(r\frac{d\phi}{dt}\right)^2 \quad (10-1-7)$$

at $r = b$, where b is the radius from the center of the cathode to the edge of the anode, $V = V_0$, and $dr/dt = 0$, when the electrons just graze the anode, Eqs. (10-1-5) and (10-1-7) become

$$\frac{d\phi}{dt} = \frac{1}{2}\omega_c \left(1 - \frac{a^2}{b^2}\right) \quad (10-1-8)$$

$$b^2 \left(\frac{d\phi}{dt}\right)^2 = \frac{2e}{m}V_0 \quad (10-1-9)$$

Substitution of Eq. (10-1-8) into Eq. (10-1-9) results in

$$b^2 \left[\frac{1}{2}\omega_c \left(1 - \frac{a^2}{b^2}\right)\right]^2 = \frac{2e}{m}V_0 \quad (10-1-10)$$

The electron will acquire a tangential as well as a radial velocity. Whether the electron will just graze the anode and return toward the cathode depends on the relative magnitudes of V_0 and B_0 . The *Hull cutoff magnetic equation* is obtained from Eq. (10-1-10) as

$$B_{0c} = \frac{\left(8V_0 \frac{m}{e}\right)^{1/2}}{b \left(1 - \frac{a^2}{b^2}\right)} \quad (10-1-11)$$

This means that if $B_0 > B_{0c}$ for a given V_0 , the electrons will not reach the anode. Conversely, the cutoff voltage is given by

$$V_{0c} = \frac{e}{8m} B_0^2 b^2 \left(1 - \frac{a^2}{b^2}\right)^2 \quad (10-1-12)$$

angular frequency. Since the magnetic field is normal to the motion of electrons that travel in a cycloidal path, the outward centrifugal force is equal to the pulling force. Hence

Cyclotron

$$\frac{mV^2}{R} = eVB \tag{10-1-13}$$

where R = radius of the cycloidal path
 V = tangential velocity of the electron

The cyclotron angular frequency of the circular motion of the electron is then given by

$$\omega_c = \frac{V}{R} = \frac{eB}{m} \tag{10-1-14}$$

The period of one complete revolution can be expressed as

$$T = \frac{2\pi}{\omega} = \frac{2\pi m}{eB} \tag{10-1-15}$$

Since the slow-wave structure is closed on itself, or "reentrant," oscillations are possible only if the total phase shift around the structure is an integral multiple of 2π radians. Thus, if there are N reentrant cavities in the anode structure, the phase shift between two adjacent cavities can be expressed as

$$\phi_n = \frac{2\pi n}{N} \tag{10-1-16}$$

where n is an integer indicating the n th mode of oscillation. In order for oscillations to be produced in the structure, the anode de voltage must be adjusted so that the average rotational velocity of the electrons corresponds to the phase velocity of the field in the slow-wave structure. Magnetron oscillators are ordinarily operated in the π mode. That is

$$\phi_n = \pi \quad (\pi \text{ mode}) \tag{10-1-17}$$

$$\beta_0 = \frac{2\pi n}{NL} \tag{10-1-18}$$

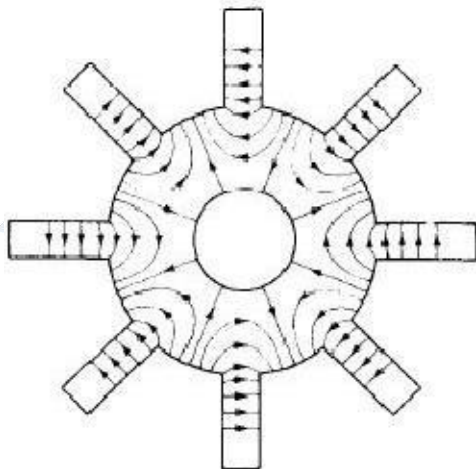


Figure 10-1-3 Lines of force in π mode of eight-cavity magnetron.

Maxwell's equations subject to the boundary conditions. The solution for the fundamental $cf>$ component of the electric field has the form [1]

$$E_{\phi 0} = jE_1 e^{j(\omega t - \beta_0 \phi)} \quad (10-1-19)$$

where E_1 is a constant and β_0 is given in Eq. (10-1-18). Thus, the traveling field of the fundamental mode travels around the structure with angular velocity

$$\frac{d\phi}{dt} = \frac{\omega}{\beta_0} \quad (10-1-20)$$

where ω_c can be found from Eq. (10-1-19). When the cyclotron frequency of the electrons is equal to the angular frequency of the field, the interactions between the field and electron occurs and the energy is transferred. That is,

$$\omega_c = \beta_0 \frac{d\phi}{dt} \quad (10-1-21)$$

MEASUREMENT OF POWER

Power Measurement

- ✓ Power is defined as the quantity of energy dissipated or stored per unit time.
- ✓ Microwave power is divided into three categories – low power (less than 10mW), medium power (from 10mW to 10W) and high power (greater than 10w).
- ✓ The general measurement technique for average power is to attach a properly calibrated sensor to the transmission line port at which the unknown power is to be measured.
- ✓ The output from the sensor is connected to an appropriate power meter. The RF power to the sensor is turned off and the power meter zeroed. This operation is often referred to as “zero setting” or “zeroing.” Power is then turned on.
- ✓ The sensor, reacting to the new input level, sends a signal to the power meter and the new meter reading is observed.
- ✓ There are three popular devices for sensing and measuring average power at RF and microwave frequencies. Each of the methods uses a different kind of device to convert the RF power to a measurable DC or low frequency signal. The devices are the diode detector, the bolometer and the thermocouple.

Diode Detector

The low-barrier Schottky (LBS) diode technology which made it possible to construct diodes with metal-semiconductor junctions for microwave frequencies that was very rugged and consistent from diode to diode. These diodes, introduced as power sensors in 1974, were able to detect and measure power as low as -70 dBm (100 pW) at frequencies up to 18 GHz.

Bolometer Sensor:

Bolometers are power sensors that operate by changing resistance due to a change in temperature. The change in temperature results from converting RF or microwave energy into heat within the bolometric element. There are two principle types of bolometers, barretters and thermistors. A barretter is a thin wire that has a positive temperature coefficient of resistance. Thermistors are semiconductors with a negative temperature coefficient.

Thermistor elements are mounted in either coaxial or waveguide structures so they are compatible with common transmission line systems used at microwave and RF frequencies.

Power meters are constructed from balanced bridge circuits. The principal parts of the power meter are two self-balancing bridges, the meter-logic section, and the auto-zero circuit. The RF Bridge, which contains the detecting thermistor, is kept in balance by automatically varying the DC voltage V_{rf} , which drives that bridge. The compensating bridge, which contains the compensating thermistor, is kept in balance by automatically varying the DC voltage V_c , which drives that bridge. The power meter is initially zero-set (by pushing the zero-set button) with no applied RF power by making V_c equal to V_{rf0} (V_{rf0} means V_{rf} with zero RF power). After zero-setting, if ambient temperature variations change thermistor resistance, both bridge circuits respond by applying the same new voltage to maintain balance.

If RF power is applied to the detecting thermistor, V_{rf} decreases so that

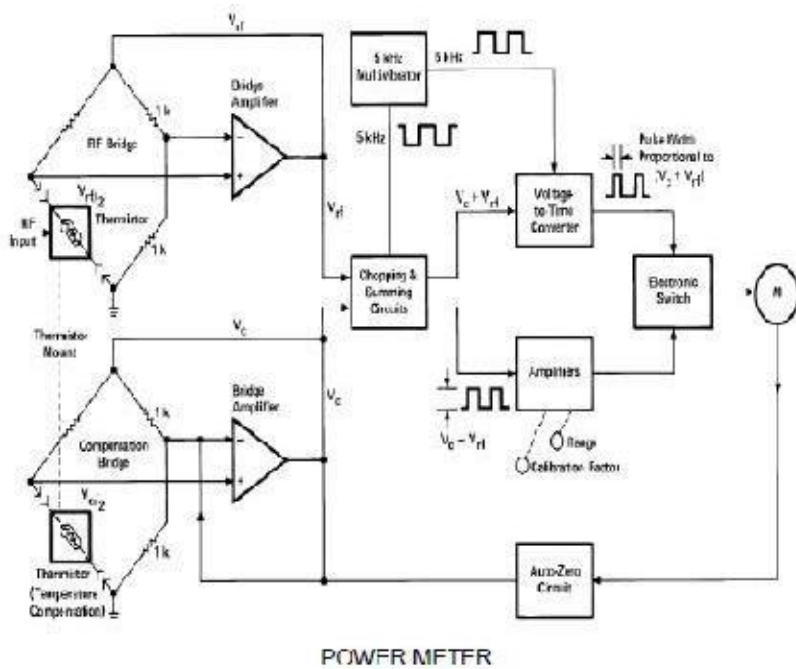
$$P_{rf} = \frac{V_{rf0}^2}{4R} - \frac{V_{rf}^2}{4R}$$

Where P_{rf} is the RF power applied and R is the value of the thermistor resistance at balance. But from zero-setting, $V_{rf0} = V_c$ so that

$$P_{rf} = \frac{V_c^2 - V_{rf}^2}{4R}$$

Which can be written

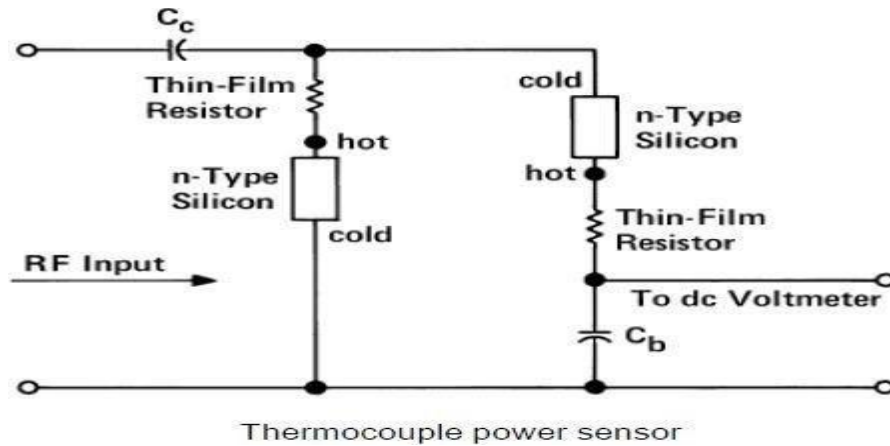
$$P_{rf} = \frac{(V_c - V_{rf})(V_c + V_{rf})}{4R}$$



Thermocouple Sensors

Thermocouple sensors have been the detection technology of choice for sensing RF and microwave power since their introduction in 1974. The two main reasons for this evolution are: 1) they exhibit higher sensitivity than previous thermistor technology, and 2) they feature inherent square-law detection characteristic (input RF power is proportional to DC voltage out).

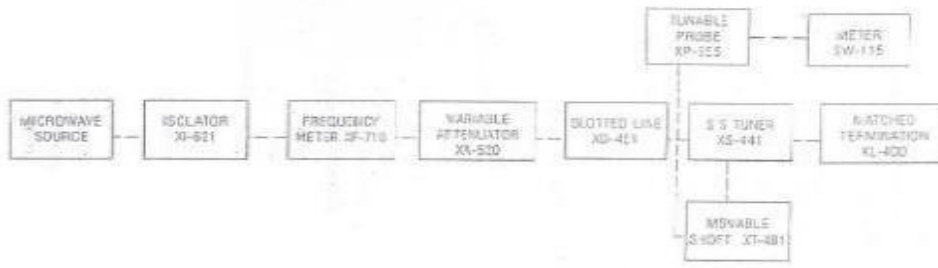
Since thermocouples are heat-based sensors, they are true “averaging detectors.” Thermocouples are based on the fact that dissimilar metals generate a voltage due to temperature differences at a hot and a cold junction of the two metals. The power sensor contains two identical thermocouples on one chip, electrically connected as in Figure.



The thermocouples are connected in series as far as the DC voltmeter is concerned. For the RF input frequencies, the two thermocouples are in parallel, being driven through coupling capacitor C_c . Half the RF current flows through each thermocouple.

Each thin-film resistor and the silicon in series with it have a total resistance of $100\ \Omega$. The two thermocouples in parallel form a $50\ \Omega$ termination to the RF transmission line. The lower node of the left thermocouple is directly connected to ground and the lower node of the right thermocouple is at RF ground through bypass capacitor C_b . The DC voltages generated by the separate thermocouples add in series to form a higher DC output voltage. The principal advantage, however, of the two thermocouple scheme is that both leads to the voltmeter are at RF ground; there is no need for an RF choke in the upper lead. If a choke were needed it would limit the frequency range of the sensor. For a square wave modulated signal the peak power can be calculated from the average power measured as where T is the time period and τ is the pulse width. □ Y P peak av P

MEASUREMENT OF WAVELENGTH AND IMPEADENCE



SET UP FOR IMPEDANCE MEASUREMENT

The impedance at any point on a transmission line can be written in the form $R+jX$

For comparison SWR can be calculated

$$S = \frac{1 + |R|}{1 - |R|}$$

Where

Reflection co-efficient

$$R = \frac{Z - Z_0}{Z + Z_0}$$

Z_0 = characteristics impedance of w/g at operating frequency

Z = load impedance. The measurement is performed in following way.

The unknown device is connected to the slotted line and the position of one minima is determined. The unknown device is replaced by movable short to the slotted line . Two successive minima positions are noted. The twice of the difference between minima position will be guidewave length. One of the minima is used as reference for impedance measurement .find the difference of reference minima and minima position obtained from unknown load. Let it be 'd'. Take a smith chart , taking '1' as centre, draw a circle of radius equal to S. mark a point on circumference of smith chart towards load side at a distance equal to d/g. join the centre with this point . find the point where it cut the drawn circle. the co-ordinates of this point will show the normalized impedance of load.

PROCEDURE:

1. Setup the components and equipments as shown in figure.
2. Setup variable attenuator at minimum attenuation position.
3. Keep the control knobs of VSWR meter as below:
Range - 50db position
Input switch - Crystal low impedance
Meter switch - Normal position
Gain(Coarse & Fine)- Mid position
4. Keep the control knobs of Klystron power supply as below
Beam voltage - 'OFF'
Mod-switch -AM
Beam Voltage knob-Fully anticlockwise
Reflector Voltage- Fully clockwise
AM- Amplitude knob- Around fully clockwise
AM- Frequency knob – Around Mid position
5. Switch 'ON' the Klystron power supply, VSWR Meter and cooling fan switch.
6. Switch 'ON' the beam voltage switch and set beam voltage around 250V-300V with help of beam voltage knob.
7. Adjust the reflector voltage to get some deflection in VSWR meter.
8. Maximize the deflection with AM amplitude and frequency control knob of power supply.
9. Tune the plunger of Klystron Mount for maximum deflection.
10. Tune the reflector voltage knob for maximum deflection .
11. Tune the probe for maximum deflection in VSWR Meter.
12. Tune the frequency meter knob to get a 'dip' on the VSWR scale and note down the frequency directly from frequency meter.
13. Keep the depth of pin S S. Tuner to around 3-4 mm and lock it.
14. Move the probe along the slotted line to get maximum deflection.
15. Adjust VSWR meter gain control knob and variable attenuator until the meter indicates 1.0 on the normal db SWR scale.
16. Move the probe to next minimum position and note down the SWR S_0 on the scale .also note down the probe position. Let it be 'd'.
17. Remove the SS tuner and matched termination and place movable short at slotted line. The plunger of short should be at zero.
18. Note the position of two successive minima position .let it be as d_1 and d_2 .Hence $\lambda_g = 2(d_1 - d_2)$.

19. Calculate

$$\frac{d}{\lambda_g}$$

20. Find out the normalized impedance as described in the theory section.

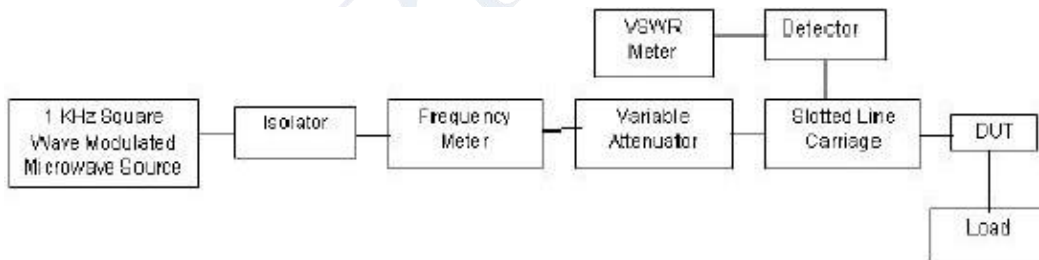
21. Repeat the same experiment for other frequency if required.

MEASUREMENT OF SWR AND ATTENUATION

In a microwave network, if load impedance and line impedance are not matched, signal fed from the source is reflected again towards source causing standing wave pattern in the network. Voltage Standing Wave Ratio is a measure used for finding the magnitude of ration of reflected signals maximum and minimum amplitudes For analyzing standing wave pattern and to find S slotted line carriage is used in laboratory.

$$S = \frac{V_{max}}{V_{min}} \quad \text{----- (1)}$$

Low VSWR Measurements: ($S < 20$)



Procedure:

1. Microwave Source is energized with 1 KHz square wave signal as carrier.
2. Tunable passive components are so adjusted to get reading across the VSWR meter in 30 dB scale.
3. Detector (Tunable probe detector) is adjusted to get maximum power across the VSWR meter.
4. Slotted line carriage is moved from the load towards source to find the standing wave minimum position.

5. By adjusting the gain control knob of VSWR meter and attenuator the reading across the VSWR meter is made as 1 or 0 dB known as normalization.
6. Again the slotted carriage is moved towards source to find the next minimum position. The reading shown at this point in the VSWR meter is the ratio of magnitude of reflected signals minimum and maximum voltages (). $\frac{V_{min}}{V_{max}}$ □
7. VSWR meter has three different scales with different ranges as specified below.
 - a) NORMAL SWR Scale 1 □ 1 – 4
 - b) NORMAL SWR Scale 2 □ 3.2 – 10
 - c) EXPANDED SWR Scale 3 □ 1 – 1.33
8. If the device under test (DUT) is having the range of VSWR 1 – 4, reading is taken from the first scale from the top (NORMAL SWR Scale 1 – 1 – 4).
9. If the device under test (DUT) is having the range of VSWR 3.2 – 10, reading is taken from the second scale from the top (NORMAL SWR Scale 2 (3.2 – 10)).
10. If the device under test (DUT) is having the range of VSWR 1 – 1.33, reading is taken from the third scale from the top (EXPANDED SWR Scale 3 (1 – 1.33)).
11. If the device under test (DUT) is having the range of VSWR 10 – 40, a 20 dB range is selected in the VSWR meter and reading is taken from the first scale from the top (NORMAL SWR Scale 1 – 1 – 4) which is then multiplied by 10 for getting the actual reading.

Possible Errors in Measurements:

1. Detector may not work square law region for both V_{max} . and V_{min} .
2. Depth of the probe in the slotted line carriage is made as minimum. If not, it may cause reflections in addition to the load reflections.
3. For the device having low VSWR, connector used for measurement must have proper matching with line impedance.
4. If the geometrical shape of the slotted line is not proper, V_{max} . (or) V_{min} . Value will not constant across the slotted line.

5. If the microwave signal is not properly modulated by a 1 KHz square wave, then signal becomes frequency modulated thereby it causes error in the V_{min} . value measured. The value becomes lower than the actual.
6. Residual VSWR of slotted line carriage may cause error in the measurements.

High VSWR Measurements - Double Minima Method - ($S > 20$)

Measurement of high VSWR needs separate procedure because the detector may not be tuned to work in square law region. An alternate method known as double minimum method is used for finding high VSWR with the same experimental set up as shown above.

Procedure:

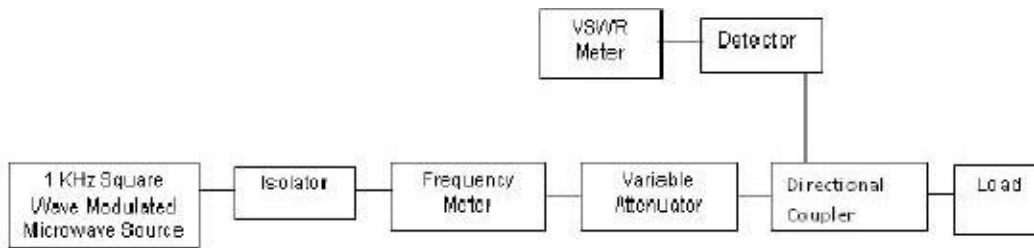
1. Microwave Source is energized with 1 KHz square wave signal as carrier.
2. Tunable passive components are so adjusted to get reading across the VSWR meter in 30 dB scale.
3. Detector (Tunable probe detector) is adjusted to get maximum power across the VSWR meter.
4. Slotted line carriage is moved from the load towards source to find the standing wave minimum position. Let it be d_1 .
5. Slotted line carriage is moved further to find the next immediate minimum position. Let it be d_2 . Now $\Delta g = 2(d_1 - d_2)$
6. By adjusting the gain control knob of VSWR meter and attenuator the reading across the VSWR meter is made as 3 dB at this minimum position.
7. By taking this point as reference, slotted line carriage is moved on either side. The points at which the VSWR meter shows 0 dB reading on both sides are noted as x_1 and x_2 .

8. High VSWR can be calculated by using the formula

$$S = \frac{\lambda_g}{\pi(x_1 - x_2)}$$

VSWR Measurements by Return Loss (Reflectometer) Method:

To overcome the difficulties faced in slotted line carriage for measuring VSWR, reflectometer can be used. Reflectometer is a device having two directional couplers combined together with ideal coupling factor and directivity. It is a four-port device.



Experimental Procedure:

1. Microwave Source is energized with 1 KHz square wave signal as carrier.
2. Tunable passive components are so adjusted to get reading across the VSWR meter in 30 dB scale.
3. Detector (Tunable probe detector) is adjusted to get maximum power across the VSWR meter.
4. Port 2 is with a movable short and is adjusted for getting the output across the detector to unity in VSWR meter. Port 3 is matched terminated.
5. VSWR meter and matched load at port4 and port 3 are interchanged. The output of the port3 is noted which should be ideally equal to the output from port 4.
6. Without disturbing the VSWR meter adjustment, the unknown load is connected at port 2 by replacing

the short and the output at port3 is noted to obtain $\frac{1}{\Gamma_L}$

directly from the VSWR meter.

Return loss = $-20 \log|\Gamma_L|$

$$VSWR = \frac{1+|\Gamma_L|}{1-|\Gamma_L|}$$

This method is well suited for loads having low VSWR. The major sources of errors are

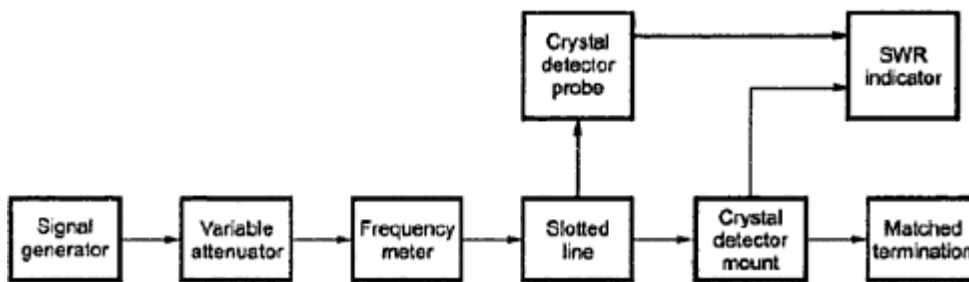
1. Unstability of the signal source causes a change of signal power level during measurement of input and reflected signals.
2. Non-ideal directional couplers and detectors are also sources of error.

Q AND PHASE SHIFT

Microwave frequency can be measured by a number of different mechanical and electronic techniques.

- ✓ Mechanical techniques
- ✓ Slotted Line Method (Indirect Method)

The standing waves setup in a transmission line or a waveguide produce minima every half wavelength apart.



These minima are detected and the distance between them is measured. From which the wavelength and frequency can be calculated by

$$\lambda_g = 2d_{\min}$$

$$f = \frac{c}{\lambda_0}$$

$$\therefore \lambda_0 = \frac{\lambda_g \lambda_c}{\sqrt{\lambda_g^2 + \lambda_c^2}}$$

where λ_0 – free space wavelength

λ_c - cut off wavelength

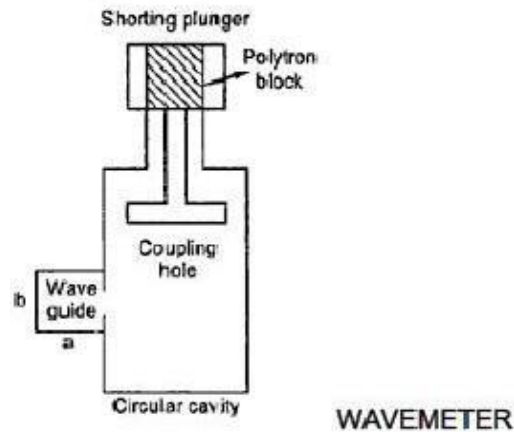
λ_g – guide wavelength

d_{\min} can be measured by the slotted line probe carriage.

Resonant Cavity Method (Direct Method)

The most commonly used type of microwave frequency meter is wave meters. It consists of a cylindrical or coaxial resonant cavity. The size of the cavity can be altered by adjustable plunger. The cavity is

designed in such a way that for a given position of the plunger, the cavity is resonant only at one frequency in the specified range.



The cavity is coupled to the waveguide through an iris in the narrow wall of the waveguide. If the frequency of the wave passing through the waveguide is different from the resonance frequency of the cavity, the transmission is not affected. If these two frequencies coincide then the wave passing through the waveguide is attenuated due to power loss. It will be indicated as a dip in the meter.

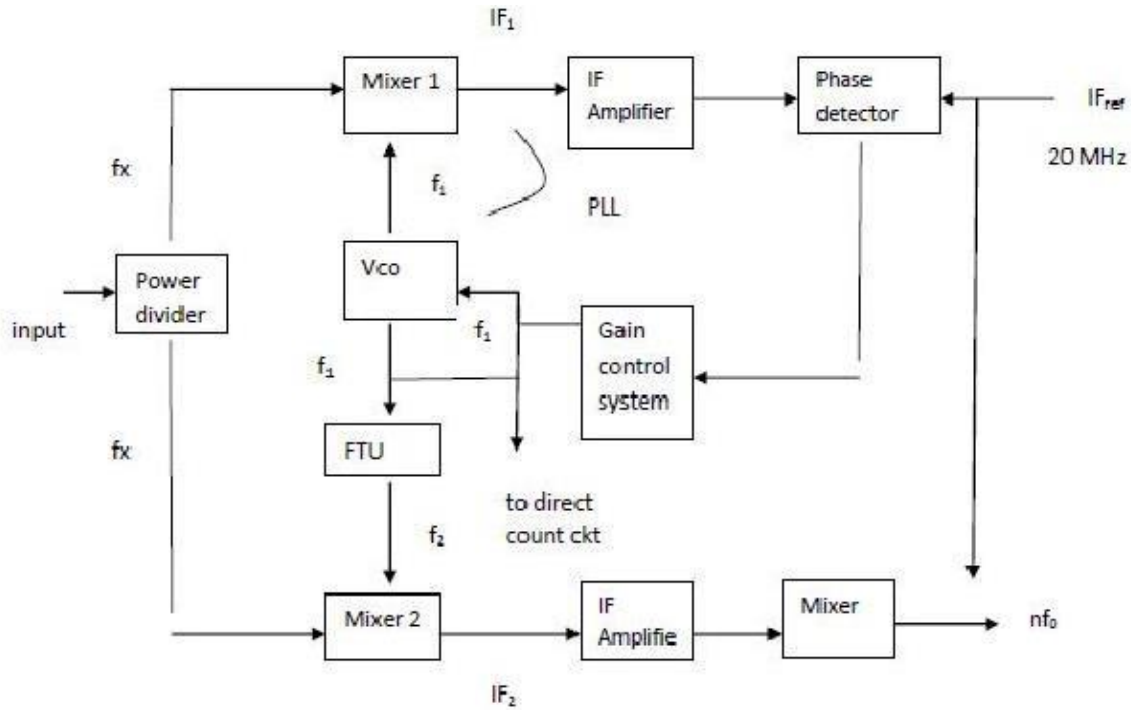
Electronic Technique

Counter Method

An accurate measurement of microwave frequency can be measured here. The input signal is divided into two equal signals by a resistive power divider. These two parts of the signal are fed to 2 mixers. The mixer 1 is used in the input PLL (Phase Locked Loop) and the mixer 2 is used to determine the harmonic number. The frequency f_1 of the input PLL is also fed to the direct counter circuits. The input PLL consists of a voltage controlled oscillator (VCO), mixer, an IF amplifier, a phase detector and a gain control block. The VCO searches over its range until an IF signal equal to 20MHz is found. Phase lock occurs when the phase detector output sets the VCO frequency f_1 such that

$$f_x = n f_1 - IF_1$$

where $IF_1 = 20$ MHz at the phase lock and f_x is the unknown frequency to be measured.



The f_1 is translated to a frequency f_2 so that

$$f_2 = f_1 \pm f_0$$

where $f_0 = 20$ MHz offset frequency. This is done by a frequency translation unit (FTU). The frequency f_2 drives the second sampler and produces a second output. IF_2 is given as

$$\begin{aligned} IF_2 &= nf_2 - f_x \\ &= n(f_1 \pm f_0) - (nf_1 - 20MHz) \\ &= \pm nf_0 + 20 \end{aligned}$$

By mixing IF_2 with IF_1 and rejecting 20 MHz and higher frequencies, nf_0 is obtained. Counting the number of zero crossing for the period of f_0 , determines the harmonic number n of the phase lock loop. The input frequency is then calculated by presetting into IF_{ref} counter, measuring f_1 and extending gate time according to number n .